Molecular characterisation of ductin, the membrane component of the gap junction and the vacuolar proton pump.

John Dunlop

This thesis is submitted in part fulfilment of the degree of Doctor of Philosophy in the University of Glasgow.

Beatson Institute for Cancer Research,
CRC Beatson Laboratories,
Bearsden, Glasgow.

Faculty of Medicine,
University of Glasgow,
Glasgow.

April 1995

ProQuest LLC.
789 East Eisenhower Parkway
P.O. Box 1346
Ann Arbor, MI 48106 – 1346

Abstract.

This thesis describes an investigation into ductin, a highly conserved and polytopic transmembrane protein which is the subunit *c* component of the vacuolar H^+-ATPase (V-ATPase) and a unique component of the connexon channel of gap junctions. The aim of the thesis was to identify regions of ductin involved in the association with other subunits of the V-ATPase and to determine the manner of ductin's synthesis and assembly into a multimeric state. Ductin has been studied using a cell-free expression system based on rabbit reticulocyte lysate and in a yeast system using a strain of conditional lethal yeast that are deficient in ductin.

A set of residues thought to be critical for the activity of ductin reside in the two conserved extramembranous loop regions, which are thought to serve as sites of contact with other subunits of the V-ATPase complex. To test their importance these loop regions were exchanged with the corresponding regions of VMA11, a protein homologous to ductin but with a distinct activity. The resulting loop chimeras of ductin were expressed in the yeast strain deficient in ductin and the activity of the chimeras was assayed. Both of the conserved loop regions were found to be sensitive to substitution, with the first loop between helices 1 and 2 having a significantly reduced activity while the second loop between helices 3 and 4 was inactive. This indicates that these conserved loop regions are important for the activity of ductin, possibly in a manner similar to that of the polar loop region of the F_1F_0-ATPase subunit *c*.

The synthesis of ductin was dependant on the presence of microsomal membranes, and ductin was inserted into this endoplasmic reticulum derived membrane, as shown by trypsin insensitivity and sodium carbonate extraction. The self-assembly of ductin into an oligomeric complex was shown by the co-immunoprecipitation of two forms of ductin using antibodies specific to one of the ductin forms. The presence of an aqueous channel in this oligomeric complex was shown by the

labelling of cysteine replacement mutants in the putative central gap junctional chanel with a membrane impermiant maleimide probe, fluoroscein-5-maleimide.

The orientation of ductin once it is inserted into the microsomal membranes was determined by two methods, firstly from the sensitivity to trypsin of a C-terminal extension, and secondly from the labelling by fluoroscein-5-maleimide of single cysteine residues. A trypsin sensitive C-terminal extension based on the mature N-terminus of β-lactamase was engineered onto ductin (Nductin-β lac) with the expectation that the ability of trypsin to cleave this extension would be determined by the orientation of ductin. After trypsin treatment two populations of Nductin-β lac were observed, one cleaved the other uncleaved, corresponding to a cytoplasmic and lumenal C-terminal location respectively. The presence of dual orientations for ductin was confirmed by the fluoroscein-5-maleimide labelling, since a single cysteine residue on either side of the microsomal membrane was only partially labelled while the membranes remained impermiant to the fluoroscein-5-maleimide.

for my friends and family; and thanks for all the help

Table of Contents.

		Page
Abstract		ii
Acknowledgements		xi
Abbreviations		xii
List of figures		xiv
List of tables		xvii
Chapter 1.	**Introduction.**	1
1.1.	General introduction.	2
1.2.	Co-translational insertion of integral membrane proteins.	3
1.2.1.	Targeting of proteins for translocation.	3
1.2.2.	The translocation machinery.	6
1.2.3.	The length of the conducting channel.	7
1.2.4.	Other components of the translocation process.	8
1.3.	Signal sequences and membrane topology.	10
1.4.	Assembly of oligomeric membrane proteins.	14
1.5.	Ductin as a model protein for membrane insertion and assembly.	15
1.6.	Ductin complexes.	16
1.6.1	Introduction.	16
1.6.2.	Gap junctions.	16
1.6.2.1.	Introduction.	16
1.6.2.2.	Structure of the gap junction.	17
1.6.2.3.	Gap junction physiology.	18
1.6.3.	The mediatophore.	19
1.6.4.	The vacuolar-type H^+-ATPase.	21
1.6.4.1.	Introduction.	21

1.6.4.2.	Subunit composition of the V-ATPase complex.	23
1.6.4.3.	Structure of the V-ATPase complex.	27
1.6.4.4.	Assembly of the V-ATPase complex.	28
1.6.5.	Evidence that the same ductin polypeptide functions as a V-ATPase, gap junction and mediatophore component.	29
1.7.	Structure of ductin.	29
1.7.1.	Introduction.	29
1.7.2.1.	Structure of subunit *c* of the F_1F_0 ATPase.	30
1.7.2.2.	Mutational analysis of subunit *c*.	31
1.7.3.	The structure of ductin.	33
1.7.4.	Mutagenesis of ductin.	36
1.7.5.	Orientation of ductin in the lipid bilayer.	37
1.7.6.	Ductin related proteins.	38
1.8.	Ductin-associated viral proteins: E5 and p12.	40
1.9.	Summary.	41
Chapter 2.	**Materials and Methods.**	43
2.1.	Materials.	44
2.1.1	Chemicals.	44
2.1.2.	Kits.	45
2.1.3.	Equipment and Plasticware.	46
2.1.4.	Plasmids.	46
2.1.5.	Antiserum.	47
2.1.6.	Bacterial Host.	47
2.1.7.	Yeast culture media and buffers.	47
2.1.8.	Water.	47
2.2.	Methods.	48

2.2.1.	Nucleic acid Procedures.	48
2.2.1.1.	Growth, transformation and storage of competent cells.	48
2.2.1.2.	Preparation of nucleic acids.	49
2.2.1.2.1.	Plasmid minipreparations: alkali lysis method.	49
2.2.1.2.2.	Large scale plasmid preparations (Qiagen tip 500 plasmid kit).	50
2.2.1.2.3.	Preparation of total RNA from yeast.	50
2.2.1.2.4.	Preparation of oligonucleotides.	51
2.2.1.3.	Enzymatic manipulation of DNA.	52
2.2.1.3.1.	Restriction digests.	52
2.2.1.3.2.	Dephosphorylation of 5' phosphate groups from plasmid DNA.	52
2.2.1.3.3.	Ligation of DNA fragments.	52
2.2.1.3.4.	Agarose gel electrophoresis.	53
2.2.1.4.	Purification and quantitation of nucleic acids.	53
2.2.1.4.1.	"Wizard" DNA purification system.	53
2.2.1.4.2.	Purification of nucleic acids by phenol/chloroform extraction.	54
2.2.1.4.3.	Concentration of nucleic acids.	54
2.2.1.4.4.	Quantitation of nucleic acids.	55
2.2.1.5.	Sequencing of double stranded DNA.	55
2.2.1.6.	Polymerase Chain Reaction (PCR).	56
2.2.1.7.	Reverse transcriptase-PCR (RT-PCR).	56
2.2.1.8.	*In vitro* RNA transcription	57
2.2.2.	Protein procedures.	57
2.2.2.1.	Protein preparation.	57
2.2.2.1.1.	Polyacrylamide slab gel analysis of proteins.	57
2.2.2.1.2.	Western analysis.	59

2.2.2.1.3.	Protein assay.	60
2.2.2.1.4.	Immunoprecipitation.	60
2.2.2.1.5.	Alkali extraction of microsomal membranes.	61
2.2.2.1.6.	Proteolysis reactions.	61
2.2.2.2.	*In vitro* translation.	62
2.2.2.3.	Chemical modification of cysteine residues.	62
2.2.2.4.	Preparation of vacuolar membranes.	63
2.2.2.5.	Vacuolar-ATPase assay.	63
2.3.	PCR constructs.	64
2.4.	Transformation of yeast.	65
Chapter 3.	**Results.**	66
3.1.	Introduction.	67
3.2.	Expression of chimeric forms of ductin in *S. cerevisiae*.	70
3.2.1.	Introduction.	70
3.2.2.	Cloning of VMA11 cDNA.	73
3.2.3.	Characterisation of the *vat c* and *NUY43* yeast strains.	73
3.2.4.	Expression of Nductin and VMA11 in yeast.	77
3.2.5.	Construction of ductin chimeras.	77
3.2.6.	Transformation of yeast.	82
3.2.7.	RT-PCR analysis of yeast transformed with loop chimeras.	82
3.2.8.	Expression of ductin chimeras in *S. cerevisiae.*	84
3.2.9.	Western analysis of yeast transformed with ductin chimeras.	86
3.2.10.	Construction and expression of further mutations to the double loop chimera	86

3.2.11.	Discussion.	91
3.2.11.1.	Replacement of the conserved loop regions of ductin.	91
3.2.11.2.	Additional mutation of the 1-2/3-4 loop chimera to VMA11.	92
3.2.11.3	The yeast expression system as a tool.	93
3.3.	Synthesis and assembly of ductin.	94
3.3.1.	Introduction.	94
3.3.2.	Examination of an *in vitro* expression system-β-lactamase.	94
3.3.3.	Synthesis of squid rhodopsin.	97
3.3.4.	Synthesis of Nductin.	99
3.3.5.	Membrane insertion of Nductin.	101
3.3.6.	Orientation of ductin in the microsomal membranes.	101
3.3.6.1.	Introduction.	101
3.3.6.2.	Construction of Nductin-β lac.	103
3.3.6.3.	Trypsin digestion of Nductin-β lac.	106
3.3.6.4.	Chemical modification of ductin by fluorescein-5-maleimide (FM).	117
3.3.7.	The role of charge in determining the orientation of Nductin-β lac.	124
3.3.8.	Orientation of VMA11.	125
3.3.9.	The assembly of ductin complexes.	128
3.3.9.1.	Introduction.	128
3.3.9.2.	Immunoprecipitation of ductin complexes.	130
3.3.9.3.	The assembly of Bductin E139R.	136
3.3.9.4.	Chemical modification of ductin complexes by FM.	136

3.4.	Discussion.	142
3.4.1.	The *in vitro* translation system.	142
Chapter 4.	**General Discussion.**	144
4.1.	Role of the conserved loop regions.	145
4.2.	Role of VMA11.	149
4.3.	Orientation of ductin in microsomal membranes.	151
4.4.	Assembly of ductin complexes.	158
References		163

Acknowledgements

I would like to thank my supervisor Dr Malcolm Finbow for all his help and advice. In addition, my thanks to Liam Meagher, Dr John Pitts and all the other members of R5 for all their contributions. I would also like to acknowledge the financial support of the Medical Research Council and the Cancer Research Campaign.

Declaration.

The work described in this thesis was performed personally unless otherwise acknowledged.

Abbreviations.

A_x	$Absorbance_{wavelength}$
ATP	adenosine 5' triphosphate
Bductin	bovine ductin
bp	base pairs
BFA	Brefeldin A
BPI	bactericidal/permeability-increasing protein
BPV	bovine papillomavirus
cAMP	3', 5' cyclic adenosine monophosphate
cDNA	complementary DNA
CIP	calf intestinal alkaline phosphatase
cm	centimetre
Da	Dalton
DCCD	dicyclohexyl carbodiimide
DNA	deoxyribonucleic acid
ECL	enhanced chemiluminescent
EDTA	ethylenediaminetetra-acetic acid, disodium salt
EGF	epidermal growth factor
ER	endoplasmic reticulum
EM	electron microscopy
FTIR	Fourrier transformed infra-red
g	gram
GJIC	gap junctional intercellular communication
hr	hour
IMP	intramembranous particle
k	kilo
l	litre
μ	micro
m	milli
M	molar
mA	milliamps
MES	2-N-morpholinoethane sulphonic acid
min	minutes
mol	mole
MOPS	4-morpholinepropanesulphonic acid
MP	membrane pellet
mRNA	messenger RNA
n	nano
Nductin	*Nephrops* ductin
NAC	nascent-polypeptide-associated complex
nm	nanometre
oligo	oligonucleotide
ORF	open reading frame
o/n	overnight
PAGE	polyacrylamide gel electrophoresis
PBS	phosphate buffered saline
PCR	polymerase chain reaction
RER	rough endoplasmic reticulum
rpm	revolutions per minute

RNA	ribonucleic acid
RNase	ribonulease
SDS	sodium dodecyl sulphate
sec	second
SRP	signal recognition particle
TEMED	tetramethylenediamine
TPA	12-O-tetradecanoylphorbal-13-acetate
tris	2-amin-2-(hydroxymethyl) propane-1,3-diol
UV	ultraviolet
V	Volts
v/v	volume for volume
W	Watts
w/v	weight for volume
X-gal	5-bromo-4-chloro-3-indolyl-β-D-galactoside

Amino acid one and three letter codes

A	Ala	Alanine
C	Cys	Cysteine
D	Asp	Aspartic acid
E	Glu	Glutamic acid
F	Phe	Phenylalanine
H	His	Histidine
I	Ile	Isoleucine
K	Lys	Lysine
M	Met	Methionine
N	Asn	Asparagine
P	Pro	Proline
Q	Gln	Glutamine
R	Arg	Arginine
S	Ser	Serine
T	Thr	Threonine
V	Val	Valine
W	Trp	Tryptophan
Y	Tyr	Tyrosine

List of figures.

		Page
Figure 1.	Model of the co-translational insertion of integral membrane proteins.	5
Figure 2.	Classification of integral membrane protein orientation.	11
Figure 3.	Model subunit structure of the F_1F_0ATPase.	22
Figure 4.	Structural model for the yeast V-ATPase.	24
Figure 5.	Proposed orientation of ductin in the gap junction and the V-ATPase complex.	39
Figure 6.	Sequence alignment of 16-kDa proteins.	71
Figure 7.	Partial sequence of PCR cloned VMA11 cDNA.	75
Figure 8.	Loop chimeras of ductin.	80
Figure 9.	Partial sequence of the PCR cloned 1-2 loop chimera.	81
Figure 10.	RT-PCR analysis of yeast transformed with loop chimeras of Nductin.	83
Figure 11.	Growth of transformed yeast at pH 7.5.	85
Figure 12.	Western analysis of the 1-2 loop chimera.	87
Figure 13.	A model depicting the character of the proposed surfaces of the four α-helix bundle of Nductin.	90
Figure 14.	Synthesis and insertion of β-lactamase into microsomal membranes.	96
Figure 15.	Membrane insertion and orientation of squid rhodopsin.	98
Figure 16.	Synthesis and insertion of Nductin into microsomal membranes.	100
Figure 17.	Trypsin digestion of Nductin.	102

Figure 18. The predicted band pattern of Nductin-β lac before and after trypsin treatment. 104

Figure 19. PCR strategy for the generation of the extended Nductin, Nductin-β lac. 105

Figure 20. Synthesis and insertion of Nductin-β lac into microsomal membranes. 109

Figure 21. Trypsin digestion of Nductin-β lac. 111

Figure 22. Time course of trypsin digestion of Nductin-β lac in microsomal membranes. 113

Figure 23. Time course of trypsin digestion of β-lactamase and squid rhodopsin in microsomal membranes. 115

Figure 24. Time course of trypsin digestion of Nductin-β lac and β-lactamase in microsomal membranes. 116

Figure 25. Disposition of Nductin in the bilayer showing the positions of the residues replaced by cysteine, S6 and S44. 118

Figure 26. Labelling of β-lactamase by fluoroscein-5-malimide (FM). 120

Figure 27. Labelling of the cys6 and cys44 substitutions of Nductin by FM. 122

Figure 28. Labelling of the cys6 and cys44 substitutions of Nductin by FM in the presence of SDS. 123

Figure 29. Time course of trypsin digestion of NductinKK-β lac and β-lactamase in microsomal membranes. 126

Figure 30. Time course of trypsin digestion of NductinAA-β lac and β-lactamase in microsomal membranes. 127

Figure 31. Time course of trypsin digestion of VMA11-β lac and β-lactamase in microsomal membranes. 129

Figure 32. Self-assembly of ductin complexes. 131

Figure 33. Association of Nductin-β lac with VMA11. 133

Figure 34. Non-association of Nductin with PPA1. 134

Figure 35. Non-association of Nductin with squid rhodopsin. 135

Figure 36. Self-assembly of ductin complexes is not disrupted by the E139R mutation. 137

Figure 37. Disposition of Nductin in the bilayer showing the positions of the residues replaced by cysteine, S25, L27 and A29. 138

Figure 38. Labelling of the cys25, cys 27 and cys29 substitutions of Nductin by FM. 140

Figure 39. Labelling of the cys25, cys27 and cys29 substitutions of Nductin by FM in the presence of SDS. 141

Figure 40. Proposed scheme of the insertion of ductin leading to dual orientations and the segregation of the assembly of the V0 of the V-ATPase from the connexon of gap junction. 152

Figure 41. A model depicting the relative position of residues on the surfaces of the four α-helix bundle of Nductin. 155

List of tables.

		Page
Table 1.	Genotype of S. cerevisiae strains, NUY43 and vat c.	72
Table 2.	Nucleotide sequence of flanking primers.	74
Table 3.	Nucleotide sequence of internal primers for Nductin chimeric polypeptides.	78
Table 4.	pH growth characteristics of Nductin, VMA11 and the loop chimeras.	76
Table 5.	Functional properties of *vat c* strains expressing mutagenised Nductin.	88
Table 6.	pH growth characteristics of F24L, Y31I and F24L/Y31I.	preceeding 91
Table 7.	Nucleotide sequence of internal primers for Nductin-β lac and VMA11-β lac fusion polypeptides.	107
Table 8.	Nucleotide sequence of 5' primers containing a T7 RNA polymerase site.	108

Chapter 1. Introduction.

1.1. General introduction.

The eukaryotic cell maintains a network of vesicles and endomembranes that separates the contents of these organelles from the bulk cytoplasm. A cell is faced with the problem of targeting proteins to and into these organelles while maintaining the integrity of the organellular membranes. The majority of organellar proteins (excluding mitochondria and chloroplasts), as well as plasma membrane proteins and secretory proteins, reach their final destination through a common entry point in the transport system, that of the endoplasmic reticulum (ER) (Ng and Walter, 1994).

Much of the work that has been done on the process of protein translocation through the lipid bilayer has focused on secretory proteins or proteins that only contain a single transmembrane domain. Integral membrane proteins that contain a number of segments that pass through the lipid bilayer have been less well studied but are presumed to use the same machinery as secretory proteins.

To date our understanding of membrane proteins has lagged considerably behind that of water soluble proteins. Of particular note is the lack of structural information for membrane proteins. The few membrane proteins for which high resolution structural information is available include the porins, the photosystem I, bacteriorhodopsin and light harvesting complex (Deisenhofer et al., 1985; Henderson et al., 1990; Weiss et al., 1991; Kuhlbrandt et al., 1994). This lack of information limits our understanding of processes that are fundamental for membrane proteins, such as folding and assembly. Whether basic principles that apply to non-membranous proteins also hold for membrane proteins is an open question, since there is little information on how the hydrophobic environment present in the lipid bilayer alters the interactions of amino acids. It increasingly looks as if the process of folding and assembly of non-membranous proteins is an assisted process, with the various members of the chaperonin family guiding the

folding process along the correct pathway (Frydman et al., 1994). It is not known if an analogous system exists for integral membrane proteins.

Ductin is a multi-membrane pass channel (polytopic) protein present in gap junctions, the vacuolar ATPase complex and the mediatophore (Finbow et al., 1995) and on which a number of structural studies have been performed. Although there is no high resolution data available, the basic features of ductin have been confirmed through a variety of techniques. Basically, it consists of four α-helical transmembrane regions probably arranged as a bundle embedded in the membrane (Holzenburg et al., 1993). Ductin would appear to be a suitable model protein with which to study the process by which polytopic membrane proteins are inserted into the membrane and the process of folding and assembly into their final quaternary structure occurs.

1.2. Co-translational insertion of integral membrane proteins.

1.2.1. Targeting of proteins for translocation.

Proteins destined for translocation either into or across the ER contain an N-terminal "signal sequence", which consists of a hydrophobic stretch of residues, flanked on the N-terminus by polar/charged residues (see section 1.3.). The signal sequence causes the nascent polypeptide as it emerges from the ribosome, to be directed to the translocation machinery situated in the ER (for refs see reviews, High and Stirling, 1993; Rapaport, 1992). The targeting process is mediated by the signal recognition particle (SRP) which binds to the signal sequence once it has emerged from the ribosome. While the nascent polypeptide-ribosome complex is targeted to the ER by the bound SRP, the translation of the polypeptide pauses (Walter and Blobel, 1981). The arrest in elongation is lifted once the ribosome-SRP complex has bound to the ER.

The interaction between the SRP and the signal sequence only occurs once the signal sequence has fully emerged from the ribosome. Before this, the emerging signal sequence is in contact with another complex, the nascent polypeptide-associated complex, (NAC) (Wiedmann et. al., 1994). The NAC consists of a heterodimer, NAC α (33k) and NAC β (21k), that is associated with the ribosome but can be extracted by high salt buffers. The NAC binds to all nascent polypeptides after at least 35 amino acids have been translated. Only in the case of signal peptides is the NAC later replaced by the SRP. The NAC appears to prevent inappropriate interactions between the SRP and emerging polypeptides such that only polypeptides with a signal sequence are bound by the SRP and so transported to the ER for translocation. In the absence of the NAC, the SRP is capable of targeting cytoplasmic proteins for translocation, albeit at reduced efficiency compared to polypeptides containing a signal sequence (Wiedmann et. al., 1994). For cytoplasmic proteins, the NAC may act as an adapter between ribosomes and the cellular folding and transport machineries, thereby protecting the nascent polypeptide from inappropriate interactions.

The SRP consists of 6 subunits complexed with a 7S RNA, each with a known specific role (Siegel and Walter, 1988). The SRP54 subunit binds with its 22kDa C-terminus domain to the signal sequence. The amino-terminal 33kDa domain of SRP54 contains a GTP binding site which is thought to be responsible for the GTP-dependency of protein targeting. The hydrolysis of GTP is thought to control the entry of the nascent polypeptide into the translocation channel (Gilmore, 1993). The SRP is recognised by a receptor (SR) present in the membrane of the ER, which brings the SRP-ribosome complex into contact with the translocation site (figure 1).

Figure 1. Model of the co-translational insertion of integral membrane proteins.

The cotranslational membrane insertion of integral membrane proteins begins when the nascent polypeptide first emerges from the ribosome and is bound by nascent polypeptide-associated complex (NAC), to prevent inappropriate interactions. The first region of the polypeptide to emerge is the signal sequence, which once fully exposed is bound by the signal recognition particle (SRP), in place of the NAC. The binding of SRP causes a pause in the translation of the polypeptide, and during this period the ribosome-nascent polypeptide-SRP complex is directed to the rough endoplasmic recticulum (RER) membrane and the SRP receptor. The SRP receptor brings the complex containing the nascent polypeptide into contact with the translocation machinery. The translocation machinery consists of the Sec61p complex and TRAM, with the Sec61p complex providing the major component of the translocation channel. Once the ribosome-nascent polypeptide binds to the translocation machinery the SRP and SRP receptor dissociate from the complex. The translation of the nascent polypeptide then resumes, with the polypeptide entering the translocation channel as a helical hairpin. Processing of the polypeptide is carried out by the signal peptidase, if a cleavable signal sequence is present, and the oligosachharyl complex. Regions of the polypeptide that become membrane incorporated move laterally in some unknown manner and so enter the lipid bilayer.

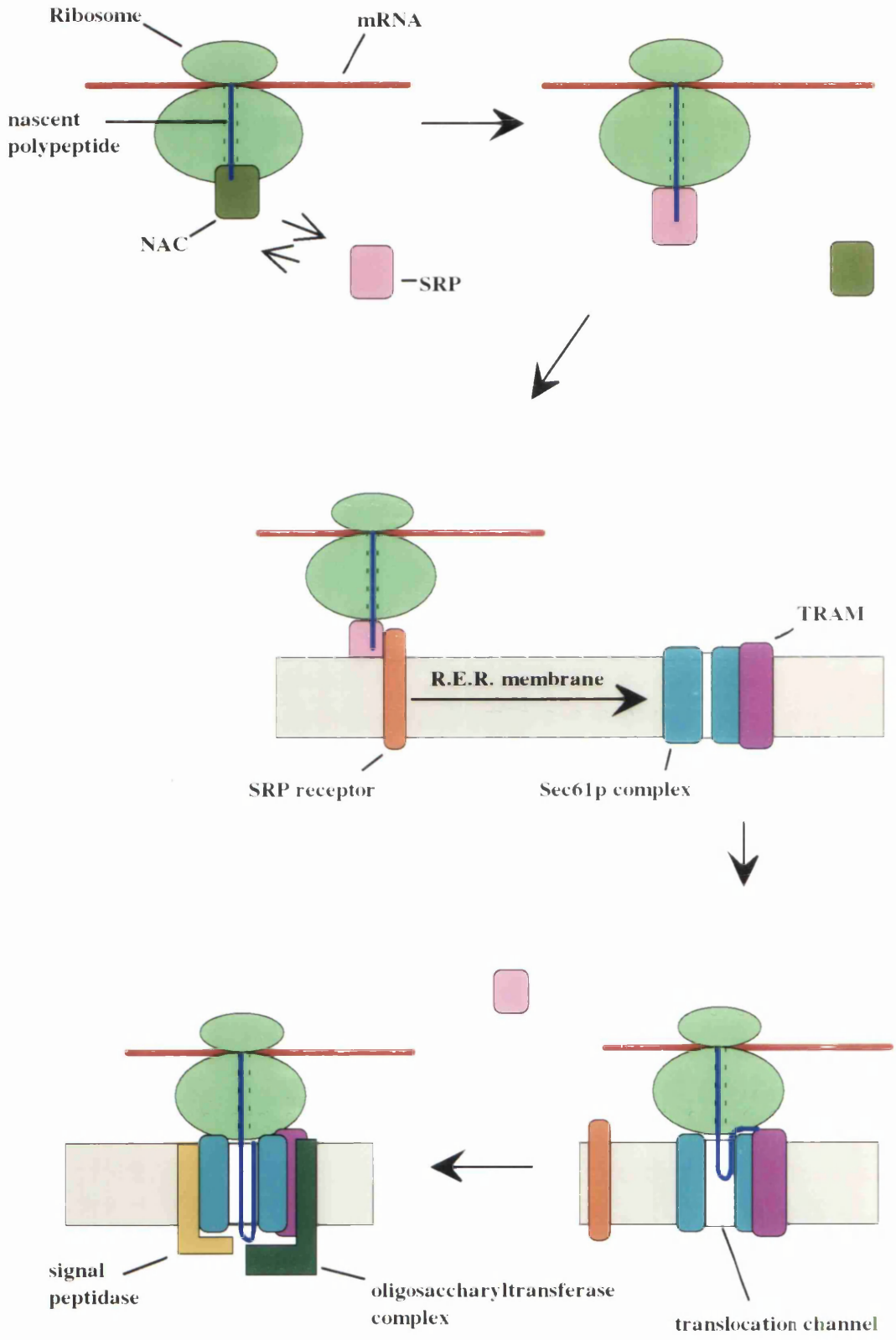
Ribosome
mRNA
nascent
polypeptide
NAC
SRP
TRAM
R.E.R. membrane
SRP receptor
Sec61p complex
signal
peptidase
oligosaccharyltransferase
complex
translocation channel

1.2.2. The translocation machinery.

The site of translocation is now generally accepted to be composed of proteinaceous subunits (Gilmore, 1993). Some of the earlier models on the translocation process proposed that a polypeptide could pass directly through the lipid bilayer due to a local distortion caused by the signal sequence. Recent results, however, indicate that there is a distinct protein-conducting channel present in the ER (Simon and Blobel, 1991). Also, studies using fluorescent probes incorporated into the signal sequence show that the probes are at all times in an aqueous environment and do not encounter a hydrophobic environment during translocation (Crowley et. al., 1993;1994). The signal from the fluorescent probes is quenched in the presence of iodide ions. Quenching of the fluorescent probes is only possible when the iodide ions gained access to the conducting channel from the lumen of the ER. The iodide ions could not gain access to the conducting channel from the cytoplasmic end, indicating that the ribosome forms a tight seal with the translocating machinery that prevents access to iodide ions. The conducting channel is gated at the lumenal surface, since the iodide ions could only quench the fluorescent probes after 70 amino acids had been translated (Crowley et. al., 1994). Reconstitution experiments have also shown that the translocation of proteins is dependent on the presence of a protein complex, which presumably constitutes the conducting channel (Gorlich and Rapoport, 1993). When the translocation machinery was reconstituted into pure phospholipid, the minimum requirement for active translocation was the SRP receptor and the Sec61p complex. Either of these two components alone was not capable of translocation.

The mammalian Sec61p complex from the reconstitution experiments consists of three components α,β, and γ, with Sec61α probably contributing the most to the translocating channel (Gorlich and Rapoport, 1993). Sec61α was initially found in *Saccharomyces cerevisiae* via genetic screening for translocation defects and is encoded by an essential gene (Deshaies and Schekman, 1987; Rothblat et. al.,

1989; Stirling et. al., 1992). Homologs of Sec61α are now known to be present in mammals and have been shown to be adjacent to polypeptide chains passing across the membrane of the mammalian or yeast ER (Gorlich et. al., 1992a; Musch et. al., 1992; Sanders et. al., 1992). In mammals, it is tightly associated with membrane-bound ribosomes (Gorlich et. al., 1992a), suggesting that the nascent chain is transferred directly from the ribosome into a protein-conducting channel that includes Sec61p and that it is Sec61p that acts as the ribosome receptor (figure 1). The efficiency of translocation in the reconstituted system differed between different secretory proteins; preprolactin could be translocated by SRP receptor and Sec61p complex alone, whereas the translocation of prepro α-factor also required the presence of the protein TRAM (Gorlich and Rapoport, 1993).

TRAM (for translocating chain-associating membrane protein) was first implicated in the translocation process after being chemically cross-linked to a secretory protein early on during translocation (Gorlich et. al., 1992b). TRAM is a glycosylated 36kDa protein that is predicted to have eight transmembrane segments. When TRAM was added back to a reconstituted translocation system, it was found to stimulate the translocation of preprolactin and was essential for the translocation of prepro-α factor and pre-β-lactamase. The cross-linking of TRAM indicates that it is in direct contact with translocating nascent chains after their release from SRP and so must be involved early in translocation (Gorlich et. al., 1992b).

1.2.3. The length of the conducting channel.

The protein environment of translocation intermediates for preprolactin was studied in greater detail by refining the technique of cross-linking (Mothes et. al., 1994). Single photoreactive lysine analogues were introduced at a series of sites over the whole length of a nascent polypeptide which was stalled in translation due to the lack of a stop codon. The cross-linking pattern of the lysine analogues was

found to depend on the length of the stalled polypeptide. Long translocation intermediates that had the signal peptide cleaved off were found to cross-link exclusively to Sec61α over a region of 40 amino acids that was predicted to span the translocation channel. The N-terminal amino acids, that had exited from the translocation channel, did not cross-link to Sec61α, but instead were cross-linked to a variety of unidentified products. Short translocation intermediates which had their signal sequences uncleaved were found to have 80 amino acids cross-linked to Sec61α. In addition the two most N-terminal lysines were found to cross-link with TRAM. In all cases, 30 amino acids do not cross-link, presumably due to burial in the ribosome. Immediately after this buried region, the translocated polypeptide cross-links to Sec61α, implying direct transfer between ribosome and translocation complex. The long intermediates only have half the number of residues in contact with Sec61α compared to the short intermediates, presumably due to their transmembrane orientation, with the N-terminus in the lumen, while the short intermediates are still in a hairpin in the conducting channel (where the N-terminus is in contact with TRAM). It would appear that Sec61α is the main component of the translocation channel and at least partially surrounds the translocating polypeptide, which agrees with earlier results from the reconstitution experiments (Mothes et. al., 1994).

1.2.4. Other components of the translocation process.

In the yeast *S. cerevisiae*, genetic screening methods have been used to identify a number of genes, that are necessary for the translocation of preproteins into the ER. The genes identified in this manner were SEC61, SEC62 and SEC63, which have now been cloned. These genes encode integral membrane proteins which, along with Sec71p, Sec72p (Deshaies et. al., 1991; Feldheim and Schekman, 1994) and BiP (Brodsky and Schekman, 1993), exist in a multiprotein complex involved in the process of translocation.

BiP, also called Kar2p, had already been implicated in the process of translocation in yeast when mutants in this gene caused an accumulation of untranslocated secretory preproteins (Vogel et. al., 1990). BiP has been cross-linked to the α-factor precursor during the translocation process, and is able to influence the interaction of Sec61p with the translocating α-factor (Sanders et. al., 1992). In the mammalian system, BiP does not appear to be involved in actual translocation, but it does seem to enhance the process and provide a vectorial element to translocation. The lumenal contents of mammalian microsomes (vesicles derived from the ER), which are mainly composed of BiP and GRP94 (also called proline disulphide isomerase, PDI), provide bias to the transport of preprolactin (Nicchitta and Blobel, 1993). In the absence of the lumenal contents, preprolactin was seen to experience signal cleavage as normal, but then to undergo retrograde movement back into the cytoplasm (Nicchitta and Blobel, 1993). A similar observation was made for a truncated version of the bactericidal/permeability-increasing protein (BPI); when truncated to 221 amino acids, BPI undergoes the processing events indicative of translocation, but it was found in the cytoplasm (Ooi and Weiss, 1992). Normal translocation was restored in the presence of a stop codon, or when an extra 32 amino acids were present on the C-terminus. The presence of the stop codon may trigger an event that prevents retrograde movement of the translocating polypeptide, while the addition of the 32 amino acids coincides with a discrete folded domain within BPI. It would appear that lumenal alterations to translocating polypeptides provides a vectorial nature to the passage of polypeptides through the translocation machinery, and that the conducting channel itself is passive (Ooi and Weiss, 1992).

Other proteins that are involved in translocation include the signal peptidase, which cleaves off the signal peptide to produce the mature polypeptide (Jackson and Blobel, 1977), and the oligosaccharyltransferase complex, which causes the addition of high mannose oligosaccharides (Hubbard and Ivatt, 1983). Both of

these polypeptide modifying enzymes are, however, non-essential for the process of translocation (Gorlich and Rapoport, 1993).

1.3. Signal sequences and membrane topology.

The signal sequence that directs a polypeptide to the membrane is contained within the amino acid sequence of the polypeptide (Blobel, 1980), and consists of a hydrophobic domain flanked by polar/charged residues. There is no homology at the amino acid level between signal sequences, though the function of these regions has been conserved over a wide evolutionary distance (Walter and Lingappa, 1986).

Integral membrane proteins that contain a single transmembrane domain are classified according to their final orientation in the membrane, and by whether an N-terminal cleavable signal sequence was used to direct the protein to the membrane (High and Dobberstein, 1992). Type I proteins have a N-terminal cleavable signal sequence and are subsequently anchored in the membrane by a more C-terminal "membrane anchor sequence" (figure 2). The N-terminus of type I proteins is exposed on the extracellular side of the membrane. Type II proteins have the opposite orientation in the membrane from that of type I and do not have a cleavable signal sequence (figure 2). For type II proteins, the signal sequence serves a second function, that of the membrane anchor sequence, with the N-terminus exposed on the cytoplasmic face of the membrane, an example of which is the paramyxovirus HN protein (Hiebert et. al., 1985). The final category is for type III proteins, which have the same orientation as type I proteins but have no cleavable signal sequence (figure 2). Instead, as for type II proteins, the signal sequence also acts as the membrane anchor, an example being the influenza A M_2 protein (Lamb et al., 1985). Orientation studies have shown to date that type I

Figure 2. Classification of integral membrane protein orientation.

Integral membrane proteins have been classified according to their orientation in the lipid bilayer and the presence or absence of a cleavable signal sequence. Type I membrane proteins have their N-terminus located in the lumen of the ER, are directed to the ER by a cleaved signal sequence and are anchored in the membrane by a more C-terminal membrane anchor sequence. For type II membrane proteins the N-terminus is cytoplasmically located, and the signal sequence also acts as a membrane anchor, with no cleavage of the signal sequence. Type III membrane proteins have non-cleavable signal sequence which acts as a membrane anchor, but unlike type II proteins, the N-terminus is located in the ER lumen. Secreted proteins have a cleavable signal sequence but no membrane anchor regions, thus they are translocated through the ER membrane into the lumen.

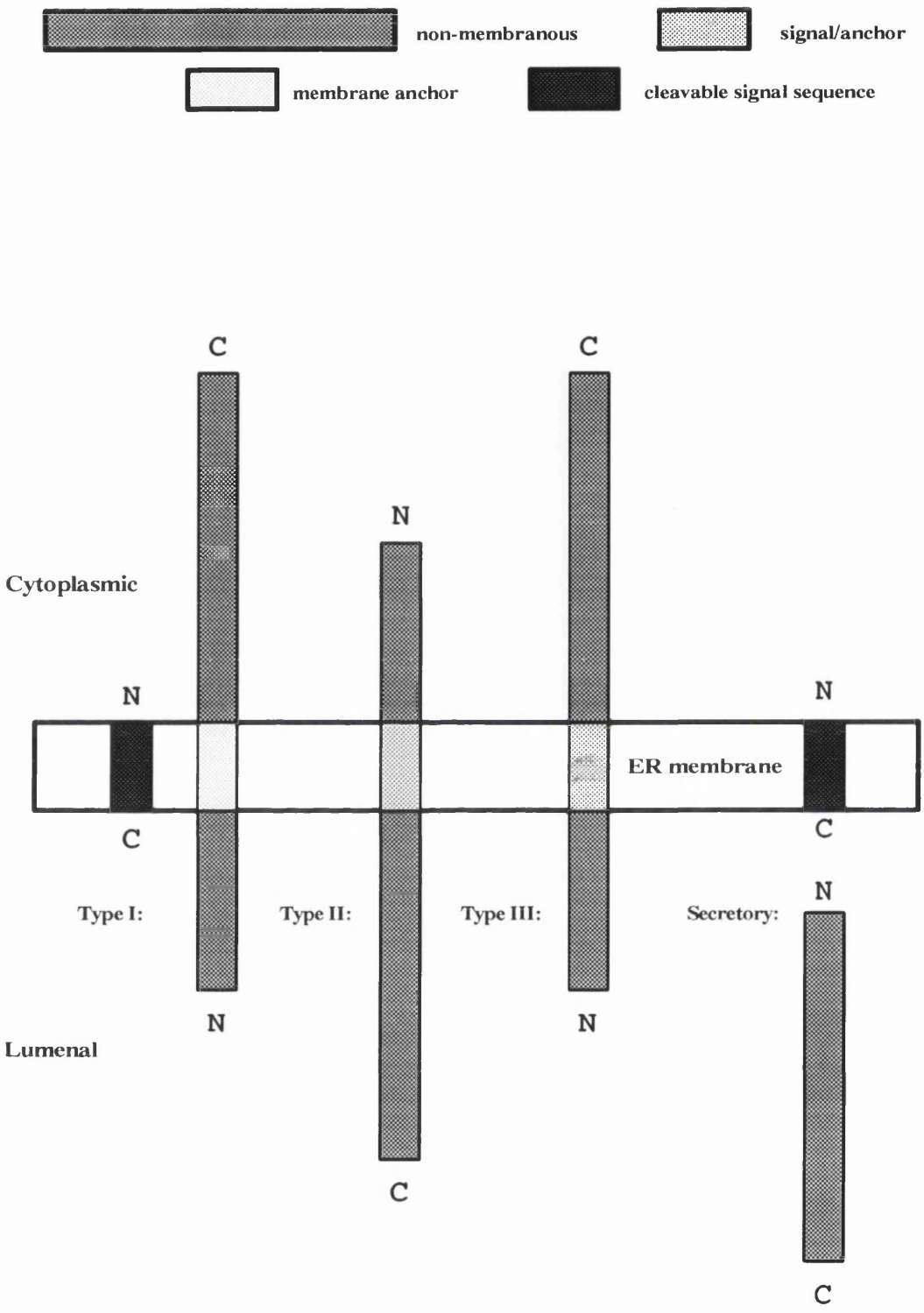
non-membranous
signal/anchor
membrane anchor
cleavable signal sequence
C
C
N
Cytoplasmic
N
N
ER membrane
C
C
Type I:
Type II:
Type III:
Secretory:
N
N
N
Lumenal
C
C

proteins are the most common, type II are less frequent, and type III are the least common (Parks and Lamb, 1993).

The insertion of the signal sequence, whether cleaved or uncleaved, is thought to occur as a loop or a helical hairpin (Shaw et al., 1988). According to the hairpin model of insertion, when the signal sequence is cleaved, the N-terminus is released into the lumen generating a type I protein, whereas if the signal sequence is not cleaved, the signal remains in the membrane and acts as an anchor (signal/anchor region or S/A region), generating the type II topology. The type III proteins do not fit neatly into the loop model, since the N-terminus would initially be on the cytoplasmic side of the membrane and must then somehow transfer across the ER. membrane.

The signals that determine which membrane type a protein belongs to can be interchanged after only a few alterations to key residues in the signal sequence. The cleaved signal sequence can act as a membrane anchor when the signal peptidase cleavage site has been altered to prevent cleavage, and results in a type II topology instead of type I (Shaw et al., 1988). In other experiments, type II proteins have been converted to type III and vice versa by mutation of the charged residues that flank the membrane anchor sequence (Parks and Lamb, 1993). Positively charged residues that flank the N-terminal end of the membrane anchor appear to be particularly influential in determining the orientation of type II proteins. The paramyxovirus HN protein has three positive residues on the N-terminal flank of the S/A region, each of which make a contribution to the orientation of HN, in particular the arginine residue that directly flanks the S/A region. Mutation of these three positive residues to either glutamine or glutamic acid caused the orientation of HN to become at least partially type III i.e. with the N-terminus exposed lumenally rather than cytoplasmically (Parks and Lamb, 1993). Changes in the charge of the region that flanks the C-terminal side of the

membrane anchor had little effect on the orientation of HN (Parks and Lamb, 1991).

Positive charges were implicated as being possible determinants of orientation when a large number of signal sequences were compared and a net positive charge was observed (von Heijne, 1984). A positive charge has been observed to flank the S/A region of type II proteins in a majority of cases. In contrast with type I and type II proteins, in most cases type III polypeptides have a net negative charge on the N-terminal flank of the S/A region. These observations led to the proposal that it was the net charge difference across the membrane that determined orientation (Hartmann et al., 1989). However, subsequent experiments did not support this hypothesis, since mutants of the asialoglycoprotein receptor H1 (a type II protein) that altered the charges flanking the S/A region did not influence the orientation in the manner predicted by the charge difference rule (Beltzer et al., 1991). These studies, as well as work on the role of the flanking charges of the paramyxovirus HN S/A region (Parks and Lamb, 1991), suggest instead that the predominant signal that determines the orientation of a type II S/A region is the positive charge present in the N-terminal flanking region. The length of the N-terminal region has also been found to have a moderating effect on the orientation of insertion; when the N-terminal region is shortened, the influence of the flanking positive charges increases (Parks and Lamb, 1993).

The signals that determine the orientation of type III proteins have proved more difficult to elucidate. Chimeric constructs that contain the N-terminal ectodomain of a type III protein (either M_2 or influenza B NB protein) were fused to the S/A region from a type II protein (HN) and expressed in cells, with their orientation subsequently determined (Parks and Lamb, 1993). When the M_2 N-terminal domain was fused, the predominant orientation was that of a type III protein, whereas when the NB N-terminal domain was fused, the predominant orientation

was type II. This suggests that there is some other factor that influences insertion into a type III orientation, and that this other factor is probably located in the S/A region (Parks and Lamb, 1993). Another observation that supports this is the length of the S/A region of the type III protein cytochrome P-450 which has been shown to influence the orientation of insertion, with longer hydrophobic segments favouring insertion into the type III orientation (Sakaguchi et al., 1992). The topology of polytopic integral membrane proteins is thought to be determined by the signals that flank the transmembrane segments and in effect they are made up from a series of signal sequences and S/A regions connected together (Lipp et al., 1989).

1.4. Assembly of oligomeric membrane proteins.

The assembly of oligomeric membrane proteins occurs in the ER after co-translational insertion into the membrane. Once assembled, these oligomers are transported to their final destination. Misfolded or misassembled complexes are degraded before they leave the ER. Hurtleyand Helenius, 1989). Little is known about the molecular events involved in subunit folding and oligomerisation.

One of the better studied oligomeric channel complexes with regard to assembly is the acetylcholine receptor (AChR). It is composed of four homologous subunits (α,β,γ, and δ) that assemble to form a pentamer with a stoichiometry of $\alpha_2\beta\gamma\delta$. There is a central aqueous channel, around which the subunits are arranged. Each subunit is cotranslationally inserted into the ER. membrane separately, and has a processed signal sequence (Popot and Changeux, 1984; Claudio et al., 1989; Unwin, 1989; Stroud et al., 1990).

The information that determines the process of assembly of the AChR appears to reside in the extracellular N-terminal domains of the α, δ, and γ subunits (Verrall

and Hall, 1992). This is also the case for other oligomeric assemblies, such as the influenza HA trimer in which the ectodomain determines assembly (Hurtleyand Helenius, 1989). The assembly of AChR proceeds at first with the rapid assembly of an intermediate $\alpha\beta\gamma$ trimer, which is followed more slowly by the addition of the δ subunit, and then the second α subunit (Green and Claudio, 1993). Addition of the δ and second α subunit requires the creation of appropriate recognition sites on the $\alpha\beta\gamma$ trimer by the correct folding of the trimer. The rapid formation of the trimer may be a consequence of the need to protect critical domains, such as the lining of the water-filled pore, from inappropriate environments that would cause misfolding or unproductive aggregation (Green and Claudio, 1993).

1.5. Ductin as a model protein for membrane insertion and assembly.

The processes that occur within the lipid bilayer during the membrane insertion of integral membrane proteins and their subsequent assembly into functional complexes, have remained relatively mysterious due to the lack of structural information for all but a few integral membrane proteins. Thus relatively few reliable model proteins are available with which to study membrane insertion and assembly. One possible model protein is ductin since it is known to consist of four α-helical membrane regions embedded in the lipid bilayer (Holzenburg et al., 1993), the arrangement of which is in the process of being confirmed (Jones et al., 1995). In addition, the ductin polypeptides are known to assemble into hexameric structures in the gap junction Finbow and Pitts, 1993). Thus, it would appear that ductin fulfils a number of criteria, that of a known structure and the ability to assemble, which make ductin a suitable model protein on which to study these processes.

1.6. Ductin complexes.

1.6.1 Introduction.

Ductin is the most highly conserved integral membrane protein known to date, and has been implicated as the structural component of three membrane complexes (Finbow et al., 1995). Ductin was isolated as part of the gap junction where it is thought to constitute a connexon, the basic channel structure of these cell surface domains (Finbow and Pitts, 1993). Gap junctions provide pathways of cell-cell communication in the tissue of metazoan animals. Ductin was also identified as belonging to the proton-translocating sector of the eukaryotic vacuolar H^+-ATPase (Arai et al., 1988; Mandel et al., 1988) and the acetylcholine-releasing complex, the mediatophore, in the pre-synaptic membrane (Israel and Dunant, 1993). The common thread between these three diverse complexes is their function in providing a means by which ions or molecules can cross the lipid bilayer. Such diversity implies that there is a high degree of functional flexibility within the structure of ductin to allow it to operate in all three complexes. This might be part of the reason, at least in metazoan animals, for the highly conserved nature of ductin, since its functional diversity would have put a constraint on changes in the structure that would not have altered function.

1.6.2. Gap junctions.

1.6.2.1. Introduction.

Gap junctions provide pathways for intercellular communication in the tissues of metazoan animals. They form at points of contact between adjacent cells and provide cytoplasmic continuity through coupled cell populations via sieve-like cell-cell channels. The channels are permeable to small ions and molecules, resulting in extensive intercytoplasmic homeostasis and co-ordination, but they are not permeable to macromolecules, allowing cells to maintain their differentiated state.

With the exception of a few cell types which become uncoupled during terminal differentiation, nearly all cells *in vivo* form gap junctions. The degree of coupling between cells varies greatly from tissue to tissue and complex patterns of compartmentation can form. Cells which follow different differentiation pathways are usually found in different compartments, the boundaries between which may or may not be associated with observable morphological features (Kam et al., 1986; Pitts et al., 1986; Pitts et al., 1988).

1.6.2.2. Structure of the gap junction.

The accepted model of the connexon has been produced by a variety of imaging techniques, such as X-ray diffraction (Makowski et al., 1977, 1984; Tibbitts et al., 1990), negative stain (Caspar et al., 1977; Sosinsky et al., 1990) and atomic force microscopy (Hoh et al., 1991). They all reveal the same basic structure, showing the connexon to be a cylinder of protein 70-75Å in length and 60-65Å in diameter, with an axial water-filled channel 15-20Å in diameter. Each connexon joins end-to-end with a connexon in the apposing membrane of another cell to provide a direct aqueous pathway between the cytoplasms of the coupled cells. Each cylinder is formed from six similar-sized subunits arranged symmetrically around the central channel.

Data based on X-ray diffraction studies suggest that about 60% of the component protein is α-helical (Tibbittset al 1990). The diffraction pattern can best be explained by arranging the protein in the membrane as a hexamer of four α-helical bundles (Tibbitts et al, 1990). The dimension data obtained was used to calculate the approximate subunit mass, which was found to be 18kDa.

These original studies were performed on mouse liver gap junctions, but have since been extended to the heart (Yeager and Gilula, 1992) and the hepatopancreas of

the lobster, *Homarus americanus* (Sikerwar et el, 1991), and in both cases the basic connexon structure and dimensions are the same as for the mouse liver. It seems likely, therefore, that connexon structure in the gap junctions isolated from different tissues and phyla is highly conserved.

The constituent protein of the connexon has been the subject of controversy in the past, there being two candidates, the connexin family of proteins and ductin. Recent work to resolve the issue appears to favour ductin as the constituent protein of the isolated connexon (Finbow and Pitts, 1993). The main evidence in support of ductin comes from structural work on isolated gap junctions, where the distinctive plaques of gap junctional arrays have been isolated under a number of different conditions and only ductin can be consistently identified as the protein responsible (Finbow and Meagher, 1992). In addition, gap junction fractions containing only ductin have been isolated from invertebrates; connexins, on the other hand, appear to be confined to the vertebrates (Finbow and Pitts, 1993). If ductin is the constituent protein of the gap junctional channel, then there is an open question as to the function of the connexin family of proteins. It seems likely that the connexins are involved in the process of gap junctional intercellular communication at some level, since there is a wealth of data indicating that connexins have an influence on gap junction activity (Dermietzel et al., 1990). It is possible that connexins could play a role in the formation of the gap junctional plaque or, alternatively, they may provide some of the observed specificity in gap junction intercellular communication (GJIC).

1.6.2.3. Gap junction physiology.

Gap junctional channels are freely permeable to ions and small cytoplasmic molecules, including metabolites and second messengers, but are impermeable to large molecules such as proteins and nucleic acids (Pitts and Simms 1977; Lawrence et al., 1978; Saez et al., 1989). The exclusion limit of the channel has

been defined by dye injection studies using fluorescent probes and metabolites of different molecular size and charge. The channels exhibit little charge selectivity and the permeability can be defined in terms of molecular weight; the exclusion limit is approximately 900 Da for mammalian cells (Flagg-Newton et al., 1979; Finbow and Pitts, 1981) and 1500 Da for arthropod cells (Simpson et al., 1977).

The structural work of Unwin and Ennis (1984) indicated that the gap junction connexon could exist in either an open or a closed state. Functional changes in the state of gap junctions have also been observed, and occur on a number of different time-scales, such as within milliseconds (Dehaan, 1988), and is reversible. The ability to rapidly and reversibly control the state of gap junctions is probably necessary to allow a rapid response to changes in the environment of the cell and is probably required in order to isolate damaged cells from their neighbours and prevent the leakage of ions and metabolites from healthy cells into them.

Changes in the state of gap junctions can occur over long timescales under the influence of a number of different agents e.g. cAMP (Hax et al., 1974), retinoids (Pitts et al., 1986), and oncogenes (Azarnia et al., 1988), as well as during the normal course of development (Lo and Gilula, 1979), though how these agents act to alter GJIC is largely unknown. Since the formation of gap junctions and the control of junctional communication involves multiple gene products (MacDonald, 1985), the number of potential target sites for the alteration of gap junctions is numerous. One such potential target is the expression level of cadherins, which have been implicated in the process of gap junction formation (Mege et al., 1988).

1.6.3. The mediatophore.

The mediatophore is a protein complex that was identified and subsequently isolated as the membrane component of the *Torpedo* electric organ responsible for

the cytoplasmic release of acetyl choline (ACh) (review see Israel and Dunant 1993). To try and understand the mechanism by which cytoplasmic ACh is released by Ca^{2+} stimulation, the release machinery was purified from synaptosomal membranes and reconstituted into artificial membranes (Israel et al., 1984). The reconstituted proteoliposomes were able to release ACh after stimulation by Ca^{2+}. The protein responsible for this activity is 15kDa in size, and is present in a 200kDa complex named the mediatophore (Israel et al., 1986). When the 15kDa protein was sequenced, it was found to be identical to ductin (Birman et al., 1990). Negative stained electron microscope images of the mediatophore indicated that it is an oligomer of 8nm diameter and with a central hole (Birman et al., 1986).

As a model system to study the molecular aspects of neurotransmitter release from cholinergic neurons, mRNA extracted from the Torpedo electric lobe was injected into *Xenopus* oocytes (Cavalli et al., 1991). ACh release by primed oocytes was dependent on Ca^{2+} concentration, and the pharmacology of release closely matched the characteristics seen in the native synapse. The mediatophore was shown to be expressed, and its activity could be specifically blocked by the presence of antisense probes directed against the *Torpedo* ductin mRNA sequence, with a concomitant loss of ACh release (Cavalli et al., 1993). Indeed, ACh release was sustained by the injection of ductin mRNA alone.

The presence of large intramembrane particles (IMP), observed by freeze fracture, during nerve pulses at the nerve-electroplaque junction has now been associated with the mediatophore (Brochier et al., 1992). The mediatophore is as yet a controversial mechanism for the release of ACh but the reconstitution of the mediatophore indicates that a ductin complex is capable of allowing the passage of large molecules by bulk flow, a property not dissimilar to that of the gap junction.

1.6.4. The vacuolar-type H^+-ATPase.

1.6.4.1. Introduction.

Vacuolar-type H^+-ATPases (V-ATPases) are a distinct class of proton-translocating enzymes responsible for the acidification of intracellular compartments in eukaryotic cells e.g. plant and yeast vacuoles, lysosomes, endosomes, clathrin-coated vesicles, chromaffin granules, synaptosomes, and amoebae contractile vacuoles (for a review see Forgac, 1989). V-ATPases are also associated with the membranes of organelles that are not measurably acidic, such as the Golgi complex, where it is speculated that the V-ATPases generate an electrical rather than a chemical gradient. Finally, V-ATPases are found on the plasma membrane of specialised cell types (renal epithelia, macrophages, neutrophils, osteoclasts, and insect midgut) where they pump protons out of the cell. From a pathophysiologic standpoint, V-ATPases are essential to nutrient uptake and processing in the food vacuole of *Falciparum* (Krogstad and Schlesinger, 1987). There is also evidence to suggest that V-ATPases may confer resistance to chemotherapeutic agents in cultured tumour cells (Marquardt and Center, 1991).

The V-ATPase is thought to have evolved from the F_1F_0 type, H^+-transporting ATPase (F_1F_0-ATPase) of eubacteria mitochondria and chloroplasts (Nelson, 1992). The F_1F_0-ATPase catalyses the synthesis of ATP during oxidative phosphorylation. This enzyme is composed of two functionally and structurally distinct sectors termed F_1 and F_0 (figure 3). The F_1 sector lies at the surface of the membrane and catalyses ATP hydrolysis, while the F_0 sector traverses the membrane and promotes H^+ transport on removal of F_1. When coupled, the two sectors function as a reversible, H^+ translocating ATPase (Senior, 1988) although the isolated F_1 has ATPase activity. In its simplest form, the F_0 sector is composed of three types of subunits, subunit *a* (31kDa), subunit *b* (17kDa) and

Figure 3. Model subunit structure of the F_1F_0 ATPase.

The F_1F_0ATPase consists of two multisubunit sectors, the cytoplasmic F_1 sector and the membrane bound F_0 sector. The F_1 sector consists of five different subunits, α,β,δ,γ, and ε, while the F_0 sector consists of three different subunits, *a*, *b* and *c*. The F_1 sector catalyses the synthesis of ATP, and the F_0 sector mediates the translocation of protons.

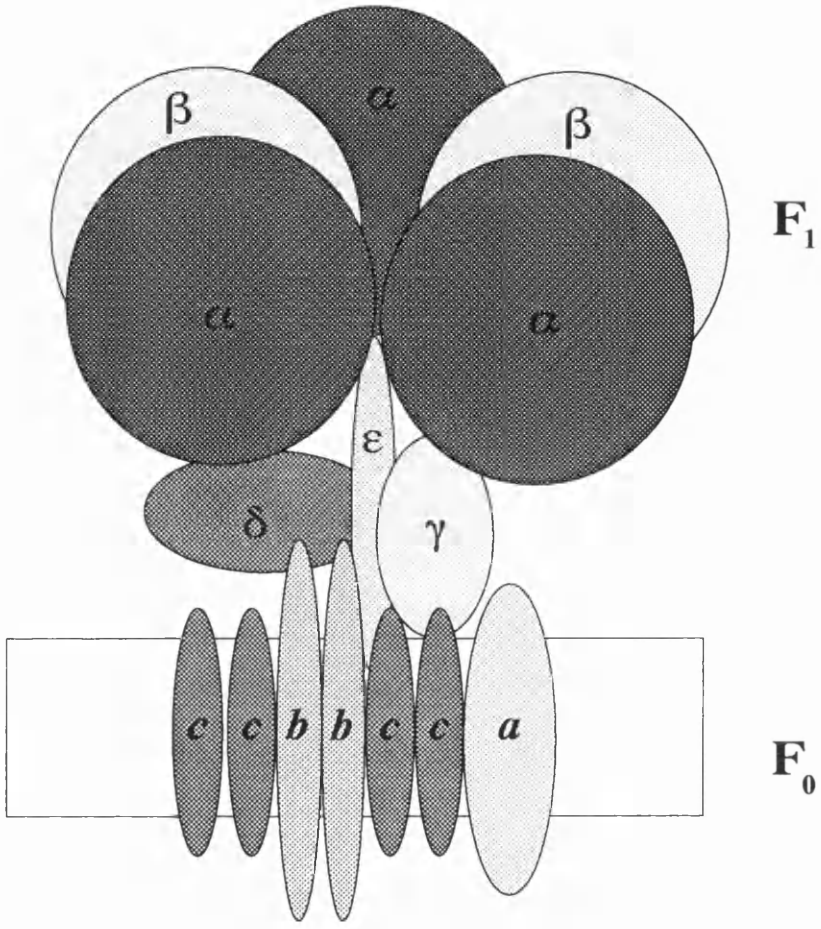
β
α
β
α
α
ε
δ
γ
c
c
b
b
c
c
a
F1
F0

subunit *c* (8kDa) and in *Escherichia coli*, these subunits are found in a ratio of 1:2:10±1 (Foster and Fillingame, 1982). Subunits *a* and *c* are both thought to play a key role in F_0-mediated H^+ translocation (Senior, 1988; Fillingame, 1992).

1.6.4.2. Subunit composition of the V-ATPase complex.

The V-ATPase complex consists of two sectors, a peripheral sector, V_1, that is the site of ATP hydrolysis, and a membrane embedded sector, V_0, which mediates the translocation of protons across the lipid bilayer (Arai et al., 1988). The overall structure of the V-ATPase is similar to that of the F_1F_0-ATPase. Both V_1 and V_0 are assemblies of a number of different subunits, which are now in the process of being defined. The V-ATPase complex has been isolated from a number of sources, including *Saccharomyces cerevisiae* vacuoles and bovine brain clathrin-coated vesicles (Kane et al., 1989; Xie and Stone, 1986).

On the basis of co-purification and immunoprecipitations studies, the yeast V-ATPase complex appears to be composed of at least nine subunits of molecular weight 100-, 69-, 60-, 54-, 42-, 32-,36-, 27-, and 17-kDa (Kane et al., 1989; Bauerle et al., 1993). Six of the subunits are part of the peripherally bound V_1 sector (69-, 60-, 54-, 42-, 32-, and 27-kDa), and the remaining three subunits (100-, 36- and 17-kDa) compose the hydrophobic V_0 sector (figure 4). In all species examined, the multimeric enzyme has at least three subunits in common, the equivalent of the 69-, 60-, and 17-kDa polypeptides. The structural genes encoding these three subunits have been highly conserved among the various plant, animal, and fungal species so far examined, and even exhibit limited homology with the corresponding subunits in the F_1F_0 -ATPase. The V-ATPase 69-kDa ATP-binding catalytic subunit and the 60-kDa ATP-binding regulatory subunit are peripherally associated with the cytoplasmic face of the vacuolar membrane, whereas the 17-kDa proteolipid is an integral membrane subunit thought to form the proton translocating pore (Kane, 1989; Forgac, 1989; Umemoto, 1990; Noumi,

Figure 4. Structural model for the yeast V-ATPase.

A) a model illustrating the arrangement of V_1 and V_0 subunits within the V-ATPase complex. B) subunit arrangement of V_1 and V_0 sectors after separation of the two sectors. The V_0 sector is not capable of translocating protons after separation from the V_1 sector, but the V_1 sector is still capable of ATP hydrolysis.

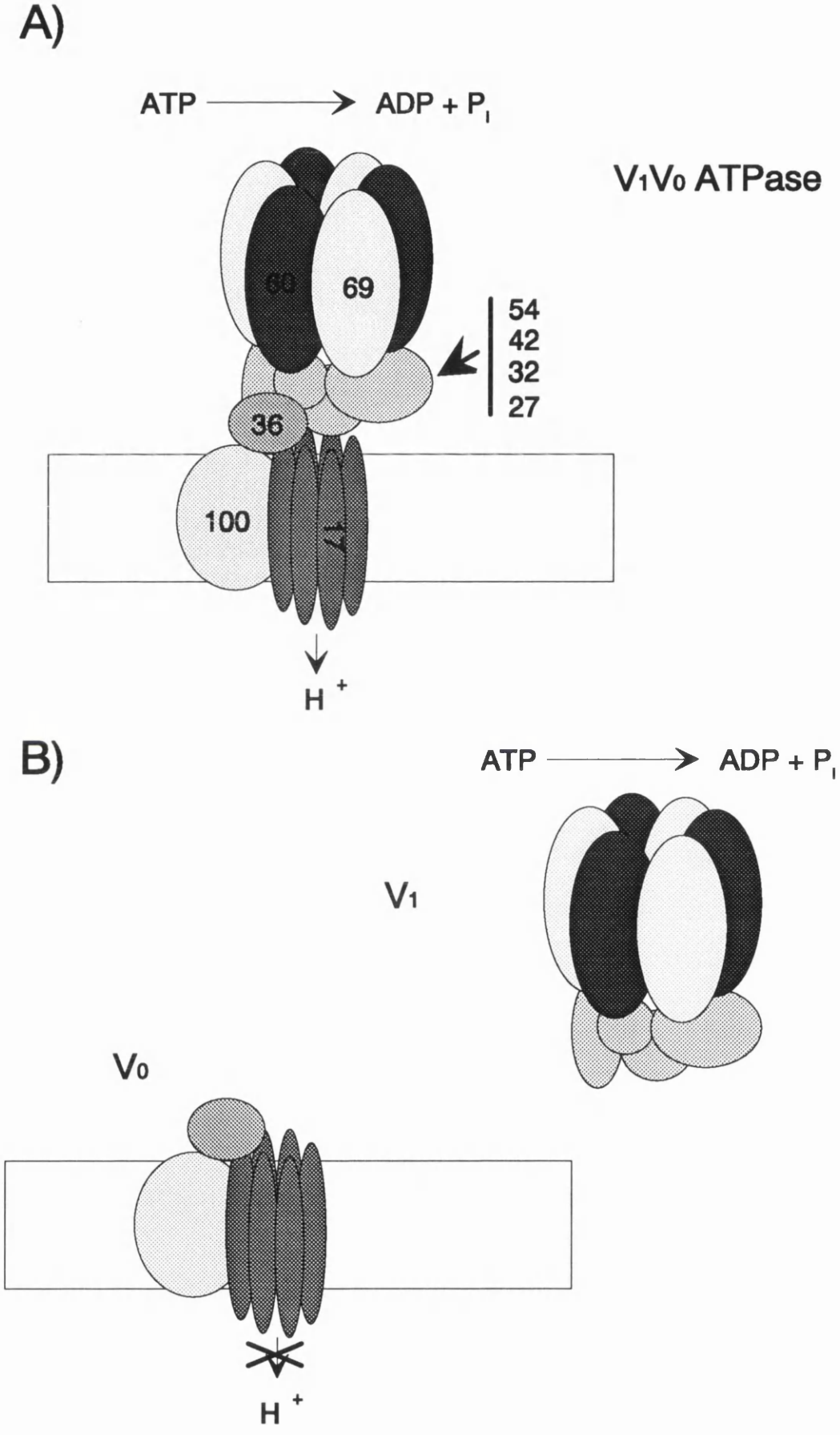
A)
ATP
ADP + P
V1V0 ATPase
60
69
54
42
32
27
36
100
17
H +
B)
ATP
ADP + P
V1
V0
H +

1991). In fact, the 17kDa was found to be the same as ductin, once the amino acid sequences for both polypeptides became available and could be compared (Finbow et al., 1992). The 69-, 60- and 17-kDa subunits are thought to be present in the ratio 3:3:6, with all the other subunits present as a single copy (Arai et al., 1988).

The yeast system has allowed the previously identified subunit components of the V-ATPase complex to be cloned and sequenced. The structural genes encoding the 100-kDa polypeptide (VPH1; Manolsen et al., 1992), 69-kDa polypeptide (VMA1; Hirata et al., 1990), 60-kDa polypeptide (VMA2; Anraku et al., 1989; Nelson et al., 1989; Yamashiro et al., 1990), 42-kDa polypeptide (VMA5; Beltran et al., 1992; Ho et al., 1993), 36-kDa polypeptide (VMA6; Bauerle et al., 1993), 27-kDa polypeptide (VMA4; Foury, 1990), and the 17-kDa proteolipid (VMA3; Nelson and Nelson, 1989; Umemoto et al., 1990) have now been isolated. In total, 14 *S. cerevisiae* genes have been identified as essential for V-ATPase activity (Manolson et al., 1994), implying that a number of non-structural genes are also required for V-ATPase activity. In this category is the VMA11 gene product, which shows a high degree of homology to the VMA3 gene, but which could not be isolated as part of the final active V-ATPase complex (Umemoto et al., 1991). Likewise, the VMA12 gene product did not co-isolate as part of the V-ATPase complex, but was essential for activity; the absence of Vma12p destabilised the V_0 sector, and as a consequence the whole complex was affected (Hirata et al., 1993). The VMA13 gene product, a 54-kDa polypeptide, is also essential for V-ATPase activity (Ho et al., 1993), but unlike the previous two gene products it was identified as part of the active V-ATPase complex. The presence of this polypeptide in the complex was probably missed in earlier studies since it co-migrates with degradation products of the other subunits (Ho et al., 1993).

Mutant alleles have been constructed in yeast by replacing the chromosomal copy of each of these genes with the corresponding cloned gene mutagenised *in vitro*.

Mutants lacking any one of these vacuolar membrane ATPase (*vma*) subunits fail to acidify the vacuole and display a characteristic set of phenotypes, including failure to grow in medium buffered to neutral pH and increased sensitivity to Ca^{2+} in the medium (Nelson and Nelson, 1990). Vacuolar membranes isolated from *vma* mutants exhibit no ATPase activity attributable to the V-ATPase, supporting the biochemical assignment of these gene products as subunits of the enzyme or as necessary for activity.

One putative subunit of the yeast V-ATPase that does not fit this pattern is the STV1 (Similar to VPH1) gene, which encodes an integral membrane polypeptide of 102-kDa with 54% identity with the peptide sequence of Vph1p (Manolson et al., 1994). STV1 disruptants have no detectable phenotype, but when the gene is overexpressed, it can partially compensate for the disrupted VPH1 gene. This partial substitution of Vph1p by overexpressed Stv1p is thought to be due to mislocalisation of Stv1p to vacuoles where it functionally replaces Vph1p. At normal expression levels, Stv1p did not co-localise with Vph1p. These observations could be explained if Stv1p, in a similar fashion to Vph1p, targets the assembly of common V-ATPase subunits, but to an organelle other than the vacuole (Manolson et al., 1994).

It seems likely that an individual cell uses a number of subunit isoforms of the V-ATPase complex to provide different organelles with distinct pH environments; multiple forms of the 58-kDa (B) subunit of the bovine clathrin-coated vesicle V-ATPase have been identified in the same cell line (Puopolo et al., 1992). It has also been reported that the V-ATPase isolated from purified bovine kidney brush-border membranes differs from the enzyme isolated from kidney microsome preparations in several ways, including pH optimum, substrate selectivity, and affinity for ATP, all of which may alter the activity of the enzyme in a manner which would affect organelle pH (Wang and Gluck 1990). It has been suggested

that this could be due to isoforms of the B subunit providing the V-ATPase complex with differential properties (Puopolo et al., 1992). Two isoforms of the 116-kDa polypeptide of bovine brain have also been identified, which arise by an alternative splice mechanism. The two isoforms exhibited a tissue-specific distribution and again, may play a role in altering the V-ATPase activity (Peng et al., 1994).

1.6.4.3. Structure of the V-ATPase complex.

Images of the V-ATPase complex from membranes of a number of organelles have now been produced by electron microscopy of negatively stained preparations. A ball and stalk structure was observed for the V-ATPase of *Neurospora crassa* vacuoles, which superficially resembled the F-type ATPase of mitochondrial membranes but appeared to differ from the mitochondrial enzyme in size and in structural details (Bowman et al., 1989). The overall similarity between the V- and F- type ATPases suggests that some of the high resolution structural details now known about the F_1 sector (Abrahams et al., 1993,1994) may apply to the V_1 sector. A more detailed EM. study of the *N. crassa* V-ATPase indicated the presence of a prominent cleft in the peripheral V_1 sector (Dschida and Bowman, 1992). This feature was also seen in detached V_1 sectors, suggesting that the major subunits are held together at the base of the head component in the region attached to the stalk. Other distinct features that were observed include a prominent stalk and additional basal components. The globular head of the enzyme, which contains the ATP binding subunits, appears to be held 6.6nm above the surface of the membrane by a stalk that is approximately 3.1nm wide (Dschida and Bowman, 1992). One of the most intriguing aspects of the V-ATPase is the question of how changes in the ATP binding sites on V_1 can be coupled to proton movement through a membrane sector which, on a molecular scale, is very far away. V_1 detached from the membrane contains five different subunits but does

not appear to have an extended stalk. Thus, the stalk may be composed, at least in part, of membrane-associated V_0 polypeptides.

1.6.4.4. Assembly of the V-ATPase complex.

The process by which the multi-subunit V-ATPase complex is assembled has been studied in both yeast and a bovine epithelial cell line. The availability of yeast strains deficient in individual subunits has allowed the process of assembly to be studied in their absence. Early work had indicated that most of the other subunits of the yeast V-ATPase were still present in mutants lacking one subunit, although the remaining subunits often failed to reach their proper intracellular location (Noumi et al., 1991; Umemoto et al., 1990; Kane et al., 1992; Ho et al 1993). Isolation of partial assemblies from various different subunit deficient strains provided information on the steps that lead to the fully assembled complex (Doherty and Kane, 1993). Subunits of the V_1 sector can assemble in the cytosol in the absence of the V_0 sector, but require the presence of a core of subunits, the 69-, 60-, and 27-kDa subunits. In the absence of any one of these three subunits, there is no assembly of V_1 subunits. In addition, the V_0 sector can assemble in the absence of the V_1 sector, and is still targeted to vacuoles. This suggests that the vacuolar targeting determinants reside in the membrane subunits (Doherty and Kane, 1993).

The assembly of the V-ATPase complex has also been studied in a bovine kidney epithelial cell line, Madin-Darby bovine kidney (MDBK) cells (Myers and Forgac, 1993). Either the V_1 sector or the whole complex were immunoprecipitated using antibodies directed against the 73-kDa subunit (subunit A) following pulse labelling of the cells with ^{35}S. At early time-points after labelling, the V_0 subunits appeared to be less abundant than the V_1 subunits, which suggested that the newly synthesised V_1 subunits were assembled onto pre-existing V_0 sectors. Blockage of vesicle transport by Brefeldin A (BFA) did not inhibit the assembly of the V-

ATPase complex, indicating that the process of assembly probably occurs in the E R, prior to distribution of the complex throughout the cell. The assembly of the V_1 subunits was rapid, followed by the slightly slower association of the completed complex with the membrane (Myers and Forgac, 1993).

1.6.5. Evidence that the same ductin polypeptide functions as a V-ATPase, gap junction and mediatophore component.

The isolation of ductin from three functionally diverse complexes, the gap junction, the V-ATPase complex and the mediatophore raises the question of whether the same polypeptide or merely closely related polypeptides are responsible. If the former, only a single gene would be expected. Multiple genetic loci for ductin were found in man (Hasebe et al., 1992), but only a single genetic locus for ductin has been found in *Drosophila melanogaster* (Finbow et al., 1994). In addition, the ductin cDNA from *Nephrops* and *Drosophila* can rescue *S. cerevisiae* defective in V-ATPase function, in which the *VMA3* gene has been inactivated (Holzenburg et al., 1993; Finbow et el., 1994). The single genetic locus in *Drosophila* and the interchangability of ductin between species suggest that the same polypeptide is part of the V-ATPase complex and the gap junction, and also presumably the mediatophore.

1.7. Structure of ductin.

1.7.1. Introduction.

Ductin has been isolated from a large number of species, and as described above there is a remarkable degree of conservation within the amino-acid sequence, even between such diverse organisms as yeast, plants and humans (Holzenburg et al., 1993). The highest degree of homology between the various ductins is in the putative transmembrane regions, and in the extramembranous domains that connect helices 1 to 2 and 3 to 4 (Figure 6). In fact, the only regions of ductin that do not

show a strong degree of conservation are at the N- and C- termini, and the extramembranous region between helices 2 and 3. The high degree of absolute conservation within the transmembrane domains would argue that the residues necessary for optimal ductin activity were set early on in the evolution of the polypeptide.

The N- and C- terminal halves of ductin have homology with each other and the F_1F_0-ATPase subunit *c*, suggesting the gene encoding ductin arose by gene duplication (Mandel et al., 1988). Highest homology is found in the transmembrane domains, and one conserved residue of note is the acidic aminoacid present in helix 2 of subunit *c* and helix 4 of ductin which in both polypeptides is thought to play a central role in the process of proton translocation and is labelled by dicyclohexyl carbodiimide (DCCD) (Finbow et al., 1992). The similarity in sequence and biochemical properties between subunit *c* and ductin suggests that the two proteins may in fact have similar roles and structures.

1.7.2.1. Structure of subunit *c* of the F_1F_0 ATPase.

Subunit *c* is thought to consist of a hairpin of two α-helical regions, connected by a polar loop region (Fillingame, 1992). Evidence for such a structure has come from a number of sources, including NMR and mutagenesis. The NMR studies were performed on purified subunit *c* that had been solubilised in a chloroform-methanol-water solution (Girvan and Fillingame, 1993). The folding of subunit *c* in this solution is thought to be similar to that found in the native F_0, since subunit *c* retains the ability to react with DCCD at residue Asp61. This reagent abolishes H^+ translocation in both the F_1F_0 ATPase and the V-ATPase (Hoppe and Sebald, 1984; Arai et al., 1987). The NMR study confirmed that 60-85% of the protein is α-helical and that the α-helical regions are present in the membrane traversing regions (Girvan and Fillingame, 1993). No structure assignments could be made for the polar loop region. The proximity of Ala24 to Asp61 was confirmed when

the DCCD nitroxide analogue, NCCD, was used to label Asp61 (Girvan and Fillingame, 1994). The effect of NCCD labelling was to broaden ^1H resonances in both helix 1 and 2, including Ala24 and Ala25, showing that these two residues lie 12Å from Asp61. The constraints introduced by these distances were used to refine a molecular model of subunit *c*, the basic features of which are the two α-helices that curve slightly around each other at approximately 20°, connected by the polar loop region to complete the hairpin structure (Girvan and Fillingame, 1994). One aspect of this model is the clustering of aromatic residues at both ends of the transmembrane segments, a feature seen in other membrane proteins which may be important in stabilising the segments in the membrane (Weiss et al., 1991).

1.7.2.2. Mutational analysis of subunit *c*.

The mutational analysis of subunit *c* has centred on two regions, the residues in close proximity to Asp61 and the residues of the polar loop region. H^+ translocation is abolished when Asp61 is mutated to either Asn or Gly (Hoppe et al., 1980,1982; Mosher et al., 1983). Although Asp61 is essential in the process of H^+ translocation, its function can be replaced in the double mutant Ala24Asp/Asp61Gly, though the activity of this double mutant was 4-24% of wild-type (Miller et al., 1990). This mutant emphasises the importance of the carboxyl group in the middle of the transmembrane region and confirms the close proximity of the two transmembrane domains in the hairpin model. Since the double mutant did not show wild-type activity, third site suppressor mutants with optimised activity were isolated (Fraga et al., 1994). Two types of optimising mutations were isolated, either on subunit *c* or on subunit *a*. The subunit *c* mutations localised to residues 53-75 of helix 2, and of particular interest were Phe53, Met57 and Met65. These three residues are thought to line the same face of the helix as Asp61, and to form a continuous hydrophobic pocket with Ile28 and Leu31 from helix 1 into which Asp61 and Ala24 would extend. The majority of the second set of mutations were in residues Ala217, Ile221 and Leu224 of subunit *a*, which

suggests a close functional relationship between this region and Asp61 of subunit *c* (Fraga et al., 1994). Efforts to maximise the activity of the Ala24Asp mutant by replacing Asp61 with a number of different residues yielded only three active mutants, Asp61Asn/Gly/Ser, which suggests that the packing of residues in this region is quite stringent (Zhang and Fillingame, 1994).

A number of mutants have been generated for the polar loop region of subunit *c*, focusing on the conserved residues Arg41-Gln42-Pro43. A common feature of mutations to these three residues is the uncoupling of H^+ translocation from ATP hydrolysis. The first mutant to show the uncoupled phenotype was Gln42Glu (Mosher et al., 1985), in which the ability to translocate protons was unaffected, as was ATPase activity, but the two properties were not coupled with each other. The F_0 sector from the Gln42Glu mutant was found to bind normally to F_1 but this in itself was not enough to recouple ATP hydrolysis and proton translocation. Other mutations have since been generated in Arg41, Gln42 and Pro43. Not all the mutations were found to disrupt the function of the F_1F_0 ATPase, such as Pro43Ser/Ala and Gln42Gly/Ala/Val, which is surprising in light of the conserved nature of these residues (although they did show some small reduction in activity which was related to uncoupling). Another uncoupling mutant has been reported, that of the Arg41Lys mutant (Fraga et al., 1994), where again the assembly of the F_1 and F_0 sectors appears to be normal but there is no coupling of ATPase activity with proton translocation.

A potential site of interaction for the polar loop within the F_1 sector was identified when second site suppressor mutants of Gln42Glu were isolated (Zhang et al., 1994). Of the four suppressor mutants isolated, all occurred at the same residue in subunit ε of the F_1 sector, at Glu31. Glu31 is in the most conserved region of subunit ε and lies close to the γ subunit. The N-terminal region of subunit ε is essential for promoting F_1 and F_0 binding, while the C-terminal region is inessential

and is close to subunit β (Kulki et al., 1988). The second site suppressor mutants of Gln42Glu do not prove that a direct interaction occurs between the polar loop region of subunit *c* and the N-terminal region of subunit ε, but they do show a potential pathway for the coupling of H^+ translocation to ATP hydrolysis (Zhang et al., 1994). This pathway starts at Asp61 and passes up through the polar loop region to subunit ε, which connects with subunit γ and then on to the α and β subunits. There is evidence to support the role of subunit ε and subunit γ in the coupling between catalytic sites and proton translocation via changes in the conformation of these two subunits (Capaldi et al., 1994).

In summary, the combination of structural work and mutational analysis shows that subunit *c* is composed of a hairpin of transmembrane α-helices connected by a single extramembranous loop, which faces the F_1 sector. Thought to be of critical importance in proton translocation is Glu61, which may form a H^+ binding site and is consistent with the X-ray diffraction analysis on isolated gap junctions.

1.7.3. The structure of ductin.

Based on the homology between ductin and subunit *c* the structure of ductin would be predicted to consist of two subunit *c* type helical hairpins i.e. four α-helices, with each α-helix connected by a short extramembranous loop region (Tibbits et al., 1990). This prediction has indeed been borne out by studies on the structure of ductin. The first studies on the structure of ductin were based on the use of hydropathy plots of the primary sequence, which showed that ductin has four highly hydrophobic regions, each of which is long enough to traverse the lipid bilayer as an α-helix (Mandel, et al., 1988: Finbow et al., 1992). The assumption that ductin is composed primarily of regions of α-helix has been confirmed using Fourier transform infrared spectroscopy (Holzenburg et al., 1993). Using this method, ductin was found to have a high α-helical content corresponding to at least 60% of the protein. An additional 20% of the protein may be in an extended

β-like structure, while the rest of the protein showed no assignable structure. The amide I IR spectrum of ductin bears a strong resemblance to that of bacteriorhodopsin, which is composed predominantly of transmembrane α-helices (Henderson et al., 1990), thus supporting the validity of the assignments made for ductin. The spectra of ductin could be measured over a range of temperatures, from 15- 95 °C, indicating that the polypeptide is extremely stable with respect to heat denaturation (Holzenburg et al., 1993).

The resistance of ductin isolated from the gap junctions of *Nephrops norvegicus* to proteolysis by a number of proteases shows that ductin is highly resistant to proteolytic degradation, with no observable change in migration in a SDS-PAGE gel following protease treatment (Finbow et al., 1992). This suggests that ductin has at most only small regions outwith the protection of the lipid bilayer, and indeed only the first few residues of the N-terminus were found to be removed by pronase. The α-helical regions of ductin are probably present in the lipid environment of the membrane, with only short connecting regions exposed to the non-lipid environment.

The EM analysis of ductin isolated from *Nephrops norvegicus* showed the functional unit to be a star-shaped hexamer of protein arranged around a central channel which runs perpendicular to the plane of the membrane (Holzenburg et al., 1993). The central channel is 1.5nm in diameter, while the complex has an overall diameter of 7.5nm. The calculated mass of the complex is consistent with the assembly of ductin into hexamers. Using the structure of subunit *c* as a framework as well as data from the EM. images, a three dimensional model of the structure of ductin has been developed (Finbow et al., 1992). The basic feature of the model is the packing of the four α-helices into a tightly packed bundle. The helices are arranged sequentially in an anti-parallel fashion tilted at a similar angle with respect to each other. Such an arrangement of the proposed α-helical transmembrane

segment of ductin would be consistent with a tandem repeat of two 8kDa halves, because it preserves the symmetry of the location of equivalent helices (i.e. helices 1 and 3 and helices 2 and 4). It also prevents crossing over of the short extramembranous loops. The hexameric assembly present in the connexon of the gap junction was generated by symmetrically placing six repeats of the four α-helix bundle around a central axis. The estimated dimensions of this model assembly are consistent with the observed dimensions of the connexon channel hexamer when viewed by electron microscopy (Holzenburg et al., 1993).

The four transmembrane helices were packed so as to minimise the number of non-hydrophobic residues exposed to the lipid bilayer such that the polar surfaces present on all the helices were facing the centre of the four α-helical bundle (Finbow et al., 1992). When so arranged, there is a near-continuous hydrophobic surface created on the exterior of the bundle. The one exception occurs on the outside surface of helix 1, where there are hydrophilic residues passing across the lipid bilayer. This region has features in common with the lining of other putative transmembrane pores (Unwin, 1989). When helix 1 is placed closest to the axis of symmetry of the ductin hexamer there is the potential for a water-filled pore. The diameter of such a pore would be 12-14 Å, sufficient in size to allow the passage of the low molecular solutes associated with passage through the gap junction (Finbow et al., 1992). Such a pore is, however, too large to allow selective proton transport, which implies that proton selectivity is provided by other subunits or other transport sites. An alternative site for the selective transport of protons is the centre of the four helical bundle of each ductin monomer. The presence of the DCCD reactive glutamic acid within this region makes it an attractive site (Finbow et al., 1992).

The model of ductin has been used to predict residues likely to be important in the function of ductin, and on the basis of this modifications to ductin have been

carried out. One strategy that has been used to probe the structure of ductin is the chemical modification of single cysteine replacement mutants (Jones et al., 1994). Single cysteine residues were placed in three distinct locations, either exposed to the lipid bilayer, or facing into the centre of the four helical bundle, or facing into the central aqueous channel. Cysteine residues in the centre of the four helical bundle were found to be resistant to chemical modification, while residues exposed to the lipid bilayer were chemically modified by lipid soluble reagents (Jones et al., 1995). The cysteine residues facing the central aqueous channel were labelled by aqueous soluble reagents. The results obtained from the modification of cysteine residues were consistent with the model of ductin's structure and have allowed the model to be refined.

1.7.4. Mutagenesis of ductin.

Extensive site specific mutagenesis of the ductin from *S. cerevisiae* (*VMA3*) has been carried out and a number of inactive polypeptides were obtained (Noumi et al., 1991). The conserved glutamic acid in helix 4 was mutated to a number of different residues but only the conservative substitution of an aspartic acid was able to show any activity, indicating that this residue is sensitive to substitution and liable to be important for the activity of ductin. Other residues close to this glutamic acid were also found to be sensitive to substitution, such as tyr142 (Noumi et al., 1991). Substitution sensitive residues were found throughout the polypeptide, some of which were used to isolate second site suppressor mutants, in the expectation of identifying regions in close proximity (Supek et al., 1994). The suppressor mutants that were isolated seemed to act by compensating for the change in volume of the original mutations. One such mutant was val138leu which was rescued by either val55ala, or met59val, or ile130thr. These second site mutants are either on the second or fourth helix, confirming the close proximity of these two helices (Supek et al., 1994).

1.7.5. Orientation of ductin in the lipid bilayer.

The orientation of ductin in the V_0 sector is thought to be N- and C- termini lumenal, as this is the case for subunit *c* in the F_0 sector (Fraga and Fillingame, 1989). This orientation would allow the conserved loops between helices 1-2 and helices 3-4 to act as the site of subunit association with the V_1 sector (Finbow et al., 1992). This region, by analogy with subunit *c*, would be the site of coupling between the V_0 and V_1 sectors and presumably cytoplasmically exposed to perform this function.

However, ductin present in the gap junction is thought to be orientated such that its N- and C- termini are exposed to the cytoplasm; i.e. opposite to the orientation of ductin in the V_0 sector of the V-ATPase. Evidence for ductin's orientation in the gap junction comes from studies using antipeptide antibodies directed against the N-terminus of mouse ductin as well as from protease studies (Finbow et al., 1993). The protease studies involved the digestion of isolated gap junctional plaques with pronase, with the result that only the N-terminal region was cleaved. This indicates that the N-terminus is exposed on the cytoplasmic face of the gap junctional plaque. The antipeptide antibodies were able to cause the agglutination of suspensions of mouse liver gap junctions into large feathery clumps, and the agglutination was inhibited by addition of the peptide (Finbow et al., 1993). The accessibility of the antigenic site in the intact gap junction suggests that the N-terminus of mouse ductin lies on the exposed cytoplasmic face of the gap junction, and this is further supported by the observation that when these antipeptide antibodies were injected into a cell line, dye coupling was blocked (Finbow et al., 1993).

When these same antipeptide antibodies were used in binding studies on bovine chromaffin granules, a rich source of the vacuolar ATPase, no binding was observed. Only after the chromaffin granule membranes were broken was the

antipeptide antibody able to bind to membrane, indicating that the antigenic site was present on the lumenal face of the chromaffin granules (Finbow et al., 1993). This result is consistent with the N-terminus of ductin in V_0 being lumenal. While able to inhibit gap junctional communication the anti-peptide antibodies were unable to inhibit ATP hydrolysis or proton pumping by the chromaffin membranes, whether they were broken or whole. This discrepancy in the ability of the antipeptide antibodies to have an effect on the two transport functions of ductin may be a result of their being located in different parts of ductin. The results from these studies suggests that ductin has two membrane orientations (figure 5) (Finbow et al., 1992, 1993). If this is the case then ductin would appear to contravene the present dogma concerning the orientation of membrane proteins, which holds that membrane proteins have only a single orientation.

1.7.6. Ductin related proteins.

To date, three ductin-related proteins have been isolated from *S.cerevisiae*, VMA 11, TFP3 and PPA1 (see figure 6). The protein that shows the highest homology with ductin is VMA 11, which has a 56.7% amino acid identity and significant coincidence (Umemoto et al., 1991). A comparison of the sequence of VMA11 and ductin indicates that the conserved regions of ductin are also conserved between ductin and VMA11 except the extramembranous regions between helices 1-2 and helices 3-4. A gene product for VMA 11 was not identified by biochemical means, although in *VMA 11*-disrupted cells no active vacuolar ATPase was detected. It has been suggested that VMA 11 is somehow involved in the assembly of the V-ATPase, but is not necessary for the activity of the final complex (Umemoto et al., 1991).

The second ductin-related protein is a truncated version of VMA 11 and is called TFP3 (Shih et al., 1988). The TFP3 gene was identified as a result of its ability to confer resistance to the drug trifluorperazine, when overexpressed. The

Figure 5. Proposed orientation of ductin in the gap junction and the V-ATPase complex.

The proposed transmembrane disposition of ductin in either the gap junction or the V-ATPase is to the left of the schematic models of each complex. The N- and C- termini of ductin in the gap junction are exposed on the cytoplasmic face, while the N- and C- termini of ductin in the V-ATPase complex are exposed on the lumenal face of the membrane.

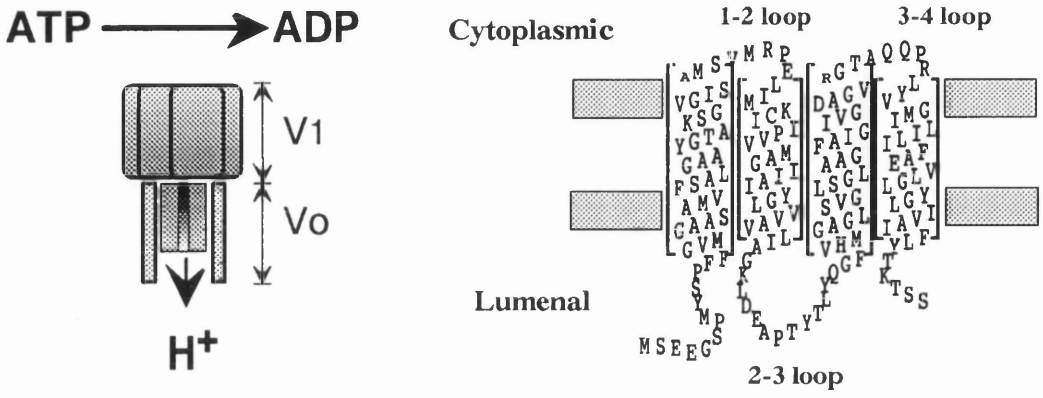

Vacuolar ATPase

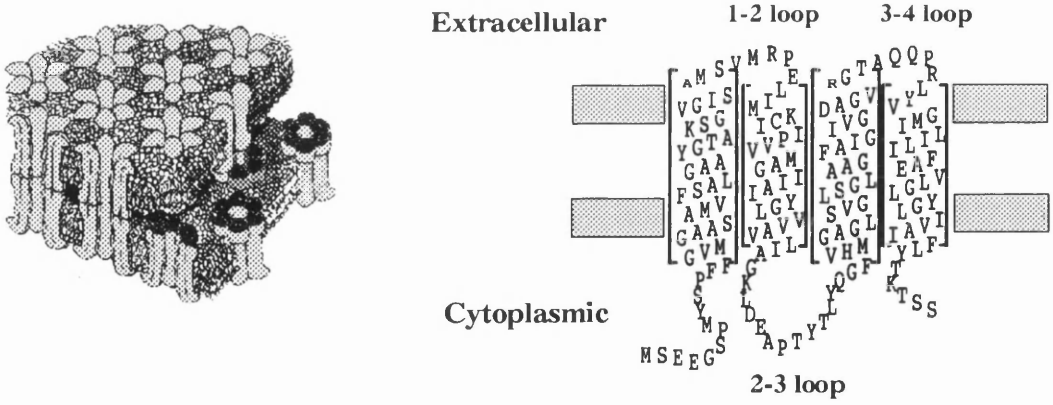

Gap Junction

polypeptide ends halfway through the third transmembrane domain, and has a deletion of seven residues in the first transmembrane region.

The third homologous protein is PPA1, which appears to be essential to the viability of cells (Apperson et al., 1990), unlike ductin for which deficiency is conditionally lethal. The PPA1 polypeptide has an N-terminal extension and the critical glutamic acid is located on the second transmembrane helix rather than on the fourth. The homology that the three proteins VMA 11, TFP3 and PPA1, have with ductin suggests that they may possess a transport function similar to that of ductin.

1.8. Ductin-associated viral proteins: E5 and p12.

Ductin has been found to complex with a number of short hydrophobic viral proteins; the functional significance of these interactions is not, as yet, fully understood. The fact that ductin is the target of viral proteins underlines the important role that ductin plays in the cell and presumably the viral proteins affect the activity of ductin as part of the viral life-cycle. The first viral protein to be shown to bind to ductin was the bovine papillomavirus type 1 (BPV1) E5 oncoprotein (Goldstein and Schlegel, 1990; Goldstein et al., 1991). This short polypeptide is 44 amino acids in length has a transforming activity and appears to consist of two domains; an N-terminal hydrophobic region which is membrane-spanning, and a C-terminal hydrophilic domain, thought to contain the oncogenic function of E5 (DiMaio et al., 1986; Horwitz et al., 1988).

The importance of the E5-ductin interaction in the transforming ability of E5 is, as yet, unclear. What is known, is that the binding of E5 to ductin is necessary, but not sufficient, for transformation (Kulke et al., 1992; Goldstein et al., 1992b). Most of the work on E5 has been focused on the ability of E5 to activate a number of growth factor receptors, such as platelet derived growth factor receptor

(PDGFR) and epidermal growth factor (EGFR) (Petti et al., 1991; Petti and DiMaio, 1992; Cohen et al., 1993; Nilson and DiMaio, 1993; Straight et al., 1994). Ductin has been shown to be present in the E5-PDGFR complex, and to bind to PDGFR in the absence of E5 (Goldstein et al., 1992a). The function of ductin in such a complex is unknown, but may reflect a role for the vacuolar ATPase in the process of receptor recycling, where the control of vesicular pH is important (Finbow et al., 1991). Alternatively, E5 may target only the gap junction form of ductin and thus affect intercellular communication (Angel Alonso, Heidelberg; unpublished result). Changes in intercellular communication are thought to be important in the process of tumour progression, although the relevance of this to the normal life-cycle of the papillomavirus is as yet unclear.

The newly identified HTLV-I protein p12 shows some sequence homology with BPV1 E5 over certain stretches, and contains a glutamine residue in a putative transmembrane region, a property again reminiscent of E5 (Franchini et al., 1993). Although p12 was unable to induce focus formation, it could dramatically increase, in a dose-dependant manner, the transforming ability of E5. The implication of the above observations is that p12 acts in a similar way to E5, possibly through their common target protein, ductin. p12 has been shown to bind to IL-2 β and α chains (Franchini et al., 1993) though it is not clear whether ductin is present in this complex. The overall similarity between E5 and p12, with respect to their structure, binding to growth factor receptors and binding to ductin suggests that they act through a common mechanism which could be mediated by ductin.

1.9. Summary.

The diversity of function that ductin exhibits suggests that ductin plays an important role in the life of a cell. This idea is supported by the fact that ductin is a target for viral proteins (see above) and that the loss of ductin from *Drosophila* is

lethal (Finbow and Kaiser, personal communication). Ductin's diversity raises a number of questions with regard to how the cell is able to direct the same protein to three functionally and locationally diverse complexes. Consequently, it would seem important to determine the mechanisms that lead to ductin becoming incorporated into the gap junction, the V-ATPase and the mediatophore. The likely starting point for this localisation process is the synthesis and membrane insertion of ductin, so this would seem a logical place to begin an investigation into how ductin becomes part of three different complexes.

One of the outstanding questions posed by previous studies on ductin is how it becomes incorporated into the gap junction and the V-ATPase in two opposite orientations, that is the N- and C- termini exposed cytoplasmically in the gap junction but in the V-ATPase they are exposed to the lumen of the vacuole (Finbow et al., 1993). Where the two orientations of ductin are generated could be important with respect to how the cell determines the orientation of other membrane proteins.

In studying how ductin becomes incorporated into the lipid bilayer it is likely that more general questions regarding the insertion of membrane proteins will also be answered since ductin is a good model integral membrane protein. So far the process of protein translocation through the ER membrane has been investigated with either secretory proteins, such as preprolactin (Mothes et al., 1994), or with single transmembrane pass proteins, such as VSV G protein (Gorlich and Rapoport, 1993). Similar studies have as yet not been extended to polytopic membrane proteins of which ductin would be a suitable candidate, not least because with regard to at least one property, that of membrane orientation, ductin may provide a clearer insight into the processes of membrane insertion than would otherwise be possible with the present model proteins used to study the translocation process.

Chapter 2. Materials and methods.

2.1. Materials.

2.1.1 Chemicals.

All chemicals were of "AnalaR" grade and obtained from BDH Chemicals Ltd., Poole, Dorset, England or Sigma Chemical Co. Ltd., Poole, Dorset, England, except those from the suppliers listed below.

Supplier- Amersham International PLC, Amersham, Bucks, England.

$\alpha[^{35}S]$dATP αS [600Ci/mmol] Hybond-ECL

L-[^{35}S] methionine [>1000Ci/mmol]

Supplier- B.R.L.(U.K.), Gibco Ltd., Paisley, Scotland.

All restriction enzymes, T4 DNA ligase and buffer concentrates were obtained from BRL except where otherwise indicated.

Supplier- Boehringer Mannheim UK Ltd., Lewes, East Sussex, England.

Calf intestinal alkaline phosphatase

DNA molecular weight markers (I-VII)

Supplier- J. Burrough (FAD) Ltd., Witham, Essex, England.

Ethanol

Supplier- Cambridge BioScience, Cambridge, England.

fluorescein maleimide

Supplier- Central Services, Beatson Institute.

L-broth

Supplier- Difco Labs., Detroit, Michigan, USA.

Bacto-tryptone Bacto-yeast extract

Bacto-agar Yeast nitrogen base

Supplier- Eastman Kodak Co., Rochester, New York, USA.

Duplicating film X-ray film (XAR-5)

Supplier- Fuji Photo Co. Ltd., Japan

X-ray film (RX)

Supplier- Gateway PLC, Glasgow, Scotland.

Marvel, dried non-fat milk powder

Supplier- Gibco Europe, Life Technologies Ltd., Paisley, Scotland.

2.5% Trypsin

Supplier- ICN Pharmaceuticals Ltd., Thame, England.

Yeast lytic enzyme (Zymolase)

Supplier- Severn Biotech Ltd.

30% acrylamide/0.8% bisacrylamide

Supplier- Rathburn Chemicals Ltd., Walkerburn, Scotland.

Phenol (water saturated)

Supplier- Whatman International Ltd., Maidstone, England.

3MM chromatography paper

2.1.2. Kits

Supplier- AMS Biotechnology, Witney, England.

mMessage mMachine kit (Sp6 and T7), from Ambion Inc.

Supplier- Amersham International PLC, Amersham, Bucks., England.

ECL Western Blotting analysis system

Supplier- Perkin Elmer Cetus, Norwalk, USA.

Gene Amp RNA PCR core kit

Supplier- Pierce and Warriner, Chester, England.

Micro BCA protein assay reagent

Supplier- Promega, Southampton, England.

Rabbit reticulocyte lysate systems, nuclease treated

Canine pancreatic microsomal membranes

Supplier- Qiagen Ltd, Dorking, England.

Qiagen tip 500 plasmid kit

Supplier- R&D Systems Europe Ltd., Abingdon, England.

TA cloning kit, from Invitrogen

Supplier- United States Biochemical, Ceveland, Ohio, USA.

Sequenase version 2.0

2.1.3. Equipment and Plasticware

Main pieces of equipment are referred to in the appropriate sections. Plasticware was obtained from the Beatson Institute stores, and the following companies are the suppliers of the most commonly used items:

Supplier- Bibby-sterilin Ltd, Stoney, Staffs., England.

Bacteriological dishes (90 mm)

Supplier- Griener Labortechnik Ltd., Dursley, England.

Eppendorf tubes

Supplier- Labsystems, Basingstoke, England.

Pipette tips (200 and 500 ml)

Supplier- Molecular Bio-Products, San Diego, California.

Aerosol Resistant Tips (20µl, 200µl and 1000µl)

2.1.4. Plasmids.

pBluescript SK Stratagene, San Diego, USA.

pYES2 Invitrogen

pCRII Invitrogen

pCYS6 0.5kb cys6 cDNA fragment cloned into the BamHI site of pYES2. A gift from P. Jones, University of Leeds, England.

pCYS25 0.5kb cys25 cDNA fragment cloned into the BamHI site of pYES2. A gift from P. Jones, University of Leeds, England.

pCYS27 0.5kb cys27 cDNA fragment cloned into the BamHI site of pYES2. A gift from P. Jones, University of Leeds, England.

pCYS29 0.5kb cys29 cDNA fragment cloned into the BamHI site of pYES2. A gift from P. Jones, University of Leeds, England.

pCYS44 0.5kb cys44 cDNA fragment cloned into the BamHI site of pYES2. A gift from P. Jones, University of Leeds, England.

pBluescript-Nductin 0.5kb Nephrops ductin cDNA fragment cloned into the BamHI site of pBluescript. A gift from P. McLean, Beatson Institute.

2.1.5. Antiserum.

Rabbit anti-*nephrops* ductin polyclonal (N2)

A gift from Dr. M.E. Finbow, Beatson Institute, Glasgow (Leitch and Finbow, 1990).

Sheep anti-rabbit horseradish peroxidase-linked whole antibody

Amersham International PLC, Amersham, Bucks., England.

2.1.6. Bacterial Host.

Competant E.coli DH5α were obtained from B.R.L., Gibco Ltd.

2.1.7. Yeast culture media and buffers.

YEP medium- 1% yeast extract, 1% peptone and 2% (wt/vol) raffinose. To induce expression from the pYES2 expression plasmid an additional 2% galactose was included. To make YEP plates 2% bactoagar was included. Transformed cells were grown on minimal plates containing 0.67% yeast nitrogen base, 2% raffinose, 2% bactopeptone 2% bactoagar and supplemented with (10 µg/ml) histidine, adenine, and tryptophan for *vat c* cells, or histidine, adenine, leucine, and lysine for *NUY43* cells.

2.1.8. Water.

Distilled water for solutions was obtained from a Millipore MilliRO 15 system, and for nucleic acid procedures it was further purified on a Millipore MilliQ system.

2.2. Methods.

2.2.1. Nucleic acid Procedures.

2.2.1.1. Growth, transformation and storage of competent cells.

The competant *E.coli* strain DH5α, (which is suitable for transformation with plasmid DNA) was purchased from B.R.L. and stored at -70°C. Competant DH5α cells for transformation were thawed on ice, gently mixed and aliquoted 20μl/Eppendorf tube. Unused competant cells were refrozen on dry ice before returning to the -70°C freezer. To each 20μl of competant cells, 1μl of diluted ligation mix (see section 2.2.1.3.3.) or plasmid of interest were added and incubated for 30 minutes on ice. The DH5α cells were then heat shocked at 42°C for 45 seconds and then incubated for 2 minutes on ice, after which 80μl of SOC medium (2% bacto-tryptone, 0.5% bacto-yeast extract, 9mM NaCl, 2.5mM KCl, 10mM $MgCl_2$, 20mM glucose) was added and the cells shaken at 225 rpm for 1 hour in a 37°C incubator, to allow the expression of the antibiotic resistance marker, ampicillin. The DH5α cells were then spread onto agar plates (1.5% agar in L-broth) containing 100μg/ml of ampicillin, and the plates incubated upside down at 37°C overnight to allow the formation of colonies. Colonies were picked using sterile pipette tips, transferred to a universal container containing 3ml of L-broth containing 100μg/ml of ampicillin and incubated for 4-6 hours at 37°C in a shaking incubator to enable subsequent plasmid preparations (see section 2.2.1.2.2.) or storage (see below).

In order to identify colonies of transformed sells that contained exogenous DNA inserted into the multiple cloning site within the β-galactosidase marker of the plasmid, transformed DH5α cells were plated on X-gal plates (1.5% agar plates on which 20ml of 2% X-gal had been spread prior to plating out). The β-galactosidase marker normally gives rise to a blue colour when cells containing the undisrupted parental plasmid are grown in the presence of the chromogenic substance X-gal, while cells containing recombinant plasmid with an DNA insert in the multiple cloning region causes the disruption of the β-galactosidase gene and gives rise to colourless colonies which can easily be identified and picked for further analysis (as described below).

Glycerol stocks for the storage of DH5α cells found to contain the required plasmid were prepared by mixing 1ml of DH5α culture with 1ml of 40% glycerol and frozen in Eppendorf tubes at -70°C.

2.2.1.2. Preparation of nucleic acids.

2.2.1.2.1. Plasmid minipreparations: alkali lysis method.

Small scale bacterial culture of 2-3ml were grown from a single colony for 6-8 hours at 37°C with vigorous shaking. 1.5ml of this culture was poured into an Eppendorf tube and centrifuged for 30 seconds. The medium was removed and the pellet resuspended in 300μl of Solution I (50mM Tris, 10mM EDTA, pH8.0, RNase at 100μg/ml) with vigorous vortexing. 300μl of Solution II (0.2 M NaOH, 1% SDS) was added, then mixed and left at room temperature for 5 minutes. The alkali solution was neutralised with 300μl of Solution III (2.55M KAc, pH4.8) and once this was thoroughly mixed it was centrifuged for 15 minutes at 4°C. 800μl of the supernatent was then transferred to a fresh Eppendorf tube. The plasmid DNA was precipitated by adding 600μl of isopropanol before centrifugation for 15 minutes at room temperature. The supernatant was discarded and the pellet was

washed in 70% ethanol before being dried. The DNA pellet was resuspended in 30µl of water and stored at -20°C.

2.2.1.2.2. Large scale plasmid preparations (Qiagen tip 500 plasmid kit).

Bacteria were grown in a 500ml L-broth culture, containing 50µg/ml ampicillin, overnight at 37°C with shaking. The bacteria were pelleted by centrifugation at 500rpm for 10 minutes in a Sorval centrifuge (GS-3 rotor). The supernatant was removed the pellet was resuspended in 10ml of buffer P1 (50mM Tris, 10mM EDTA, pH8.0, RNase at 100µg/ml). Then, 10ml of buffer P2 (0.2 M NaOH, 1% SDS) was added and incubated at room temperature for 5 minutes. To this, 10ml of buffer P3 (2.55M KAc, pH4.8) was mixed, then incubated on ice for 20 minutes. The precipitated material was pelleted by centrifugation at 4°C for 30 minutes at 10000rpm in a Sorval centrifuge (HB-4 rotor). The supernatant was removed promptly and applied to a Qiagen-tip 500 column that had previously been equilibriated with 10ml of buffer QBT (750mM NaCl, 50mM MOPS, 15% ethanol, pH7.0, 0.15% Triton X-100). Once the supernatant had passed through the column 2x 30ml of buffer QC (1.0M NaCl, 50mM MOPS, 15% ethanol, pH7.0) was washed through. The plasmid DNA was eluted off the column by passing through 15ml of buffer QF (1.25M NaCl, 50mM MOPS, 15% ethanol, pH8.2). The DNA was precipitated with 0.7 volumes of isopropanol, then pelleted by centrifugation at 10000rpm at 4°C for 30 minutes in a Sorval centrifuge (HB-4 rotor). The DNA pellet was washed with 70% ethanol and allowed to air dry before being redissolved in 500µl of water and stored at -20°C.

2.2.1.2.3. Preparation of total RNA from yeast.

100ml of logarithmically growing yeast cells (OD_{600} 1-3) were collected by centrifugation at 3000rpm for 5 minutes at 4°C. The pelleted cells were resuspended in 10ml of sodium acetate buffer (50mM NaAc, 10mM EDTA, pH5.0). To this was added $^1/_{10}$ vol 10% SDS and 1.2 vol of prewarmed phenol

(65°C). The sample was incubated at 65°C for 5 minutes with intermittent short vortexing. Subsequently, the sample was cooled down quickly to room temperature in a dry ice-ethanol bath. The organic and the aqueous phases were separated by centrifugation at 3000rpm for 10 minutes at room temperature. The lower organic phase was removed, leaving the interphase and the pellet of unbroken cells. The remaining aqueous phase and cell debris was extracted again, as described above, with an equal volume of prewarmed phenol (65°C). After separation the aqueous phase was transferred to a fresh tube and to this was added 1 vol. of chloropane (50% phenol, 50 % chloroform and 0.8% 8-hydroxyquinoline), followed by vortexing for 2 minutes and separation of the phases by centrifugation. The aqueous phase was transferred to a fresh tube, 1/10 vol of 3M NaAc (pH5.3) and 3 vol ethanol were added, and the RNA was precipitated at -20°C for 2 hours. The precipitated RNA was collected by centrifugation at 3000rpm for 15 minutes at 4°C, and the pellet washed with 70% ethanol. After being dried the pellet was redissolved in 600ml of water and stored at -20°C.

2.2.1.2.4. Preparation of oligonucleotides.

Oligonucleotides were synthesised on an Applied Biosystems model 381A DNA synthesiser. The 5' methyl-trityl groups were removed on the machine before the oligonucleotides were eluted from the synthesis column by "washing" 5-6x with approximately 2ml of concentrated ammonia solution (29%) over a 2-3 hour period. The concentrated ammonia solution containing the oligonucleotide was then transferred to glass vials, sealed with parafilm (to prevent evaporation of the samples) and incubated overnight at 55°C. The deprotected oligonucleotides were then ethanol precipitated by adding 0.1 vol 3M Sodium Acetate and 2 vol ethanol, incubating for 15 minutes at -70°C and collecting the precipitate by centrifugation. The resulting pellets were briefly dried and resuspended in 300µl of water. 2.5µl of this solution was used for O.D. analysis (see section 2.2.1.4.4.), from which the

oligonucleotide concentration was adjusted to the appropriate concentration for either sequencing (see section 2.2.1.5.) or PCR (see section 2.2.1.6.) and the oligonucleotide solutions were stored at -20°C.

2.2.1.3. Enzymatic manipulation of DNA.

2.2.1.3.1. Restriction digests.

Small quantities of plasmid DNA, typically 1μg, were digested using 1-10 units of enzyme, (depending on the enzyme used and the number of restriction sites within the plasmid) in a total volume of 20μl which was buffered with the appropriate buffer concentrates supplied by the manufacturer of the enzyme used. Digests were carried out at 37°C for 1-2 hours and were terminated by the addition of $^1/_6$ vol of DNA gel loading buffer (0.25% bromophenol blue, 30% glycerol in water). Double digests were also performed using a suitable buffer concentrate that optimised the activity of both the enzymes; and for larger scale digests the volumes used were increased in proportion.

2.2.1.3.2. Dephosphorylation of 5' phosphate groups from plasmid DNA.

The dephosphorylation of 5' phosphate groups from 10μg of linearised plasmid DNA in water was performed by incubating the plasmid DNA with 0.1 unit of calf intestinal alkaline phosphatase (CIP) in 1x CIP buffer (10x CIP buffer is 10mM $MgCl_2$, 1mM $ZnCl_2$, 10mM spermidine, 0.5M Tris, pH 9.0) for 30 minutes at 37°C. The dephosphorylated linear plasmid DNA was phenol/chloroform extracted (see section 2.2.1.4.2.) and ethanol precipitated before being resuspended in water. Diluted dephosphorylated linear plasmid DNA was then used for ligations.

2.2.1.3.3. Ligation of DNA fragments.

The ligation of dephosphorylated vector (100ng) and purified insert DNA (2-10 molar excess) was carried out using T4 DNA ligase (1μl) and 5x ligation buffer

(2μl; supplied by the manufacturer of the enzyme) and made up to a volume of 10μl with water. Reactions were set up on ice and incubated overnight at 12-14°C. The ligation mixture was diluted 4-10x prior to being used to transform bacteria (see section 2.2.1.1.).

2.2.1.3.4. Agarose gel electrophoresis.

Non-denaturing 1% agarose gels were run to separate DNA fragments. Gels were prepared by dissolving 1g of agarose in 100ml of 1x TBE buffer (5x TBE is 0.45M Tris, 0.45 M boric acid, 12.5mM EDTA, pH8.3) by heating until the solution boiled and the agarose dissolved. The gel mix was allowed to cool to approximately 50°C before ethidium bromide (10mg/ml) was added to a final concentration of 1μg/ml. The gel was cast and allowed to set at room temperature before the comb was removed and the gel placed in the gel tank. Electrophoresis was carried out in the same buffer used to form the gel at 100V for 30-60 minutes. The DNA samples and DNA standards (Boehringer Mannheim) for electrophoresis were mixed with 1/6 vol of DNA gel loading buffer, loaded and resolved by electrophoresis. On completion of electrophoresis the size of the DNA fragments were assessed by illuminating the gel on a 312nm transilluminator and compared to the positions of the DNA standards. A photographic record of the UV illuminated gel was taken using a Polariod camera on Polaroid Type 57 high speed film or on the video (The Imager, Appligene).

2.2.1.4. Purification and quantitation of nucleic acids.

2.2.1.4.1. "Wizard" DNA purification system (Promega).

DNA fragments were separated on a low melting point agarose gel (see section 2.2.1.3.4.) and the desired band was excised under UV illumination. The excised bands were transferred to an Eppendorf tube and incubated at 70°C until the agarose was completely melted. 1ml of the resin was then added and mixed thoroughly. The resin was loaded into a column and washed with 2ml of 80%

isopropanol. The DNA was eluted from the column by adding 50µl of water, incubating for 1 minute, then spinning the eluted DNA into a fresh Eppendorf tube. The purified DNA was stored at -20°C.

2.2.1.4.2. Purification of nucleic acids by phenol/chloroform extraction.

Occasionally it was necessary to purify nucleic acids by extraction with phenol/chloroform in order to remove contaminants, such as enzymes which might otherwise interfere with subsequent cloning steps. The method used was essentially that described by Maniatis et al. (1989) and is as follows:

1) The DNA sample was mixed with an equal volume of phenol/chloroform, (freshly prepared from an equal volume of TE pH8.0 saturated phenol and chloroform/isoamyl alcohol, 24:1) until an emulsion formed.

2) The phases were separated by centrifugation for 3 minutes in a microfuge.

3) The aqueous phase was removed and extracted with an equal volume of chloroform/isoamyl alcohol (24:1). The aqueous phase was collected and transferred to a fresh Eppendorf tube. The DNA was recovered by ethanol precipitation as described below.

2.2.1.4.3. Concentration of nucleic acids.

Ethanol precipitation was used to concentrate DNA as follows:

1) To the aqueous DNA solution $^1/_{10}$ vol of 3M NaAc pH 5.2 and 2 vol of ethanol were added.

2) The sample was then mixed well and the DNA precipitated by chilling -20°C for 30 minutes.

3) The precipitated DNA was collected by centrifugation in a microfuge for 15 minutes.

4) The supernatent was discarded, and the pellet washed with 70% ethanol and briefly dried before resuspension in water at an appropriate concentration.

2.2.1.4.4. Quantitation of nucleic acids.

The concentration of nucleic acid in a solution was determined spectrophotometrically, by first calibrating the spectrophotometer (Beckman) using a water blank and then diluting the samples in water and reading the absorbancy at wavelengths 260nm and 280nm in a quartz cuvette with a pathway of 1cm. For plasmid and genomic DNA samples an A_{260} of 1 was taken to correspond to 50μg/ml, for oligonucleotides an A_{260} of 1 was taken to correspond to 35μg/ml, and for RNA an A_{260} of 1 was taken to correspond to 40μg/ml.

2.2.1.5. Sequencing of double stranded DNA.

4μg of plasmid DNA in 18μl of water was denatured by the addition of 2μl of 2M NaOH/20mM EDTA and incubated for 5 minutes at room temperature. The denatured DNA was neutralised by adding 8μl of 5M Ammonium Acetate and precipitated by adding 200μl of ethanol and incubating for 15 minutes at -70°C. The DNA was pelleted by centrifugation in a microfuge for 15 minutes, then washed with 70% ethanol and dried. The pellet was resuspended in 7μl of water, then 1μl of oligonucleotide sequencing primer (50ng/ml) and 2μl of "Sequenase" reaction buffer (U.S.B.) were added to the denatured DNA solution. The sequencing primers were annealed to the denatured DNA by heating to 65°C for 2 minutes then cooling slowly until below 35°C, then stored on ice. The sequencing reactions were then performed using the reagents provided in the "Sequenase" version 2.0 (U.S.B.) according to the manufacturers instructions. The terminated, labelled fragments were resolved on 6% polyacrylamide denaturing gels (containing 42% urea) at 50W for 2-4 hours. The gels were fixed in a solution of 12% methanol and 10% acetic acid for 30 minutes at room temperature and then dried for 1 hour at 80°C under vacuum, before autoradiography overnight at -70°C.

2.2.1.6. Polymerase Chain Reaction (PCR).

PCR amplification was carried out by a method modified from Saiki et al. (1985). Double stranded DNA was amplified in a 0.5ml microfuge tube, in a reaction volume of 100µl, containing 10mM Tris-HCl, pH8.3, 50mM KCl, 0.001% (w/v) gelatin, 0.2mM of each dNTP, 1µM 5' and 3' primers and 2.5 units of Taq DNA polymerase. The reaction mix was overlaid with 80µl of mineral oil to prevent evaporation. The amplification conditions consisted of 30 cycles; 1) a denaturation step of 60 seconds at 94°C, 2) an annealing step of 60 seconds at 55°C, and 3) a primer extension step of 30 seconds at 72°C. After the 30th cycle an extended extension incubation of 5 minutes at 72°C was carried out to ensure that all amplified DNA was double stranded. $^1/_{10}$th of the amplified DNA was examined by agarose gel electrophoresis (see section 2.2.1.3.4.). The mineral oil was extracted by mixing with 100µl of chloroform and removing the upper aqueous layer to a fresh Eppendorf tube.

2.2.1.7. Reverse transcriptase-PCR (RT-PCR) (GeneAmp RNA PCR kit).

RNA was prepared (see section 2.2.1.2.3.) and used as the template for reverse transcription and PCR amplification of cDNA. The reaction mix was set up according to the manufacturers instructions, to the following final concentrations: 5mM $MgCl_2$, 50mM KCl, 10mM Tris, pH8.3, 1mM of each dNTP, 1U/µl RNase inhibitor, 2.5µM oligo $d(T)_{16}$, 1µl of diluted RNA (<1µg), 2.5U/µl MuLV Reverse Transcriptase, and water to a volume of 20µl. The reaction mix was incubated at room temperature for 10 minutes to allow primer extension. Then the reaction mix was overlaid with 80µl of mineral oil, and heated to 42°C for 15 minutes in a DNA thermal cycler. The next step was at 99°C for 5 minutes, followed by a 5 minute step at 5°C. Once these steps were complete the reaction mix was prepared for the PCR stage. The reaction mix was made to give the following final concentrations: 2mM $MgCl_2$, 50mM KCl, 10mM Tris, pH8.3, 2.5U/100µl AmpliTaq DNA polymerase, 0.15µM 5' and 3' primers, and made up to 100µl with water. This

reaction mix was placed in a DNA thermal cycler with the following cycle: an initial step of 120 seconds at 95°C followed by 35 cycles of 60 seconds at 95°C and 60 seconds at 60°C. The final step is 7 minutes at 72°C to allow full extension. $^1/_{10}$th of the PCR DNA product was run on an agarose gel (see section 2.2.1.3.4.) and visualised under UV illumination.

2.2.1.8. *In vitro* RNA transcription

In vitro transcribed capped RNA was synthesised using the mMessage mMachine kit (Ambion). 1μg of DNA, either linearised plasmid (see section 2.2.1.3.1.) or purified PCR product, was added to the transcription reaction mix, according to the manufacturers instructions. The reaction mix was incubated at 37°C for 1 hour, then 1μl of RNase-free DNase (2U/μl) was added and incubated for 15 minutes at 37°C. The capped RNA was recovered by adding 30μl of RNase-free water and 25μl of lithium chloride precipitation solution. The reaction was mixed thoroughly, then chilled for 30 minutes at -20°C. The precipitated RNA was pelleted by centrifugation in a microfuge for 15 minutes. The supernatent was removed and the pellet washed with 70% ethanol, then dried. The pellet was resuspended in 20μl of RNase-free water and stored at -70°C.

2.2.2. Protein procedures.

2.2.2.1. Protein preparation.

2.2.2.1.1. Polyacrylamide slab gel analysis of proteins.

Protein samples were resolved according to their molecular weight using sodium dodecyl sulphate polyacrylamide gel electrophoresis (SDS-PAGE). 15cm gels were used (Atto), containing gels of varying polyacrylamide content, depending on the molecular weight of the protein being resolved, but typically 12.5% gels were used. For a single 15cm gel of 12.5% the following solutions were prepared:

30% acrylamide/ 0.8% bisacrylamide (Severn Biotech Ltd.)	10ml
Running buffer (1.5M Tris, 4% SDS, pH8.9)	6ml
water	8ml
10% ammonium persulphate(freshly prepared)	200µl
TEMED	10µl

This resolving gel mix was poured between a sandwich of two glass plates sealed on three sides with a gasket, then overlaid with isopropanol and left to polymerise at room temperature. Once set, the isopropanol was removed using Whatman 3MM filter paper and the stacking gel mix added along with the comb. The stacking gel was prepared as follows:

30% acrylamide/ 0.8% bisacrylamide	2ml
Stacking buffer (0.5M Tris, 4%SDS, pH6.7)	3ml
water	7ml
10% ammonium persulphate(freshly prepared)	100µl
TEMED	5µl

Once the stacking gel had polymerised the whole gel was transferred to an electrophoresis tank. The tank reservoirs were then filled with Tris-glycine elctrophoresis buffer (50mM Tris, 50mM glycine and 1% SDS in water). After removal of the combs, the wells were flushed out with electrophoresis buffer to remove any excess stacking buffer.

Prior to loading, protein samples had an equal volume of 2x SDS gel loading buffer added (4% SDS, 0.2% bromophenol blue, 20% glycerol and 100mM Tris, pH6.8). The protein samples were not boiled and 1% β-mercaptoethanol was added when necessary. The prepared protein samples were then loaded into the gel and resolved by electrophoresis at a constant current 30mA/gel for 2-3 hours. Once the dye front had reached the bottom of the gel, it was removed and either fixed in 10% methanol and 12% acetic acid for 1 hour, or used for western analysis (see section 2.2.2.1.2.). The fixed gel was dried under vacuum prior to autoradiography at -70°C.

2.2.2.1.2. Western analysis.

Protein samples were prepared (see section 2.2.2.4.) and resolved by SDS-PAGE (see section 2.2.2.1.1.). The gel was removed from the electrophoresis tank, then excess gel was cut away. The dimensions of the remaining gel was measured and 12 pieces of Whatman 3MM filter paper were cut to an equal size, as was one piece of nitrocellulose (ECL-hybond). The transfer of the protein samples from the gel to the nitrocellulose was performed on a Biotech semi-dry electroblotter, set up as follows:

1) 6 pieces of the cut filter paper were wetted in Anode solution 1 (0.3M Tris, 20% methanol, pH10.4), then placed on the anode plate.

2) 3 pieces of the cut filter paper were wetted in Anode solution 2 (25mM Tris, 20% methanol, pH10.4), and placed on top of the first layer of filter paper.

3) The piece of cut nitrocellulose was wetted in distilled water and placed directly onto the gel. The nitrocellulose and gel were placed on top of the filter papers with the gel uppermost.

4) On top of the gel was placed 3 more pieces of the cut filter paper that had been wetted in Cathode solution (40mM 6-amino-n-hexanoic acid, 20% methanol, pH7.2).

5) this assembly of filters was coverd with the cathode plate and the electroblotting performed at a current of $0.8mA/cm^2$ for 1 hour.

Once the transfer was complete, the nitrocellulose filter was blocked by shaking in 100ml of wash buffer (WB) (10x WB: 0.9%NaCl, 10mM Tris-HCl, pH7.4) containing 5% Marvel for 1 hour at room temperature. The nitrocellulose filter was washed in WB containing 0.1% Tween-20 for 2-3x 10 minutes. The filter was then incubated with the primary antibody diluted to the appropriate concentration in WB, for 1-4 hours at room temperature. After this the nitrocellulose filter was washed for 3x 10 minutes in WB containing 0.1% Tween-20. The anti-rabbit horseradish peroxidase secondary antibody was diluted 1:1000

in WB containing 0.1% Tween-20, then incubated with the nitrocellulose filter for 1 hour at room temperature. The final wash step was at least for 3x 15 minutes with WB containing 0.1% Tween-20 at room temperature. The detection step consisted of incubating the filter in an equal volume of ECL detection reagents 1 and 2 for 1 minute at room temperature. The excess detection solution was drained off the nitrocellulose filter and this was then wrapped in Saran wrap. The chemiluminescent signal was detected using X-ray film (Fugi-XR) during exposures of between 1 second and 20 minutes.

2.2.2.1.3. Protein assay.

The Micro BCA Protein assay kit (Pierce and Warriner) was used to spectrometrically determine the protein concentration of dilute solutions. The manufacturers instructions were followed and are summarised as follows: The BCA reagent was made by adding 200µl of reagent C (4% cupric sulphate pentahydrate) to 4.8ml of reagent B (4% bicinchoninic acid, (BCA)), then 5ml of reagent A was added. 5µl of the protein solution was made up to 20µl with water, then 20µl of 1% SDS was added, after which 460µl of water was added. To this diluted sample 500µl of the BCA reagent was added and after shaking, was incubated for 60 minutes at 60°C. The O.D. at 562nm was measured on a spectrophotometer, and the protein concentration calculated from a standard graph.

2.2.2.1.4. Immunoprecipitation

Samples were immunoprecipitated (IP) by first solubilising 10µl of translation reaction mixture in 200µl of RIPA buffer (25mM Tris-HCl pH 7.4, 150mM NaCl, 0.1% SDS, 0.5% DOC, 0.5% Triton X-100, 1µg/ml aprotinin). Rabbit polyclonal antiserum to *Nephrops* gap junctions (N2) at 1:100 dilution was then added and incubated at 4°C for 1h with agitation. 10µl of a Protein A sepharose bead (Sigma) slurry in phosphate buffered solution (PBS) was subsequently added,

followed by a further incubation at 4°C for 1h with agitation. The beads were collected by centrifugation and washed three times in 200µl of RIPA buffer. Bound protein was stripped off the beads by resuspending the beads in 10µl of 2x SDS-PAGE loading buffer.

2.2.2.1.5. Alkali extraction of microsomal membranes

The Na_2CO_3 extraction was performed on microsomal membranes that had been pelleted using a Beckman Benchtop Ultracentrifuge at 50000 rpm for 1 hour. The pellet was resuspended in 200µl of 100mM Na_2CO_3, pH 11.5 and incubated at 4°C for 1 h. The membrane fraction was separated from the carbonate releasable fraction by recentrifugation and the pellet fraction resuspended in MP buffer.

2.2.2.1.6. Proteolysis reactions

Following translation, the reactions were cooled on ice, and tetracaine HCl was added to a final concentration of 2mM to stabilise the membranes. Trypsin digest were carried out using 2.5% Gibco BRL as a stock solution. Prior to the digest the trypsin was diluted 10x in PBS. 1µl of this diluted trypsin solution was added per 10µl of translation mix. Digests were carried out on ice for the times indicated. The proteolysis was stopped by either adding 200µl of RIPA buffer, if the samples were to be immunoprecipitated (see section 2.2.2.1.4.), or by adding 150µl of MP buffer containing aprotinin to a final concentration of 1µg/ml. Once the MP buffer was added, the microsomes were separated from the reaction mix by ultracentrifugation at 50000rpm for 60 minutes at 4°C. The pellet was resuspended in an equal volume of MP buffer then analysed by SDS-PAGE.

Rhodopsin was digested using endoproteinase glu-C (Boehringer) added to 10µl of translation mix for 60 minutes at room temperature at a final concentration of 0.01 mg/ml. The digestion mixtures were loaded immediately onto a 12.5% SDS-PAGE gel after addition of SDS loading buffer.

2.2.2.2. *In vitro* translation

In vitro transcribed RNA (see section 2.2.1.8.) was translated *in vitro* using the rabbit reticulocyte lysate system from Promega, according to the manufacturers instructions. The following components were mixed on ice in an Eppendorf tube:

Nuclease treated rabbit reticulocyt lysate	17.5µl
1mM amino acid mixture (minus methionine)	0.5µl
[^{35}S] methionine (>1000 Ci/mmol) at 10mCi/ml	2.0µl
RNase-free water	1.0µl
Microsomal membranes (Promega)	2.0µl
RNA substrate (1-2 µg)	2.0µl

The reaction mix was incubated at 30°C for 60 minutes. The reaction mix was then analysed either by SDS-PAGE (see section 2.2.2.1.1.) or was used for further procudures.

2.2.2.3. Chemical modification of cysteine residues

The cysteine specific maleimide reagent, fluorescein-5-maleimide (FM), was purchased from Cambridge BioScience. The FM was prepared in dimethylformamide to a stock concentration of 0.25M and stored at -20°C. Prior to each cysteine labelling reaction 7.5µl of the stock FM was diluted into 500µl of MP buffer to give a 3.75mM FM solution. To 12.5µl of translation mix, varying volumes of the 3.75mM FM solution were added to give the desired final concentration of FM after being made up to 104µl with MP buffer. The reaction mix was incubated at 30°C for 60 minutes, then stopped by adding β-mercaptoethanol to a final concentration of 1%. The microsomes were separated from the reaction mix by ultracentrifugation at 50000rpm for 60 minutes at 4°C. The pellet fraction was resuspended in 12.5µl of MP buffer and 2x SDS loading buffer. The labelled polypeptides were visualised by 12.5% SDS-PAGE, followed by autoradiography.

2.2.2.4. Preparation of vacuolar membranes (based on Guthrie and Fink, 1991).

1l of yeast cells were grown to mid-log phase and collected by centrifugation at 5000rpm for 5 minutes. The cells were resuspended in 100ml of 1M sorbitol and 400µl of β-mercaptoethanol. 4 units of ICN yeast lytic enzyme/ml of suspension was added, and the suspension was then incubated for 4 hours at 30°C with shaking. The spheroplasts were collected by centrifugation at 3000rpm for 5 minutes at 4°C. The pellet was resuspended in 20ml of buffer A (10mM MES/Tris, pH6.9, 0.1mM $MgCl_2$, 12% Ficoll 400) and homogenised at 4°C. The cell debris was spun out at 3000rpm for 10 miutes at 4°C, and the supernatent transferred to a polyallomer tube of appropriate size for a Beckman SW28 rotor. The sample was carefully overlaid with 13ml of buffer A and centrifuged at 60000g for 30 minutes. The white wafer floating on top of the Ficoll was collected and homogenised in 6ml of buffer A. This suspension was transferred to a polyallomer tube appropriate for a Beckman SW40 Ti rotor, then overlaid with 6ml of buffer B (10mM MES/Tris, pH6.9, 0.5mM $MgCl_2$, 8% Ficoll) and centrifuged at 60000g for 30 minutes at 4°C. The white wafer floating on the top of the Ficoll was collected and resuspended in 200µl of 2x buffer C (10mM MES/Tris, pH6.9, 5mM $MgCl_2$, 25mM KCl). The vacuolar vesicles were homogenised, then an equal volume of 1x buffer C was added. The vacuolar vesicles were stored in 10% glycerol at -70°C. All solutions were made containing 0.1mM PMSF.

2.2.2.5. Vacuolar-ATPase assay.

The following solutions were mixed in an Eppendorf tube:

25mM ATP	25µl
vacuolar vesicles	25µl
2x buffer C	125µl
water	75µl

ethanol with or w/o DCCD 5µl

This reaction mix was incubated for 1 hour at 37°C before 0.75ml of Phosphate reagent (0.5% SDS, 0.5% ammonium molybdate, 0.1% ascorbate and 2% sulphuric acid) was added. The blue colour was allowed to develop for 10 minutes before the OD was measured at 830nm.

2.3. PCR constructs

The Nductin-β lac DNA was constructed using PCR methodology (figure 19). Two overlapping PCR products were first prepared, *T7pol*ductin and β-lac*term*. *T7pol*ductin contained a T7 polymerase site, the ORF for *Nephrops* ductin and an overlap with the second PCR product. This was generated with the standard primer oligonucleotide for pBluescript (5'-GTTTTCCCAGTCACGAC) which is 5' of the T7 polymerase site in this vector, and a reverse primer oligonucleotide (5' GTGAGCAAAAACAGGAAGGCTGGAGGTCTTGGTG) which the encoded the 5 C-terminal residues of *Nephrops* ductin plus one extra base (underlined), and residues 18 to 23 of β-lactamase (*Esherichia coli*). β-lac*term* was generated using the complimentary oligonucleotide to the reverse oligonucleotide used to generate *T7pol*ductin (5' CACCAAGACCTCCAGCCTTCCTGTTTTTGCTCAC), and a reverse oligonucleotide primer (5' GCGAGCTCGTTTACCCGGCGTCAACACGGG) which encoded residues 80 to 85 plus two extra bases together with an in-frame termination codon (underlined) and *Xho*1 restriction site. After "Wizard" spin column purification (Promega) of the PCR products, they were hybridised and used as a template for PCR to generate Nductin-β lac DNA using the standard primer olignucleotide with the reverse olignucleotide used to generate β-lac*term*.

The VMA11 gene was cloned by PCR from yeast genomic DNA (Promega) into the TA cloning vector (Invitrogen) with the following oligos, 5'

CCGGATCCGTAAACATGTCAACGCAACTCG (*VMA11-5' BamHI*) and 3' CGACTCGAGATCAACTTTTGACTCATTCAG (*VMA11-3' XhoI*) (table 2). The N-terminal mutants were constructed by PCR using the same oligonucleotides as were used for Nductin-β lac except for the 5' oligo, which contained a T7 promoter site upstream of the ATG start site, and were as follows; NductinAA-β lac, 5' GGATCCTAATACGACTCACTATAAGGAGGCTCAAAA**ATG**TCTGCAGCGG GTAGTCCT, and NductinKK-β lac, 5' GGATCCTAATACGACTCACTATAGGGAGGCTCAAAA**ATG**TCTAAAAAGG GTAGTCCT. The initiation ATG sequence is shown in bold and the underlined sequences are the sites of glutamic acid substitutions. The PCR products were used directly without purification, for *in vitro* transcription. The single cysteine replacement mutants cys6, cys25, cys27, cys29 and cys44 were obtained from Dr. P. Jones, Leeds University. A T7 RNA polymerase site was placed immediately upstream of the ATG codon by a PCR based strategy using the oligos *T7 Nductin* and *Nductin 3' antisense* (table 8). The PCR product was used directly for the in vitro transcription of capped RNA.

2.4. Transformation of yeast

Yeast cells were transformed according to the method described by Elble, (1992), which was based on a modified lithium acetate procedure. 0.5ml of yeast culture was pelleted by a 30 second spin in a microcentrifuge and the supernatent was removed. 1μg of transforming DNA was mixed into the pellet of yeast cells. 0.5ml of PLATE (40% PEG 4000, 0.1M LiAc, 0.01M Tris-HCl, pH7.5, and 1mM EDTA) was added and mixed with the yeast cell pellet. The samples were incubated overnight at room temperature, then spread directly onto selective plates (see section 2.1.7.). The bottom 100μl of the overnight mixture, which contained most of the yeast cells that had settled, was spread on the plates.

Chapter 3. Results.

3.1. Introduction

One of the aims of this thesis is to establish the importance of the conserved loop regions between the putative transmembrane helices 1 & 2 and 3 & 4 for the activity of ductin in the V-ATPase complex. These regions have been proposed to be exposed on the cytoplasmic face of the membrane and act as possible sites of interaction with the other subunits of the V-ATPase (Finbow et al., 1992). This proposal stems from the high conservation of these loops and from the known orientation of the F_0 subunit *c* (Fraga and Fillingame, 1989). In addition, N-terminally directed antibodies to ductin bind preferentially to the lumenal surface of chromaffin granular membranes, consistent with this orientation. Therefore, changing residues in these loop regions would be expected to cause a disruption in the activity of ductin and hence the V-ATPase. However, as reviewed in the Introduction, there is direct evidence based upon proteinase and immunological studies for the N-terminus of ductin being cytoplasmic when part of the gap junction (Finbow et al., 1993). That is, the ductin polypeptide has the opposite orientation in gap junctions from that of the ductin polypeptide in the V_0 sector. This would allow the conserved loop regions to act as the site of contact between the apposing connexons of the gap junction, and in so doing they would play an important role in both the V-ATPase and the gap junction.

A second aim of this thesis is to identify the mechanism of insertion of ductin; is it through the standard ER machinery or is it by some other mechanism? The insertion of integral membrane proteins is thought to occur using the same machinery that has been identified previously as being responsible for the translocation of secretory proteins across the ER membrane. Single transmembrane pass proteins of either orientation also use the Sec61 complex as their means of insertion into the lipid bilayer (Gorlich and Rapoport, 1993). Regardless of the number of transmembrane passes, integral membrane proteins are

generally thought to use the same insertion machinery and to have only a single orientation.

If ductin does have two orientations in the membrane the question arises of how and where this occurs. Since ductin does not appear to fit in with the general assumption about membrane proteins having a single orientation, then it cannot be assumed that ductin is inserted into the lipid bilayer using the general translocation machinery of the ER. It could be that ductin may utilise some post-translational insertion mechanism, as appears to be the case for synaptobrevin (Kutay et al., 1995), to facilitate its insertion with two orientations into the lipid bilayer. Such a mechanism could be based on, for example, the chaperone family of proteins. Alternatively, ductin could be inserted into the membrane using the ER machinery but in a single orientation and subsequently undergo some mechanism, such as asymmetric membrane fusion, that results in the generation of the second orientation.

A third aim of this thesis is to investigate the process of self-assembly for ductin. Once ductin has been inserted into the membrane it must undergo an assembly process that eventually leads to either the final gap junction complex or the final V-ATPase complex. In the case of the gap junction only ductin has so far been identified as a constituent protein of the connexon channel, so at the very least ductin is capable of self-assembly into the hexameric connexon, which may then undergo further assembly into the final gap junction complex. For the V-ATPase there are at least 8 different subunits present in the final complex (Kane et al., 1989) and the six ductin polypeptides present in the V-ATPase must be assembled with the other subunits into the final complex.

To pursue the aims of this thesis two systems were used, a yeast expression system, and an *in vitro* translation system. The yeast expression system is based on

strains of *S. cerevisiae* that are deficient in either ductin or VMA11, leading to the *vma* phenotype. The main characteristic of this phenotype is a restricted pH growth range, *vma* cells grow at pH 5.5 but not at pH 7.5 (Nelson and Nelson, 1990). The growth at pH 7.5 of the deficient strains can be restored by transforming the cells with an expression plasmid containing the missing protein. This allows mutated forms of ductin or VMA11 to be tested for activity by introducing the mutant forms into the appropriate deficient strain of yeast and testing for growth at pH 7.5. The benefit of this system is that it allows the effect of mutations to either ductin or VMA11 to be tested for their effect on the activity of the V-ATPase. The assay itself, comparing the growth of the transformed cells at either pH 5.5 or pH 7.5 is simple and quick to perform.

The *in vitro* translation system is a cell-free system that allows the translation of individual RNA species. Since the proteins being expressed using this system are membrane proteins, the translation system can be supplemented with microsomal membranes to allow the integration of the membrane proteins into a lipid bilayer and thus act as a model for the insertion of membrane proteins into the lipid bilayer. This cell-free system has been used previously for other integral membrane proteins, such as the aquaporin, nodulin 26 (Miao et al., 1992), to study the topology of these proteins. Results obtained using this system have been reproduced with alternative systems, as was the case for the hepatitis B virus large envelope protein (Bruss et al., 1994; Ostapchuk et al., 1994).

3.2. Expression of chimeric forms of ductin in *S. cerevisiae*.

3.2.1. Introduction

The conserved extramembranous loops between the putative transmembrane helices 1 & 2 and 3 & 4 (from now on referred to as helices 1-2 and 3-4) of ductin are thought to be the sites of interaction between the apposing connexons of the gap junction and the interface between the V_0 and V_1 sectors of the V-ATPase. The analogous loop region of the F-type subunit *c* is also conserved, and has been shown to be important in connecting the translocation of protons in F_0 with ATP hydrolysis in F_1 (Mosher et al., 1985) (see section 1.7.2.2.). This would seem to indicate that the loop regions are potentially important for the activity of ductin. Previous site-directed mutagenesis studies in this region of ductin (Noumi et al., 1991) showed that the activity of ductin was not affected by single amino acid substitutions, except for the change R117A, in the 3-4 loop region, which produced an inactive form of ductin.

Although VMA11 is homologous (70% identity) to ductin, the activity of the two gene products is not interchangeable (Umemoto et al., 1991). From a sequence comparison of ductin and VMA11 (figure 6) a striking difference is seen in the 1-2 and 3-4 loop regions, in which this region in VMA11 deviates from the general conservation of residues that is seen over the rest of the amino acid sequence. Exchanging these regions, singly or in combination, between VMA11 and ductin thus provides an approach to understand the importance of the two loops in ductin activity in the V-ATPase. Such experiments also provide a strategy to identify the role of the VMA11 polypeptide. In addition, it would be expected that the chimeric polypeptides would still be capable of the proper folding since the exchanged loop regions will be present in the same context as before. The ductin and VMA11 activity of the resulting chimeras were tested by expressing them in the yeast expression system outlined above, using the yeast strains listed in table 1.

Figure 6. Sequence alignment of 16-kDa proteins.

The sequences are aligned on proline residues of the extramembranous loops between helices 1 & 2 and helices 3 & 4 as shown in Figures 7 and 11 in Finbow et al (1992). The 16-kDa protein sequences shown are the N-terminal half (denoted by "-N") and C-terminal half (denoted by "-C") of *Nephrops* (Ne), *Drosophila melanogaster* (Dr), bovine (Bo), murine (Mo), human (Hu), *Torpedo californica* (Tp), *S. cerevisiae VMA3* (Yt-N), *S. cerevisiae VMA11* (Yt-N*), *S. cerevisiae TFP3* (TFP3) and *S. cerevisiae PPA1* (Yp-N). Sequences are taken from Apperson et al., 1990; Birman et al, 1990; Finbow et al, 1992; Gillespie et al, 1991; Goldstein et al, 1991; Mandel et al, 1988; Nelson and Nelson, 1990; Shih et al., 1988; Umemoto et al, 1991). Dashes correspond to identities to the top sequence (*Nephrops*) and dots show insertions (modified from Holzenburg et al., 1993). The boxed regions correspond to the conserved extramembranous loop regions referred to in the text.

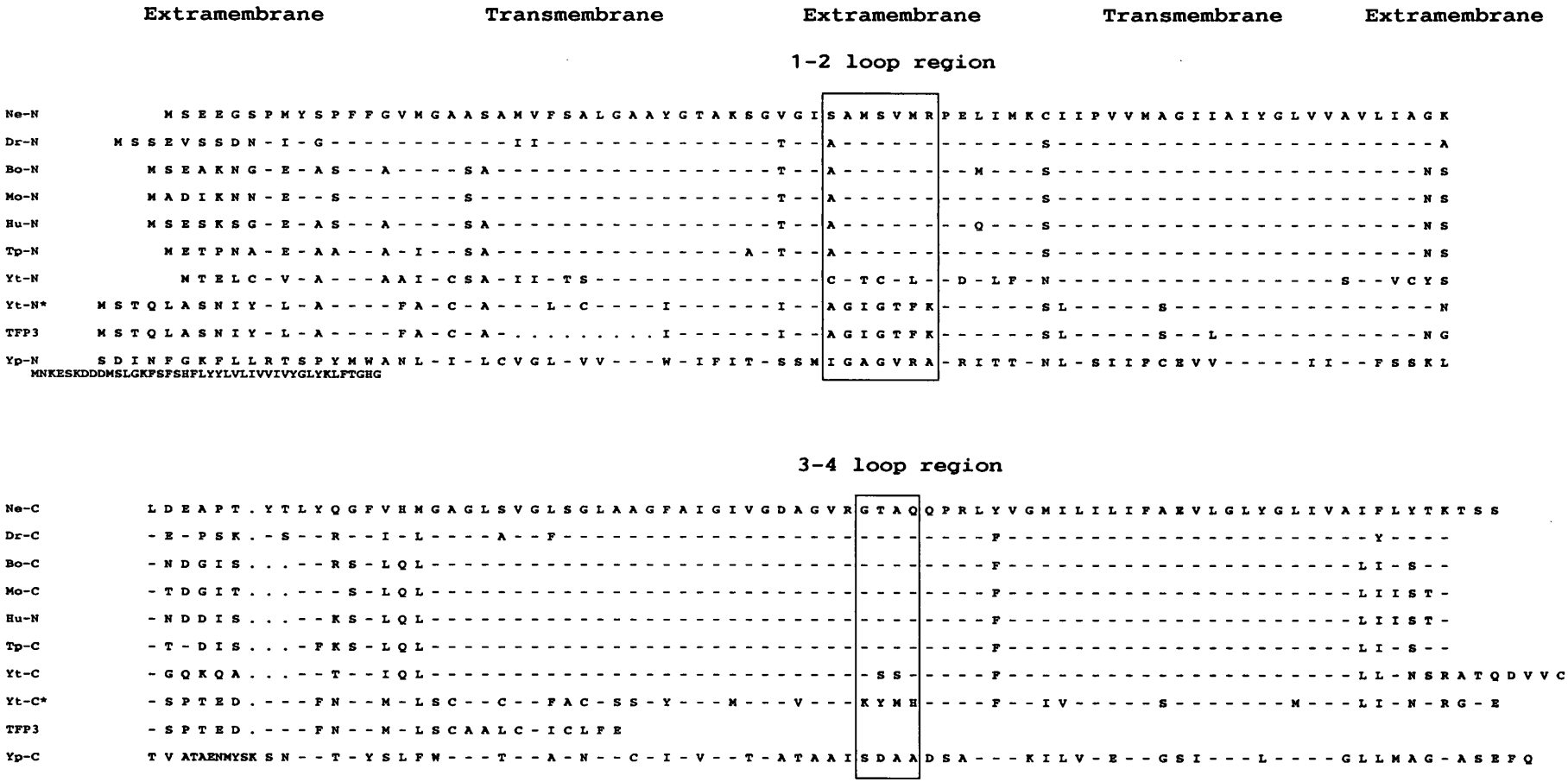
Extramembrane
Transmembrane
Extramembrane
Transmembrane
Extramembrane
1-2 loop region
Ne-N
Dr-N
Bo-N
Mo-N
Hu-N
Tp-N
Yt-N
Yt-N*
TFP3
Yp-N
MNKESKDDDMSLGKFSFSHFLYYLVLIVVIVYGLYKLFTGHG
3-4 loop region
Ne-C
Dr-C
Bo-C
Mo-C
Hu-N
Tp-C
Yt-C
Yt-C*
TFP3
Yp-C
Ne- Nephrops; Dr- Drosophila; Bo- Bovine; Mo- Mouse; Hu- Human; Tp- Torpedo; Yt- S.cere VMA3; Yt*- S.cere VMA11; TFP3- S.cere Tfp resistance; Yp- S.cere PPA1 proteolipid.
-N - N-terminal '8-kD domain'; -C - C-terminal '8-kD domain'.

Table 1. Genotype of *S. cerevisiae* strains, *NUY43* and *vat c*.

The parental strains for *NUY43* and *vat c* are in brackets.

strain	genotype
NUY43 (YPH 500)	*MATa leu2 lys2 trp1 ade2 his3 ura3* TRP1::vma11
vat c (W303-1B)	*MATa leu2 trp1 ade2 his3 ura3* LEU2::vma3

3.2.2. Cloning of VMA11 cDNA

Firstly, for these experiments it was necessary to obtain the VMA11 gene. To do this the cDNA of the VMA11 gene was cloned by PCR, using *S. cerevisiae* genomic DNA (Promega) as the template. The oligonucleotides used (table 2) were directed against the 5' and 3' ends of VMA11 and covered the start and stop codons, respectively. After the PCR step a single band of ~500bp was produced, which was cloned using the TA cloning kit (Invitrogen). The VMA11 gene was then subcloned into the pYES2 expression vector (Invitrogen) using the *BamH I* and *Xho I* restriction sites that were present in the oligonucleotides used in the PCR reaction. The subcloned VMA11 gene was sequenced (figure 7) and found to be identical to that of the reported sequence (Umemoto et al., 1991).

3.2.3. Characterisation of the *vat c* and *NUY43* yeast strains

For these experiments, appropriate "knock out" strains of S. cerevisiae were obtained. The *vat c* strain (*VMA3*$^-$) was obtained from N. Nelson (Roche Institute, Nutley, NJ) and the *NUY43* strain (*VMA11*$^-$) was obtained from Y. Anaraku (University of Tokyo, Tokyo) (table 1). In the *vat c* strain the *VMA3* gene (which codes for ductin) is disrupted by the insertion of the *Leu2* gene, while in the *NUY43* strain the *VMA11* gene is disrupted by the *trp1* gene. The growth of these strains on full media plates was tested at both pH 5.5 and pH 7.5, and for both strains growth was restricted to the pH 5.5 plates (table 4), as has been previously described (Nelson and Nelson, 1990).

Table 2. Nucleotide sequence of flanking primers.

Flanking primers

Nductin-5' BamHI:

5' CCGGATCCCTCAAAATGTCTGAAGAGGGTAG 3'

Nductin-3' XhoI:

5' CCCTCCGAGTCCATTTAGCTGGAGGTCTTGG 3'

VMA11-5' BamHI:

5' CCGGATCCGTAAACATGTCAACGCAACTCG 3'

VMA11-3' XhoI:

5' CGACTCGAGATCAACTTTTGACTCATTCAG 3'

β-*lac 3' anti*:

5' GCGAGCTCGTTTACCCGGCGTCAACACGGG 3'

Figure 7. Partial sequence of PCR cloned VMA11 cDNA.

The sequencing was performed on the pYES2 vector containing the VMA11 cDNA subcloned from the pCRII vector and for 1) a primer specific for downstream of the multiple cloning site was used, so as to read into the 3' end of the cloned cDNA. The sequencing of 2) was performed using a primer specific for upstream of the multiple cloning site, so as to read into the 5' end of the cloned cDNA. The deduced sequence for both is shown below for each, and in both cases is identical to the published sequence of Umemoto et al., 1991.

1

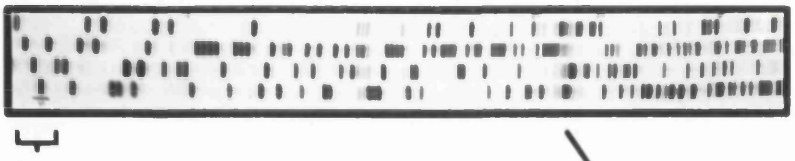

STOP

ATCATTCAGAGCCTCTAGTGTTCAAAATCAAAGCTACAATCATACCATAT
TAGTAAGTCTCGGAGATCACAAGTTTTAGTTTCGATGTTAGTATGGTATA

AACCCTAAAACTTCAGAGAAAATTAGAATCAAAACGATACCGACAAAAAG
TTGGGATTTTGAAGTCTCTTTTAATCTTAGTTTTGCTATGGCTGTTTTTC

2

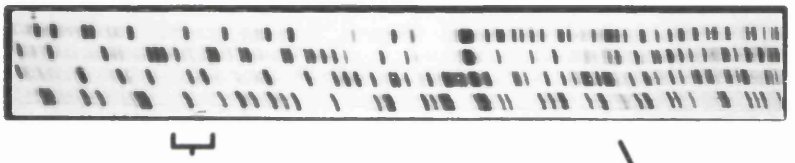

START

ATGTCAACGCAACTCGCAAGTAACATATATGCTCCATTGTACGCTCCC
TACAGTTGCGTTGAGCGTTCATTGTATATACGAGGTAACATGCGAGGG

TTTTTCGGGTTCGCAGGTTGTGCAGCTGCCATGGTGCTTTCCTGTTTG
AAAAAGCCCAAGCGTCCAACACGTCGACGGTACCACGAAAGGACAAAC

Table 4. pH growth characteristics of Nductin, VMA11 and the loop chimeras.

Growth at pH 7.5 was assayed for *vat c* and *NUY43* strains of *S. cerevisiae* after transformation with cDNA coding for Nductin, the loop chimeras (1-2, 3-4 and 1-2/3-4), and VMA11 in the pYES2 yeast expression vector. YPD agar plates were supplemented with 2% galactose to induce expression from pYES2.

cDNA	Growth at pH 7.5	
	vat c	*NUY43*
Nductin	+	-
1-2 loop	+	-
3-4 loop	-	-
1-2/3-4 loop	-	-
VMA11	-	+

3.2.4. Expression of Nductin and VMA11 in yeast

The cDNA for the *Nephrops* ductin (Nductin) was used in these experiments instead of the endogenous form of yeast ductin, VMA3, because antibodies are available to Nductin, and Nductin has been shown to incorporate into a fully active yeast V-ATPase complex (Holzenburg et al., 1993). In addition, the majority of the structural work on ductin has been performed on Nductin. Nductin and VMA11 were cloned into the pYES2 expression vector, which contains the selectable marker gene *Ura3*, allowing transformed cells to be selected. In addition, the transcription of the inserted DNA is under control of the galactose inducible GAL4 promoter. The expression vectors were transformed into the *vat c* and *NUY43* cells and transformed colonies were selected for on the appropriate selection plates. The sensitivity to pH of the transformed cells was then tested by growing them at either pH 5.5 or pH 7.5 on full media plates in the presence of glucose and galactose. The Nductin expressing *vat c* cells were able to grow at both pH values, as were the VMA11 expressing NUY43 cells (figure 11 and table 4). In contrast, the VMA11 expressing *vat c* cells grew only at pH 5.5, as was the case for the Nductin expressing NUY43 cells (table 4). These results were expected from the previous expression studies using the above strains and proteins, and in addition confirm that the PCR cloned VMA11 cDNA encodes an active polypeptide.

3.2.5. Construction of ductin chimeras

The chimeric forms of ductin were constructed by a PCR based strategy using the oligonucleotides listed in tables 2 and 3. Two types of primer were used, the first type being external and the second type being internal. The internal primers were designed such that they had regions of overlap to contiguous regions of ductin and

Table 3. Nucleotide sequence of internal primers for Nductin chimeric polypeptides.

Internal primers- ductin/VMA11 chimeric protein

Loop 3-4 antisense:

5' GTGCATATACTTCCTCACACCGGCATCTCC 3'

Loop 3-4 sense:

5' AAGTATATGCACCAACCTCGTCTGTATGTTG 3'

Loop 1-2 antisense:

5' CTTGAAAGTACCTATACCGGCAATTCCCACTCCTGATTTG 3'

Loop 1-2 sense:

5' GCCGGTATAGGTACTTTCAAGCCGGAGTTGATCATGAAG 3'

F24L antisense:

5' GGGCGCTAAGTACCATGGC 3'

F24L sense:

5' GCCATGGTACTTAGCGCCC 3'

Y31I antisense:

5' GGTGCAGCAATTGGCACTGC 3'

Y31I sense:

5' GCAGTGCCAATTGCTGCACC 3'

VMA11 (figure 8). The first PCR reaction synthesised short segments of ductin that contained regions of overlap at their ends with the neighbouring segment. The regions of overlap contained the VMA11 sequence in place of the ductin sequence. The PCR DNA fragments were purified using spin columns (Promega) to remove excess primers, that would otherwise interfere with the next PCR reaction. The purified PCR products from the first reaction were used as the template for the second PCR reaction. The external primers, specific to the N- and C- termini of ductin, were used with the appropriate set of DNA fragments to produce a full length ductin cDNA that contained VMA11 sequences for either the 1-2 loop or for the 3-4 loop.

The full length ductin chimeras were cloned into pCR II, by taking advantage of the 3' A overhang left by the Taq DNA polymerase, using the TA cloning kit (Invitrogen). The ductin chimeras were subsequently subcloned into the yeast expression vector pYES2 (Invitrogen) using the *BamH I* and *Xho I* sites in the multiple cloning site. The double loop replacement was constructed in the same manner as the single loop replacement chimeras except that the template used for the first round of PCR was the cloned 1-2 loop chimera and the internal primers used were specific for the 3-4 loop region. The full length double chimera was cloned into pCRII and subsequently subcloned into pYES2 using the *BamH I* and *Xho I* sites. All the subcloned chimeras were sequenced using the Sequenase 2.0 kit (USB) using the standard sequencing primers provided in the kit. All the chimeras had the correct sequence, both over the replaced extramembranous loops and the regions derived from Nductin as shown for the 1-2 loop chimera (Figure 9).

Figure 8. Loop chimeras of ductin.

A) Amino acid sequence of the exchanged loop regions.

The exchanged residues for the 1-2 loop region in Nductin and VMA11 correspond to residues 41-47 and 45-51 respectively, and are contained in the boxed region in figure A. The residues exchanged in the 3-4 loop region are 121-124 in Nductin and 125-128 in VMA11, as outlined in the boxed region of figure A.

B) PCR strategy for the exchange of the 1-2 and 3-4 loop regions of ductin and VMA11. Two rounds of PCR were necessary to generate the single loop chimeras, while for the double loop chimera three rounds of PCR were necessary. The first round of PCR generated a series of DNA fragments that contained regions of overlap with each other e.g. DNA fragments 1 and 5 contain a region of overlap at their 3' and 5' ends, respectively, that corresponds to the 1-2 loop region of VMA11 in place of Nductin. In the second round of PCR the DNA fragments 1 & 5, and 3 & 4, were mixed then used as the template for the generation of the full length cDNA. The double loop chimera was generated in a third round of PCR using DNA fragment 3 and the 1 & 2 DNA fragment generated in the second PCR round. The full length cDNA PCR products were cloned using the TA cloning kit (Invitrogen) and sequenced using Sequenase 2.0 (USB).

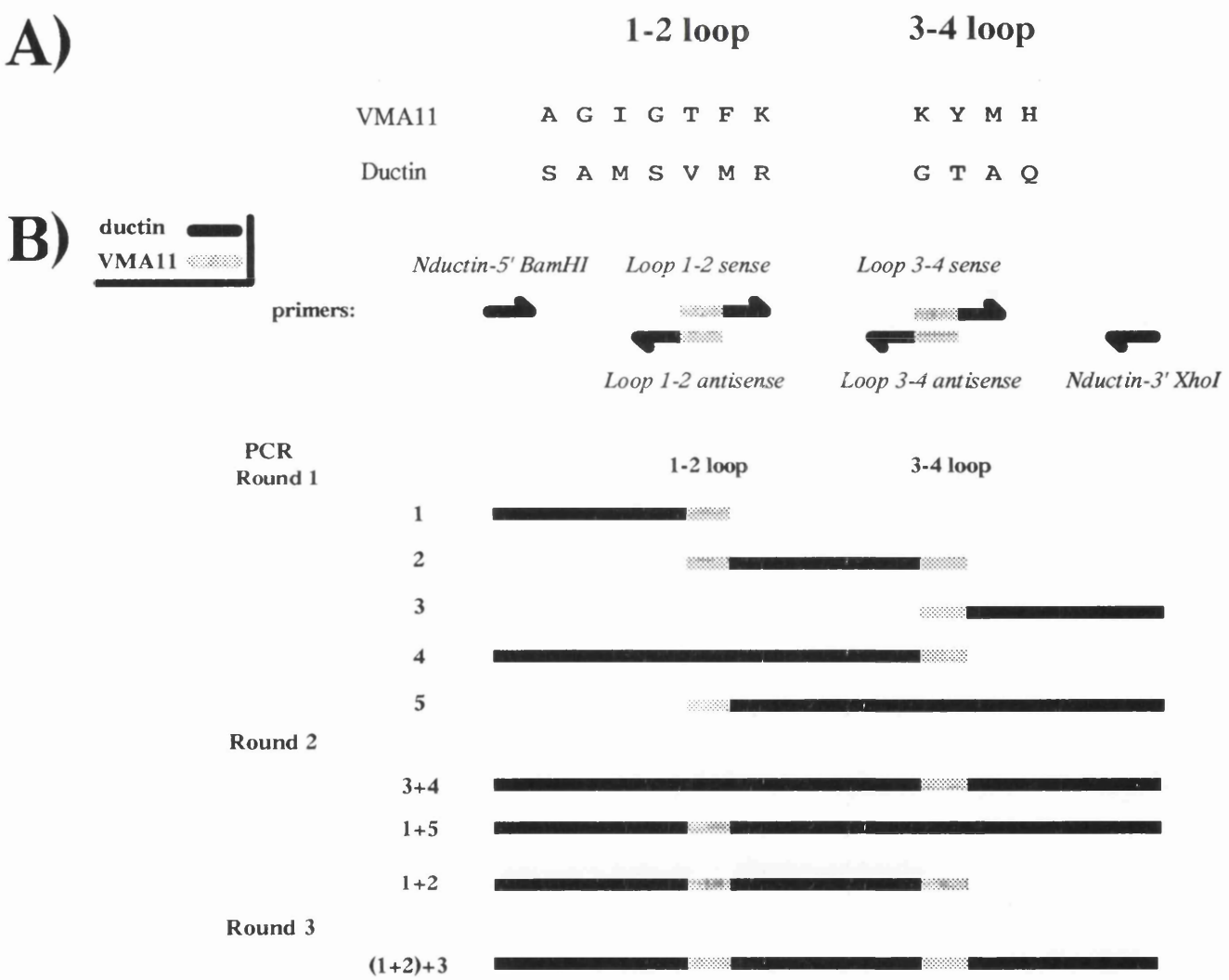
A)
1-2 loop
3-4 loop
VMA11
A G I G T F K
K Y M H
Ductin
S A M S V M R
G T A Q
B)
ductin
VMA11
Nductin-5' BamHI
Loop 1-2 sense
Loop 3-4 sense
primers:
Loop 1-2 antisense
Loop 3-4 antisense
Nductin-3' XhoI
PCR
Round 1
1-2 loop
3-4 loop
1
2
3
4
5
Round 2
3+4
1+5
1+2
Round 3
(1+2)+3

Figure 9. Partial sequence of the PCR cloned 1-2 loop chimera.

The sequencing was performed on pYES2 vector containing the 1-2 loop chimera cDNA, using a primer specific for upstream of the multiple cloning site, so as to read into the 5' end of the cloned cDNA. The deduced sequence for the 1-2 loop chimera was identical to the expected sequence.

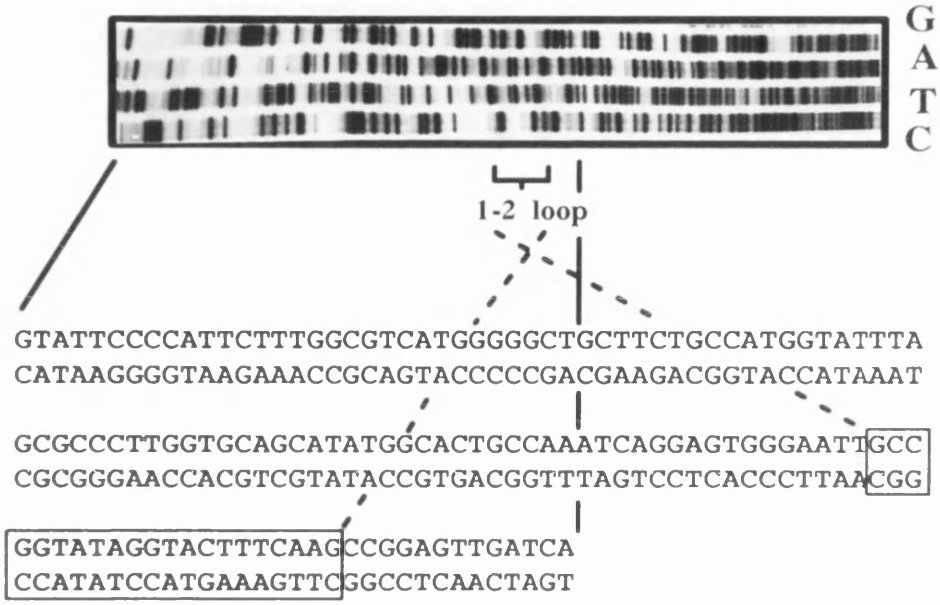
G
A
T
C
1-2 loop
GTATTCCCCATTCTTTGGCGTCATGGGGGCTGCTTCTGCCATGGTATTTA
CATAAGGGGTAAGAAACCGCAGTACCCCCCGACGAAGACGGTACCATAAAT
GCGCCCTTGGTGCAGCATATGGCACTGCCAAATCAGGAGTGGGAATTGCC
CGCGGGAACCACGTCGTATACCGTGACGGTTTAGTCCTCACCCTTAACGG
GGTATAGGTACTTTCAAGCCGGAGTTGATCA
CCATATCCATGAAAGTTCGGCCTCAACTAGT

3.2.6. Transformation of yeast

Large scale plasmid preparations were performed on the chimeric clones and the plasmid DNA was used to transform, using a modified lithium acetate protocol (Elble, 1992), both the *vat c* and *NUY43* strains of *S. cerevisiae*. The transformed yeast cells were plated out on the appropriate minimal media selection plates containing raffinose, and after 1-2 weeks of growth at 30°C transformed colonies were visible.

3.2.7. RT-PCR analysis of yeast transformed with loop chimeras

To confirm that the chimeric forms of ductin were being transcribed from the pYES2 plasmid, the transformed yeast were analysed for the presence of mRNA from the ductin chimeras. Total RNA was isolated from the yeast cells that had been transformed with the mutant forms of ductin, and which had been grown on the appropriate selective media supplemented with galactose. As mentioned above, the galactose induces the expression of genes present in the cloning region of the pYES2 vector. The total RNA was analysed for the presence of ductin transcripts by RT-PCR, using oligonucleotides specific to the 5' and 3' ends of ductin (table 2). mRNA was selected for during the reverse transcriptase step by using the oligo d(T)n primers. In all lanes a PCR product of ~500bp was observed (figure 10), the expected size for the full length Nductin chimeras, which indicated that all the transformed yeast cells analysed were expressing RNA transcripts of the ductin chimeras.

Figure 10. RT-PCR analysis of yeast transformed with loop chimeras of Nductin.

The yeast strains *vat c* and *NUY43* were transformed with the cDNA for the 1-2 loop chimera (lanes 1 and 6, respectively), the 3-4 loop chimera (lanes 11 and 5, respectively), the 1-2/3-4 double loop chimera (lanes 14 and 2, respectively), F24L (lanes 4 and 3, respectively), Y31I (lanes 13 and 9, respectively), F24L/Y31I (lanes 10 and 8, respectively), Nductin (lane 12) and VMA11 (lane 7) in the pYES2 yeast expression vector, after which total RNA was isolated from cells grown in the presence of 2% galactose to induce transcription from the GAL4 promoter. RT-PCR analysis was carried out on the total RNA using the primers *Nductin-5' BamHI* and *Nductin-3' XhoI* (table B), which are specific for the N- and C- termini of Nductin. The arrow indicates the expected size of the RT-PCR product, ~500bp. The DNA size marker is in the lanes marked VI, and the expected sizes of the DNA fragments are 2176, 1766, 1230, 1033, 653, 517, 453, 394, 298, 234, 220, and 154 bp.

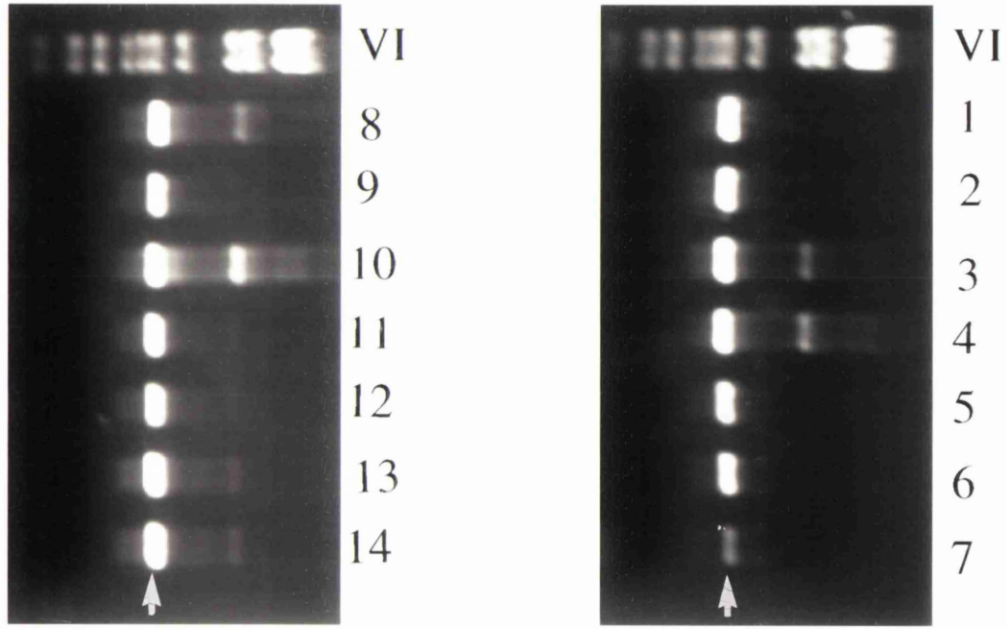
VI
8
9
10
11
12
13
14
VI
1
2
3
4
5
6
7

3.2.8. Expression of ductin chimeras in *S. cerevisiae*

The activity of the ductin chimeras was tested by transferring the transformed yeast cells onto full media plates that were pH buffered to pH 7.5 using 50mM MOPS and 50mM MES. The only transformed yeast cells able to grow at pH 7.5 are ones that are expressing an active ductin chimeric polypeptide. The expression of the ductin chimeras was induced by 2% galactose, in addition to the 2% raffinose, present in the full media. Colonies of transformed cells that could grow at pH 7.5 took 1-2 weeks to become visible and were subsequently photographed (figure 11). The growth characteristics of the ductin chimeras are listed in table 4. The three loop replacement chimeras were unable to restore the growth of *NUY43* cells at pH 7.5, while only the loop 1-2 replacement chimera was able to restore growth of the *vat c* cells at pH 7.5, but with a reduced rate of growth compared to Nductin. Neither the 3-4 loop replacement chimera or the double loop replacement chimera were able to restore growth of the *vat c* cells at pH 7.5. The V-ATPase activity of the single chimera to exhibit any growth, the 1-2 loop chimera, was tested by performing an ATPase assay on vacuoles isolated from this chimera. The ATPase activity was found to be low when compared with activity of the wild type Nductin containing V-ATPase.

The results of this experiment show firstly the importance of the two conserved extramembranous loops in the activity of ductin in the V-ATPase. Secondly, they show that the VMA11 polypeptide is unlikely to be able to function in the V-ATPase, confirming the previous results (Umemoto et al., 1991) that the VMA11 polypeptide cannot substitute for the *vat c* function.

Figure 11. Growth of transformed yeast at pH 7.5.

A) The *vat c* yeast strain grown at pH 7.5 in the presence of 2% galactose after transformation with the pYES2 expression vector containing Nductin cDNA.

B) The *NUY43* yeast strain grown at pH 7.5 in the presence of 2% galactose after transformation with the pYES2 expression vector containing VMA11 cDNA.

C) The *vat c* yeast strain grown at pH 7.5 in the presence of 2% galactose after transformation with the pYES2 expression vector containing 1-2 loop chimera cDNA.

A

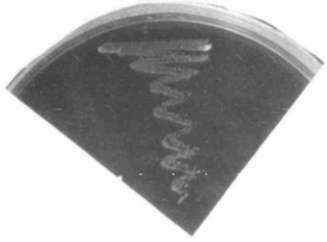

B

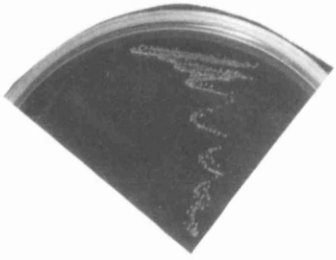

C

3.2.9. Western analysis of yeast transformed with ductin chimeras

Although having a low V-ATPase activity the 1-2 loop replacement chimera could be detected in the *vat c* cells. Vacuolar membranes were isolated using Ficoll gradients, and 7μg of the isolated vacuolar protein was loaded onto a 12.5% SDS-PAGE gel and once the protein sample was separated it was transferred to a nitrocellulose filter. The antibody used to probe the western blot was a polyclonal antisera (N2) raised against Nductin (Leitch and Finbow, 1990). A band was observed at 16kDa that was the same size as for the control Nductin that had been isolated from *Nephrops* gap junctions (Figure 12).

3.2.10. Construction and expression of further mutations to the double loop chimera.

The inability of the loop replacement chimeras to restore the growth in the NUY43 cells suggested that the difference in activity between ductin and VMA11 was not confined to the 1-2 and 3-4 loop regions and that additional regions or residues play a role in distinguishing the activity of the two polypetides. One candidate region that came to light from a mutagenesis study as possibly containing additional distinguishing features is the first transmembrane region of Nductin (Jones et al., 1994). This region was being studied as part of an effort to confirm the helical arrangement of ductin when it is part of the V-ATPase. A number of residues in the first helical region of the Nductin were mutated to cysteine and the effect on the activity of ductin assayed (table 5). Of particular note were the residues F24 and Y31, since when either were replaced by cysteine the activity of the V-ATPase was significantly reduced (Jones et al., 1994). These two residues are conserved in ductin, from fungi to higher eukaryotes, but are different in VMA11 being replaced by L and I, respectively (figure 6). These two aromatic

Figure 12. Western analysis of the 1-2 loop chimera.

Vacuolar membranes were isolated from *vat c* cells expressing the 1-2 loop chimera and the protein separated by 12.5% SDS-PAGE. After transfer onto nitrocellulose the blot was probed with the primary antibody, N2 antisera, at 1:100 dilution and the presence of antigen was visualised by chemiluminescence using the ECL-Western kit from Amersham. Lanes 1 and 2 are vacuolar membrane protein isolated from *vat c* and *NUY43* cells, respectively, expressing the 1-2 loop chimera polypeptide. Lanes 3 and 4 are different exposures of the control Nductin, isolated from gap junctions.

1-2 loop chimera

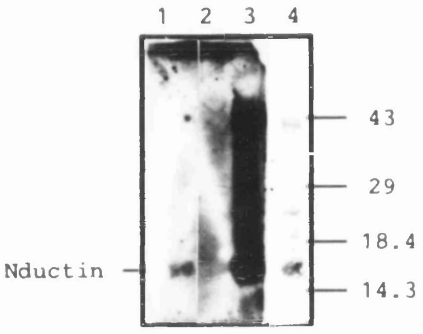

Table 5. Functional properties of *vat c* strains expressing mutagenised Nductin.

Codes refer to the changed residue, its position in the primary structure and the amino acid which has been introduced. Vacuolar membrane ATPase specific activities are expressed as μmol ATP hydrolysed/mg protein/min. Km is expressed for ATP (mM). Vacuolar membrane isolation and ATPase assay were performed as in Uchida et al., (1985). Values in parentheses reflect ATPase activity relative to that in the C54S mutant. ND, not determined (taken from Jones et al., 1994).

Mutant strain	Specific activtiy	Km	Growth at pH7.5
C54S	0.17 (100)	0.4	+
S6C	0.12 (71)	0.4	+
F24C	0.29 (171)	0.7	+/-
S25C	0.29 (171)	0.8	+/-
A26C	0.13 (76)	0.4	+
L27C	0.13 (76)	0.4	+
A29C	0.12 (71)	0.4	+
A30C	0.17 (100)	0.4	+
Y31C	ND	ND	+/-
S44C	0.15 (88)	0.4	+

residues are predicted to lie on the same face of helix 1, perhaps forming a contact between this helix and helix 4 (figure 13). Therefore, these two residues may contribute to the difference in activity between ductin and VMA11.

To test this possibility single site mutations to the residues F24 and Y31 were made, and were changed to L and I respectively in the double loop replacement chimera. In addition, the double substitution F24L/Y31I was also constructed in the double loop chimera. These substitutions were carried out with the oligonucleotides listed in Table 3 using the same PCR strategy as for the construction of the original loop replacement chimeras. As before, the full length PCR products were cloned into the pCR II vector using the TA cloning kit (Invitrogen) and subcloned into pYES2 at the *BamH I* and *Xho I* cloning sites, after which the region containing the altered nucleotides was sequenced and the changes confirmed. As for the original ductin chimeras, F24, Y31 and F24L/Y31I were expressed in both *vat c* and *NUY43* yeast cells. RT-PCR confirmed the presence of RNA products for each polypeptide (figure 10). The activity of the new ductin mutants was tested by growing the transformed cells at pH 5.5 and pH 7.5, in full media containing galactose. The results of the growth assay are shown in table 6. No growth in either the *vat c* or the *NUY43* cells was observed for F24L, Y31I or F24L/Y31I, indicating that they were still defective in restoring wild type ductin activity and that there was no new VMA11 like activity present in the ductin mutants.

Figure 13. A model depicting the character of the proposed surfaces of the four α-helix bundle of Nductin.

The amino acid sequence underneath the model correspond to residues 20 to 34 in helix 1 of Nductin, and the underlined residues have all been modified to cysteines and the subsequent effect on V-ATPase activity assayed. The two residues, F24 and Y31, are highlighted in grey since they disrupt the activity of Nductin when modified to cysteine (modified from Finbow et al., 1995).

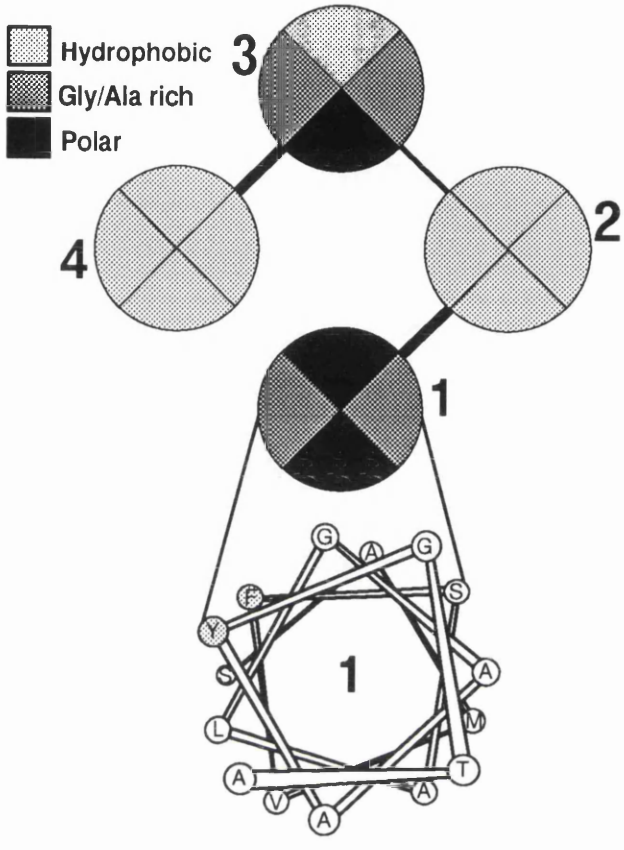

SAMV FSALGAAY GTA

Table 6. pH growth characteristics of F24L, Y31I and F24L/Y31I

Growth at pH 7.5 was assayed for *vat c* and *NUY43* strains of *S. cerevisiae* after transformation with cDNA coding for F24L, Y31L and F24L/Y31I in the pYES2 yeast expression vector. YPD agar plates were supplemented with 2% galactose to induce expression from pYES2.

cDNA	Growth at pH 7.5	
	vat c	*NUY43*
F24L	-	-
Y31I	-	-
F24L/Y31I	-	-

3.2.11. Discussion

3.2.11.1. Replacement of the conserved loop regions of ductin

The only chimeric Nductin that restored partial V-ATPase activity was the 1-2 loop chimera. A total of 7 residues were exchanged in this chimera and although a number of those residues were conservative changes, the cumulative effect of the 7 changes might have been expected to result in a complete loss of activity for the chimeric polypeptide. That this was not the case suggests that the 1-2 loop region is not crucial for the activity of ductin in the V-ATPase complex. The loss of activity that was observed, as seen in the slower growth of colonies at pH 7.5 and the low ATPase activity of isolated vacuoles does though indicate that this region has an important influence on the activity of ductin when in the V-ATPase complex.

In contrast, when the 3-4 loop region of ductin was replaced with the equivalent region of VMA11, the resulting chimeric polypeptide was not able to substitute the missing ductin activity in the *vat c* strain. Only four residues replaced in the 3-4 loop region but the character of the residues that were exchanged was much more diverse than in the 1-2 loop region. The resulting chimeric polypeptide was unable to function in the V-ATPase complex, thus the sensitivity of this region provides evidence for the importance of this region to the activity of ductin. In addition, the 1-2 and 3-4 double loop replacement ductin chimera was not able to substitute the wild-type ductin activity.

The loop replacement chimeras of ductin do not directly show that this region acts as an interface between ductin and other V-ATPase subunits, but what they do show, especially for the 3-4 loop region, is the importance of these regions for the

activity of ductin and the continuing relevance of the equivalent work on subunit *c*. In subunit *c* the loop region has an important role in the activity of the polypeptide, as has now been shown for the 3-4 loop region of ductin. It seems therefore to be no coincidence that the character of the subunit *c* loop region resembles that of the 3-4 loop region, and if so then the 3-4 loop may perform an analogous role in the activity of ductin, that of coupling the ATPase activity with H^+ translocation. The importance of these two loop regions and their location in the V-ATPase complex with regard to the possible site of proton translocation and V_0-V_1 interaction will be discussed in section 4.1.

The ductin loop replacement chimeras were also expressed in the *NUY43* strain in the prediction that the chimeric polypetides should be able to substitute the missing VMA11 activity. At this time there is no data as to what role VMA11 may perform in yeast cells, but the high degree of homology between VMA11 and ductin suggests that the two polypeptides perform similar but distinct functions. The lack of activity of the loop replacement chimeras in the *NUY43* cells indicates that this was not the case and there is more to the difference in activity between ductin and VMA11 than the differences between the 1-2 and 3-4 loop regions.

3.2.11.2. Additional mutation of the 1-2/3-4 loop chimera to VMA11

In an effort to change the activity of ductin to that of VMA11 two further residues of ductin were mutated to their equivalent residue in VMA11. The two residues were F24L and Y31I, both of which are in the first transmembrane region and have been shown to be sensitive to replacement by cysteine (Jones et al., 1994). When the double loop chimera with these additional alterations, either singly or with both present, was expressed in the *NUY43* strain there was no observable growth, indicating that the polypeptides still had no VMA11 activity. These results demonstrate that the differences between ductin and VMA11 cannot be easily

determined from the amino acid sequences of the two polypeptides and that they are more widespread than at first thought. What in fact are determines the difference in activity between the two polypeptides remains unclear and probably involves a number of regions and residues spread throughout the polypeptides.

3.2.11.3 The yeast expression system as a tool

The expression of ductin in the *vat c* strain of *S. cerevisiae* provides a convenient assay for the activity of ductin when it is part of the V-ATPase complex. This allows the effect of mutations on ductin to be tested and related to the normal activity of ductin in the V-ATPase complex. A disadvantage with this system is the inability to distinguish the cause of inactivating mutations to ductin, that is, a particular mutation can only be described as active or inactive without an understanding of why that is the case. Since the process that leads to ductin becoming incorporated into an active ATPase complex is multi-step the large number of potential failure points along that pathway can make interpreting the results of an inactive mutant ductin difficult. A similar problem has been noted while studding the assembly of phospholamban, a cardiac ion channel (Arkin et al., 1994). The mutation of residues that line the pore caused a disruption in the stability of the phospholamban complex, not a result that was expected and that could easily have been wrongly interpreted. Part of the problem could be potentially overcome if a simpler expression system could be used to examine, for example, assembly of the ductin core complex. In the following section, such a system has been used to study ductin.

3.3. Synthesis and assembly of ductin.

3.3.1. Introduction

According to the presently accepted concepts of membrane protein orientation (von Heijne, 1995) ductin should only have a single orientation, whereas the experimental evidence would suggest that ductin has two membrane orientations (Finbow et al., 1993). One of the aims of this thesis is to resolve this difference between the published data on the orientation of ductin and the accepted concepts of membrane protein orientation. As a start to this, the first steps in the synthesis of the ductin polypeptide will be studied using a model system based on cell-free expression of the polypeptide in rabbit reticulocyte lysate.

Such an approach should determine the manner of ductin synthesis, i.e. is it SRP-dependent, and how it becomes incorporated into the membrane. In addition, it should allow an approach to examine the process of assembly of ductin oligomers. This *in vitro* system has been used in other studies to examine the synthesis and insertion into the ER of polytopic transmembrane proteins (Miao et al, 1992, Skach et al, 1994, Falk et al, 1994).

3.3.2. Examination of an *in vitro* expression system - β-lactamase.

Commercial sources are available for both a rabbit reticulocyte lysate (Promega) and canine pancreatic microsomes (Promega). This lysate consists of a reticulocyte extract that has been treated with micrococcal nuclease to degrade the endogenous mRNA. This treated lysate contains the cellular components required for protein synthesis and has been optimised for the translation of added mRNA. Translation of mRNA in the presence of microsomal membranes allows a number of polypeptide processing events to be studied, including signal sequence cleavage,

membrane insertion and translocation, and core glycosylation. The processing activity of the microsomal membranes can be assayed using the control β-lactamase mRNA provided with the microsomal membranes.

Translation of β-lactamase mRNA leads to an unprocessed form of the protein of 32kDa in size (figure 14). When microsomes are added, there is an appearance of a band at ~29kDa consistent with removal of the N-terminal signal sequence of β-lactamase. These results indicate that β-lactamase has been translocated through the microsomal membrane. Further evidence for this comes from the protection afforded to the polypeptide against proteolytic degradation by the microsomal membrane. Once the processed form of β-lactamase was translated in the presence of microsomal membranes it was found to be protected from the action of trypsin in the absence but not in the presence of detergent (figure 14, lanes 2 and 3). The presence of the detergent disrupted the microsomal membranes and gave the trypsin access to the lumen where it digested the β-lactamase.

The two possible locations for a polypeptide in the microsomal membrane are in the lumen or in the lipid bilayer. To distinguish between these two possibilities the microsomal membranes can be treated with sodium carbonate at pH 11, causing the contents of the lumen to be released. The membrane fraction of the microsomes can then be separated from the lumenal contents by centrifugation in a Beckman TL-100 Ultracentrifuge at 50000 rpm for 60 minutes. When this was performed on *in vitro* translated β-lactamase it was found in the supernatant and therefore is associated with the contents of the microsomal lumen and not the membrane (figure 14, lane 6). These results confirm the location of β-lactamase after translocation as being in the lumen of the microsomal membranes, as expected for a secreted polypeptide.

Figure 14. Synthesis and insertion of β-lactamase into microsomal membrane. Control mRNA encoding β-lactamase was translated in the presence of microsomal membranes. Lanes 1, 2 and 3 are β-lactamase after treatment with (+) or without (-) trypsin and either in the presence (+) or absence (-) of triton, as indicated above each lane. In lanes 5 and 6, microsomal membranes were extracted with sodium carbonate and centrifuged to pellet integral membrane protein (lane 5, 'p') from peripheral and lumenal protein (lane 6, 's'). Lane 4 represents the microsomal membranes before extraction with sodium carbonate. The upper β-lactamase band corresponds to the unprocessed form, while the lower band has been processed by the removal of the signal sequence. The protein samples were visualised by 12.5% SDS-PAGE and autoradiography.

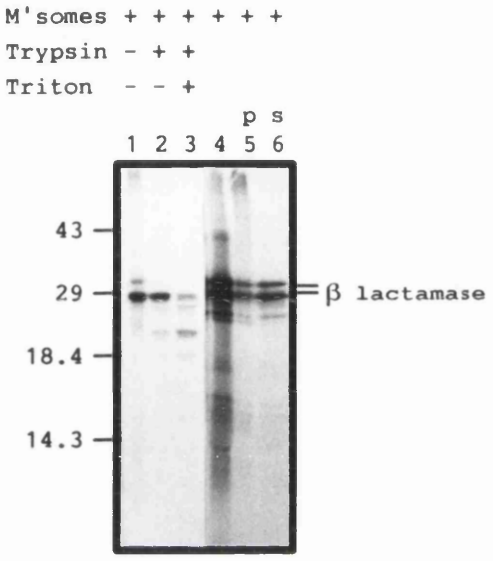
M'somes + + + + + +
Trypsin - + +
Triton - - +
p s
1 2 3 4 5 6
43
29
18.4
14.3
β lactamase

3.3.3. Synthesis of squid rhodopsin.

To characterise the microsomal membranes with respect to an integral membrane protein, as opposed to the secreted β-lactamase, squid rhodopsin was used as a model protein (Hall et al, 1991). This polypeptide is a member of the seven transmembrane α-helical receptor family in which the N-terminus is extracellular and the C-terminus is cytoplasmic (figure 15B). In isolated photoreceptor membranes, the C-terminus of squid rhodopsin was removed by endoproteinease glu-c and gave a N-terminally derived 36kDa form instead of the mature 47-kDa form (Ryba et al, 1993). The 36kDa form represented the core integral membrane section of squid rhodopsin. The correct insertion of squid rhodopsin into the microsomal membranes was tested by determining the orientation of the polypeptide after insertion. The C-terminal region of squid rhodopsin will be exposed on the cytoplasmic face of the microsomal membranes and available for cleavage by endoproteinease glu-c if the process of insertion has occurred correctly. Alternatively, if squid rhodopsin had been incorrectly inserted, then it should be resistant to the proteinase. Treatment of *in vitro* translated squid rhodopsin with endoproteinease glu-c resulted in the loss of the full length 47kDa form and the appearance of a 36-kDa product instead, indicating the presence of the correct, single orientation in the microsomal membranes (Figure 15A). The above results indicate the suitability of using the rabbit reticulocyte lysate coupled with microsomal membranes as an expression system for examining the synthesis and insertion of ductin.

Figure 15. Membrane insertion and orientation of squid rhodopsin.

A) Squid rhodopsin (Mr 47,000) was translated *in vitro* in the presence of microsomes, and then treated for the times shown with endoproteinase glu-C (V8 protease) at 0.01 mg/ml for 1 hour at room temperature, before being visualised by 12.5% SDS-PAGE and autoradiography. B) Predicted transmembrane topology of squid rhodopsin. Squid rhodopsin is a member of the G-protein receptor superfamily, and consists of seven transmembrane regions with the C-terminus exposed on the cytoplasmic face of the lipid bilayer where it is accessible to proteases (modified from Hall et al., 1991).

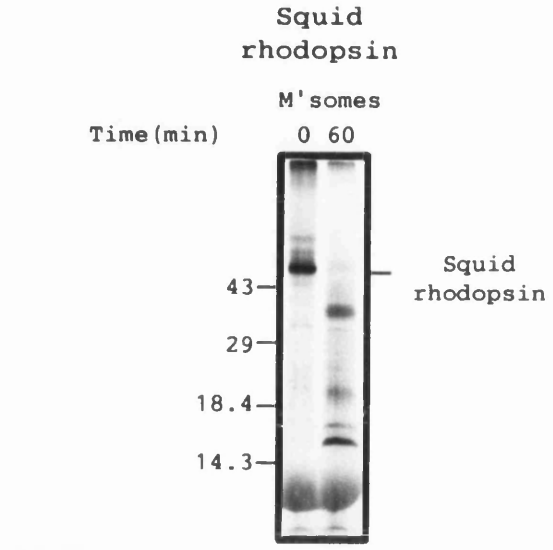
Squid
rhodopsin
M'somes
Time(min)
0 60
43
29
18.4
14.3
Squid
rhodopsin

A

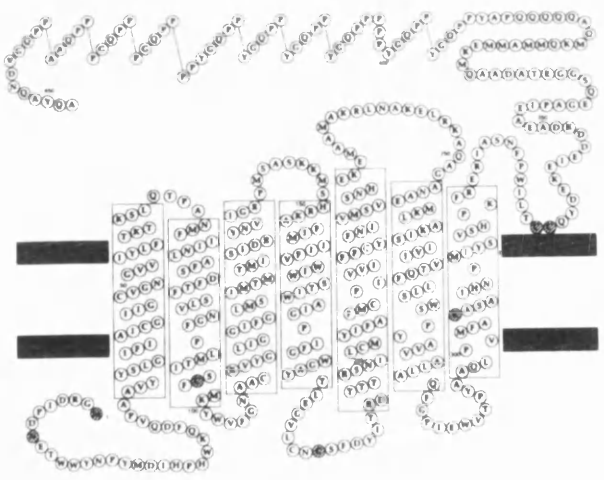

B

3.3.4. Synthesis of Nductin.

The ductin cDNA from *Nephrops norvegicus* (courtesy of P. McLean, Beatson Institute) in pBluescript (Stratagene) was used as the template to produce mRNA for translation in the *in vitro* system. The plasmid was linearised prior to *in vitro* transcription using the restriction enzyme *Xba I*, which cuts downstream of the Nductin stop codon. The linearised plasmid was purified by phenol extraction then used as a template for the production of capped mRNA by T7 RNA polymerase using the T7 mMessage mMachine kit (Ambion). The Nductin mRNA was added to reticulocyte lysate that had either no microsomal membranes present or to lysate that had been supplemented with microsomal membranes. Translated Nductin polypeptide was then immunoprecipitated using the N2 antisera and visualised by SDS-PAGE on a 12.5% gel followed by autoradiography. The efficient translation of ductin mRNA was found to be dependant on the presence of the microsomal membranes (Figure 16) since in the absence of the microsomes only a relatively small amount of ductin could be detected compared to when it was translated in the presence of microsomal membranes. The block in translation in the absence of membranes indicates that ductin is probably inserted into the microsomes using the SRP-dependent pathway, consistent with ductin being a polytopic membrane polypeptide (Walter et al, 1984).

The *in vitro* synthesised Nductin co-migrated with ductin isolated from gap junctions showing there is no signal sequence cleavage. Further evidence of SRP-dependency comes from using a wheatgerm extract translation system. In this *in vitro* system, SRP is absent and therefore SRP-dependent proteins are translated in the absence of microsomal membranes. Such an experiment showed that Nductin was indeed synthesised in wheatgerm extract in the absence of microsomal membranes (figure 16, lanes 5 and 6).

Figure 16. Synthesis and insertion of Nductin into microsomal membrane. Capped mRNA encoding Nductin was translated in the presence (lane 1, shown as '+') or absence (lanes 2, shown as '-') of microsomal membranes before immunoprecipitation with antibodies to Nephrops ductin (N2). In lanes 3 and 4, microsomal membranes containing translated Nductin were extracted with sodium carbonate and centrifuged to pellet the membrane component (lane 3, 'p') and so separate it from peripheral and lumenal protein (lane 4, 's'). In lanes 5 and 6 the Nductin mRNA was translated using the wheatgerm extract system, either in the presence (lane 5, '+') or absence (lane 6, '-') of microsomal membranes. The protein samples were visualised by 12.5% SDS-PAGE and autoradiography.

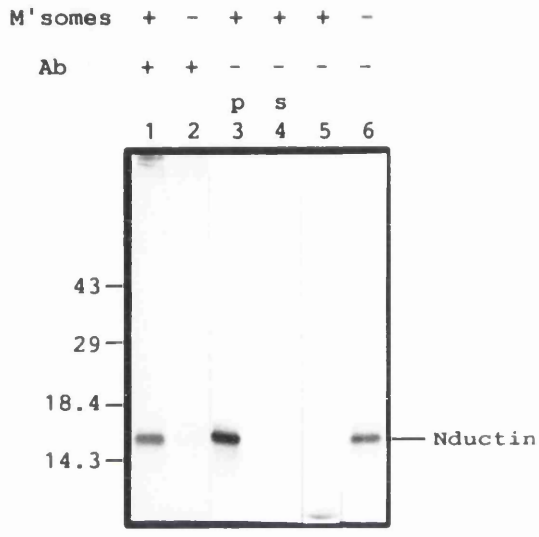
M'somes + - + + + -
Ab + + - - - -
p s
1 2 3 4 5 6
43
29
18.4
14.3
Nductin

3.3.5. Membrane insertion of Nductin.

The location of newly synthesised ductin within the microsomes was examined in the same manner as previously for β-lactamase. Nductin that had been translated in the presence of microsomes was treated with trypsin in the absence and presence of the detergent Triton X-100. Nductin was not digested by the trypsin when no detergent was present, but it was digested in the presence of detergent (figure 17). The protection of Nductin from digestion indicates that Nductin is present within the microsomal membranes or the lumen of the microsomes. To distinguish between the two possible locations within the microsomal membranes, the lumen or the lipid bilayer, the contents of the microsomal lumen were extracted using sodium carbonate, pH 11. Nductin was found to be present in the membrane fraction after centrifugation (Figure 16, lane 3). These results confirm that ductin has been inserted into the lipid bilayer of the microsomal membranes, the expected location for an integral membrane protein. The digestion of ductin by trypsin in the presence of detergents contrasts with the inability of trypsin to digest ductin isolated from gap junctions, in the presence of detergents (Finbow et al., 1984). This suggests that Nductin , although possibly present in oligomeric forms (see section 3.3.9.), is not organised into large membrane arrays of the form characteristic of gap junctions.

3.3.6. Orientation of ductin in the microsomal membranes.

3.3.6.1. Introduction.

Ductin has no post-translational processing events (e.g. signal peptide cleavage or glycosylation) that can act as markers for the orientation of ductin after insertion. To overcome this, a fusion polypeptide was made by adding 67 amino acids from

Figure 17. Trypsin digestion of Nductin.

Nductin (lanes 1, 2 and 3) was translated *in vitro* in the presence (+) of microsomal membranes (M'somes), then treated either with (+) or without (-) 0.025% trypsin, both in the absence (-) and presence (+) of 1% triton. The digest was performed for 60 minutes at room temperature and the protein immunoprecipitated using the N2 antisera, before being visualised by 12.5% SDS-PAGE and autoradiography.

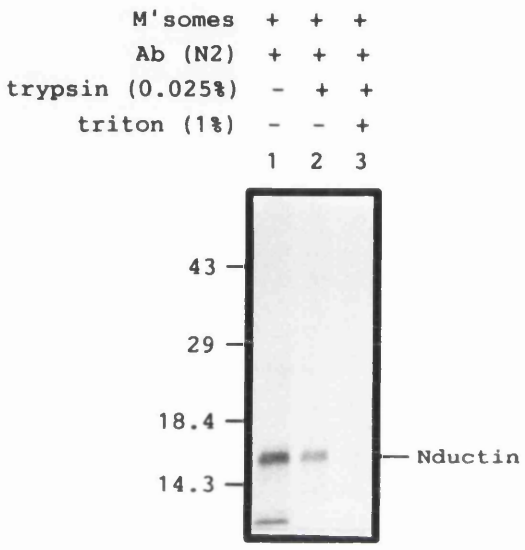
M'somes + + +
Ab (N2) + + +
trypsin (0.025%) - + +
triton (1%) - - +
1 2 3
43
29
18.4
14.3
Nductin

the N-terminus of β-lactamase to the C-terminus of Nductin (Nductin-β lac) to provide a trypsin sensitive extension. β-lactamase was chosen as the source of the extension since it is known to translocate efficiently in the microsomal membranes, does not contain any transmembrane segments, and has multiple tryptic cleavage sites, the closest one being 12 residues downstream of the C-terminus of Nductin: so the β-lactamase extension would be expected to have no influence on the insertion of the Nductin portion of the fusion polypeptide. Adding a C-terminal extension on to Nductin would not be thought to influence the orientation of the chimeric protein because on current models of membrane insertion coupled to synthesis, the C-terminal region would not be synthesised until after the N-terminus of Nductin has been inserted into the membrane (see section 1.2.3.).

Once Nductin-β lac has been inserted into the microsomal membranes the accessibility of the extension to trypsin can be determined by the orientation of insertion (figure 18). There are three possible outcomes that can be envisaged after trypsin treatment of Nductin-β lac. If the N-terminus of Nductin-β lac is exposed on the cytoplasmic face then the extension will be cleaved by trypsin, causing a shift in the migration of the polypeptide, whereas if the N-terminus is exposed on the lumenal face then there will be no trypsin digestion and no shift in migration. The presence of both digested and undigested Nductin-β lac would indicate the presence of a mixed population of polypeptides distinguishable by their orientation.

3.3.6.2. Construction of Nductin-β lac.

The fusion polypeptide Nductin-β lac was constructed using a PCR based strategy. For this approach (outlined in figure 19), two overlapping PCR products were first prepared, *T7pol*ductin and β-*lac*term. *T7pol*ductin contained a T7 RNA polymerase site, the ORF for Nductin and an overlap with the second PCR

Figure 18. The predicted band pattern of Nductin-β lac before and after trypsin treatment.

A) Model of the three potential orientation profiles for Nductin-β lac, where 1 represents Nductin-β lac having the N- and C-termini lumenally exposed, 2 represents Nductin-β lac having a mixed population of the two orientations and 3 represents Nductin-β lac having the N- and C-termini exposed on the cytoplasmic face. B) A representation of an idealised SDS-PAGE analysis of 1, 2 and 3 after treatment with trypsin, showing the digestion pattern of Nductin-β lac; with, 1- no digestion of the C-terminal extension, 2- partial digestion of the C-terminal extension, and 3- full digestion of the C-terminal extension. C) A diagram of Nductin-β lac indicating the approximate positions of potential tryptic cleavage sites. There are four lysine residues 12, 14, 35 and 53 amino acids downstream of the C-terminus of Nductin. In addition there is a arginine residue 23 amino acids downstream of the C-terminus of Nductin.

A

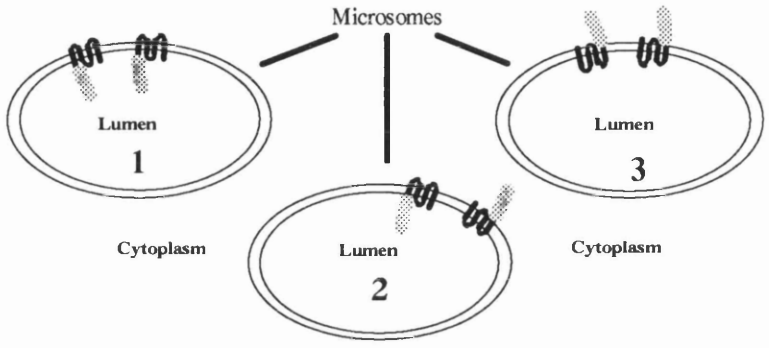
Microsomes
Lumen
1
Lumen
3
Cytoplasm
Lumen
2
Cytoplasm

B

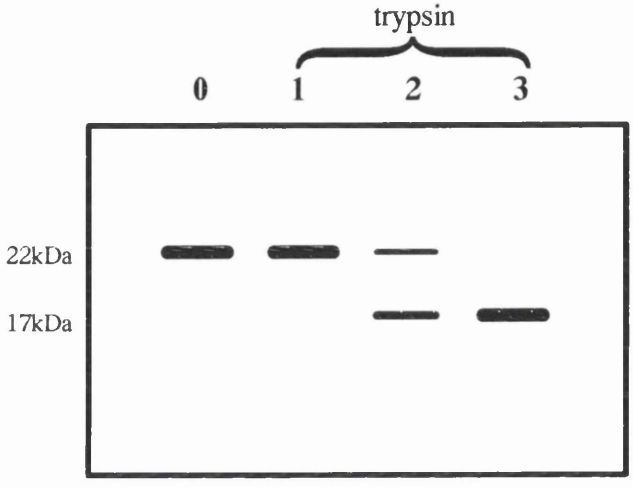
trypsin
0
1
2
3
22kDa
17kDa

C


1
155
18
**
*
*
*
85
Nductin-β lac


ductin
β-lactamase
Nductin-β lac
potential tryptic cleavage site
*

Figure 19. PCR strategy for the generation of the extended Nductin, Nductin-β lac.

Two rounds of PCR were used to generate Nductin-β lac which contained a T7 RNA polymerase site 5' of the ATG start codon for the fusion polypeptide. In the first round of PCR two DNA fragments were generated, *T7pol*ductin using the primers *T7 Nductin* and *Nductin T4A sense*, and β-*lac*term using the primers *Nductin T4A* antisense and *b-lac 3' anti*. The primers *Nductin T4A sense* and *Nductin T4A antisense* are complementary to each other, which means that the DNA fragments *T7pol*ductin and β-*lac*term have a region of overlap at their 3' and 5' ends, respectively. The region of overlap allows the two DNA fragments to anneal together and it this annealed product which is amplified during the second round of PCR. *T7pol*ductin and β-*lac*term were purified then mixed, and used for the template DNA in the second round of PCR, using the *T7 Nductin* and β-*lac 3' anti* primers to generate the full length Nductin-β lac fusion construct.

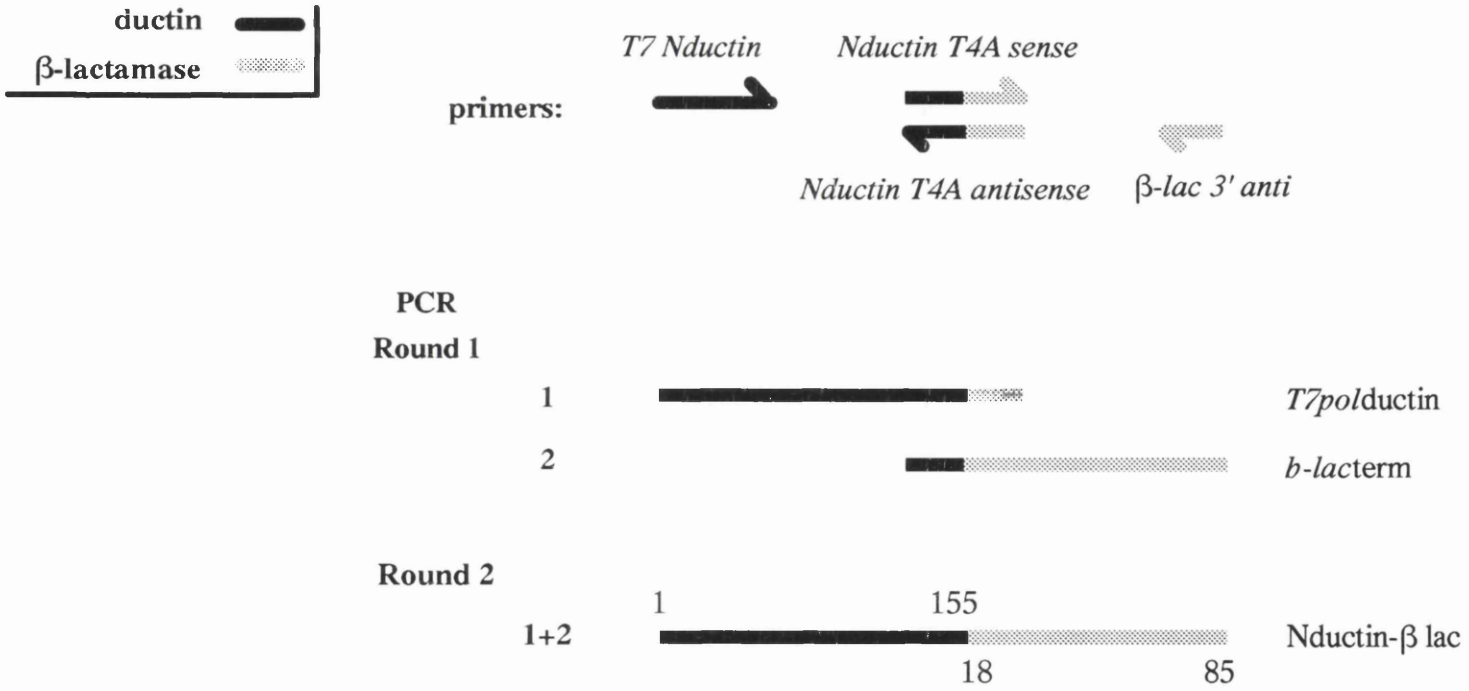
ductin
β-lactamase
primers:
T7 Nductin
Nductin T4A sense
Nductin T4A antisense
β-lac 3' anti
PCR
Round 1
1
T7polductin
2
b-lacterm
Round 2
1+2
1
155
18
85
Nductin-β lac

product. The inclusion of a T7 RNA polymerase site in *T7pol*ductin was to allow the use of the PCR DNA directly in the *in vitro* transcription reaction, as had been done for Nodulin 26 (Miao et al., 1992). Previous attempts to clone Nductin-β lac into a vector containing an upstream T7 RNA polymerase site had failed, hence the need to use the PCR DNA directly for the *in vitro* transcription. The PCR DNA was generated using the forward primer *T7 Nductin* (table 8) and the reverse primer *Nductin T4A antisense* (table 7) which encoded the 5 C-terminal residues of *Nephrops* ductin plus one extra base, and residues 18 to 23 of β-lactamase (from *Esherichia coli*). β-*lac*term was generated using *Nductin T4A sense*, the complimentary oligonucleotide to *Nductin T4A sense* (table 7) which was used to generate *T7pol*ductin, and a reverse oligonucleotide primer, β-*lac 3' anti*, which encoded residues 80 to 85 plus two extra bases together with an in-frame termination codon and a Xho1 restriction site. Excess oligonucleotides from the first round of PCR were removed by "Wizard" spin column purification (Promega) of the PCR products after agarose gel electrophoresis had separated the PCR product from the oligonucleotides. *T7pol*ductin and β-*lac*term were hybridised and used as a template for a second round of PCR, which generated the full length DNA product, Nductin-β lac, by using the external primers *T7 Nductin* and β-*lac 3' anti* (table 2).

3.3.6.3. Trypsin digestion of Nductin-β lac

Capped mRNA was transcribed directly from the Nductin-β lac PCR DNA using the T7 mMessage mMachine kit (Ambion) and then translated in the *in vitro* system. Nductin-β lac gave a band of apparent size 22-kDa on SDS-PAGE, the predicted size of the fusion polypeptide and retained the dependency on microsomes for synthesis that had been observed for Nductin (Fig 20). After the separation of the microsomal membranes from the reticulocyte lysate by centrifugation, Nductin-β lac was present in the pellet containing the membranes

Table 7. Nucleotide sequence of internal primers for Nductin-β lac and VMA11-β lac fusion polypeptides.

Internal primers-ductin fusion protein

Nductin T4A antisense:

5' GTGAGCAAAAACAGGAAGGCTGGAGGTCTTGGTG 3'

Nductin T4A sense:

5' CACCAAGACCTCCAGCCTTCCTGTTTTTGCTCAC 3'

VMA11 T4A antisense:

5' CAGCGTTTCTGGGTGTTCAGAGCCTCTAGT 3'

VMA11 T4A sense:

5' ACTAGAGGCTCTGAACACCCAGAAACGCTG 3'

Table 8. Nucleotide sequence of 5' primers containing a T7 RNA polymerase site.

T7 RNA polymerase primers

T7 Nductin:

5' GGATCCTAATACGACTCACTATAGGGAGGCTCAAAATGTCTGAA GAGGG 3'

T7 Nductin AA:

5' GGATCCTAATACGACTCACTATAGGGAGGCTCAAAATGTCTGCA GCGGGTAGTCCT

T7 Nductin KK:

5' GGATCCTAATACGACTCACTATAGGGAGGCTCAAAATGTCTAAA AAGGGTAGTCCT 3'

T7 VMA11:

5' GGATCCTAATACGACTCACTATAGGGAGGGTAAACATGTCAACG CAACTC

Figure 20. Synthesis and insertion of Nductin-β lac into microsomal membrane.

Capped mRNA encoding Nductin-β lac (lanes 1 and 2) was translated in the presence (lanes 1, '+') or absence (lanes 2, '-') of microsomal membranes before immunoprecipitation with N2 antisera, after which the protein was resolved on a 12.5% SDS-PAGE gel and visualised by autoradiography.

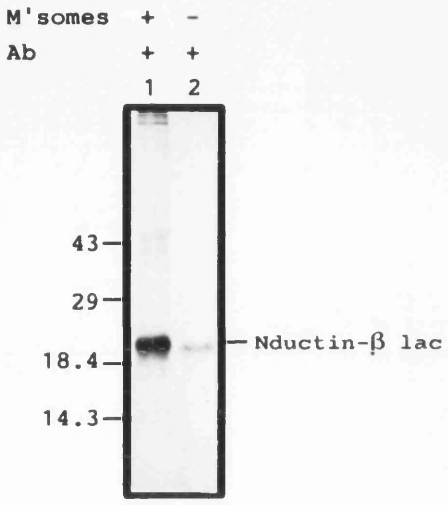
M'somes + -
Ab + +
1 2
43
29
18.4
14.3
Nductin-β lac

(figure 24), as was the case for Nductin. The β-lactamase portion of Nductin-β lac introduces a potential trypsin cleavage site 12 amino acids downstream from the C-terminus of the ductin sequence, which should lead to an identifiable increase of ~1kDa in the migration of the core membrane region of Nductin-β lac when compared to Nductin.

The translated Nductin-β lac was treated with trypsin under a number conditions including variable trypsin concentration, length of digestion and temperature at which the digest was performed. First of all, Nductin-β lac was treated with a number of different concentrations of trypsin, 0.025%, 0.05% and 0.25%, at room temperature for 30 minutes before being immunoprecipitated with the N2 antisera, in the presence of a trypsin inhibitor. At 0.025% and 0.05% trypsin the two main bands present are 22kDa and 17kDa in size, whereas at 0.25% trypsin only a faint 17kDa band was observed (figure 21). The 22kDa band co-migrates with the full length Nductin-β lac that was not treated with trypsin, while the 17kDa band corresponds in size to that predicted for Nductin-β lac after removal of the C-terminal extension at the trypsin sensitive site 12 amino acids downstream of the join between the Nductin and β-lactamase portions. At 0.25% trypsin almost all the Nductin-β lac was fully digested, leaving only a faint 17kDa band (figure 21, lane 2). At this high concentration, the near complete digestion of the 17kDa band, which is predominantly of Nductin origin, in the absence of detergents suggests there is a breakdown of the microsomal membrane. The presence of both digested and undigested Nductin-β lac at 0.025% and 0.05% trypsin is consistent with the presence of dual orientations according to the predictions made above. However, an alternative explanation for the double band pattern seen at the lower trypsin concentrations (0.05% and 0.25%) is the incomplete digestion of Nductin-β lac and not dual orientation.

Figure 21. Trypsin digestion of Nductin-β lac.

Nductin-β lac (lanes 1-6) and Nductin (lanes 7 and 8) were translated in the presence of microsomes then, where indicated, treated with trypsin at the concentrations specified. The proteins were resolved on a 15% SDS-PAGE gel after immunoprecipitation using N2 antisera. For trypsin digestion, the translation mix was treated with tetracaine-HCl, to a final concentration of 2mM, before the proteinase was added and incubated at room temperature for 30 min. The reaction was stopped by the addition of RIPA buffer containing trypsin inhibitor. The protein samples were visualised by 15% SDS-PAGE and autoradiography.

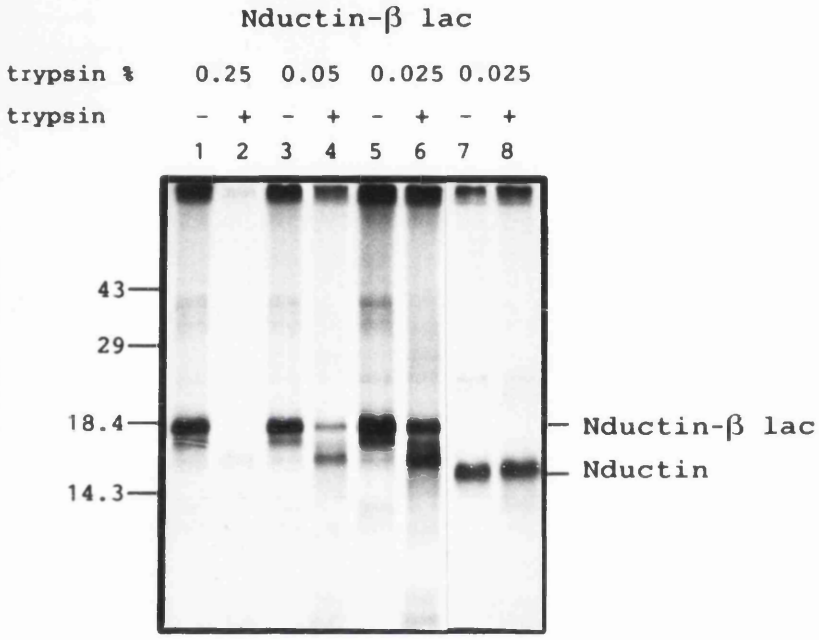
Nductin-β lac
trypsin %
0.25
0.05
0.025
0.025
trypsin
- + - + - + - +
1 2 3 4 5 6 7 8
43
29
18.4
14.3
Nductin-β lac
Nductin

To distinguish between these two possibilities, the 0.025% trypsin digest of Nductin-β lac was followed over a period of time at room temperature. Aliquots of the trypsin digestion reaction were removed at 0, 5, 10, 15 30, 60, and 90 minutes and diluted into RIPA buffer containing aprotinin to stop the trypsin digestion. The Nductin-β lac was immunoprecipitated with the N2 antibodies and visualised by SDS-PAGE and autoradiography. The 17kDa band was present after at least 5 minutes and up until 90 minutes, while the 22kDa band was lost after 15 minutes (Figure 22), but appeared to be stable during this time, again suggestive of dual orientations. However, the loss of the 22kDa band after only 15 minutes is in contrast with the earlier 0.025% trypsin digest where the 22kDa band was still present after 30 minutes. This difference could be due to either a more efficient trypsin digest in the second experiment, or the loss of microsomal membrane integrity before the end of the timecourse in the second experiment.

The same timecourse experiment was also performed on ice, not only to reduce the activity of trypsin, but also to stabilise the microsomal membranes and reduce any permeablisation of the membranes that may occur. Tetracaine-HCl was also added to further stabilise the microsome membranes. As a marker for the integrity of the microsomal membranes, the access of trypsin into the lumen of the microsomes was assayed by a timecourse trypsin treatment of β-lactamase. As long as trypsin is excluded from the lumen of the microsomes then β-lactamase should not be degraded, and any digestion of Nductin-β lac will be due to exposure on the non-lumenal surface of the microsomal membrane where trypsin has access. In addition, squid rhodopsin was digested with trypsin under the same conditions, so as to provide a measure of the rate of trypsin digestion of the cytoplasmically exposed C-terminal region of this polypeptide.

Figure 22. Time course of trypsin digestion of Nductin-β lac in microsomal membranes.

Microsomes containing the fusion protein, Nductin-β lac was translated *in vitro* in the presence of microsomal membranes before being treated with 0.025% trypsin over a 90 min period at room temperature. Prior to the trypsin digestion the microsomal membranes were treated with tetracaine-HCl to a final concentration of 2mM. The digest was stopped at the indicated time points by diluting an aliquot of the sample in RIPA buffer containing aprotinin, after which an immunoprecipitation (IP) was performed using the N2 antisera and the samples were visualised by 12.5% SDS-PAGE and autoradiography.

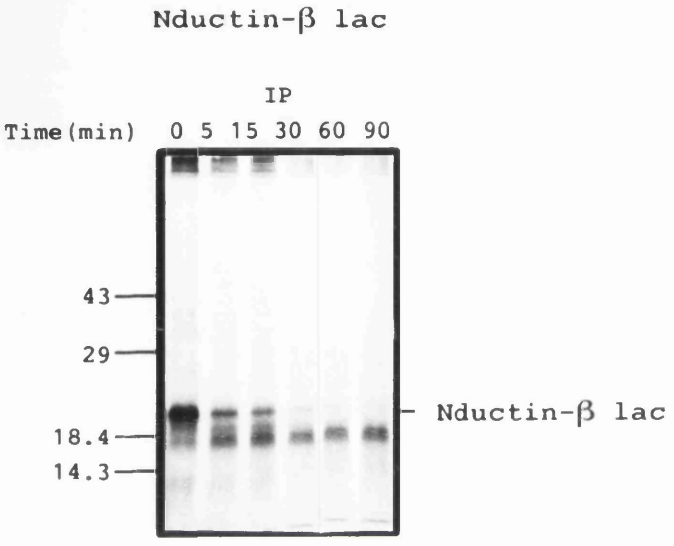
Nductin-β lac
IP
Time(min) 0 5 15 30 60 90
43
29
18.4
14.3
Nductin-β lac

To stop the action of the trypsin samples were diluted into MP buffer containing aprotinin, and the microsomes were separated from the reticulocyte lysate by centrifugation at 50000 rpm for 60 minutes. During the timecourse digestion of β-lactamase there does not appear to be any digestion of the polypeptide until between 60 and 90 minutes (figure 23). For the trypsin digestion of squid rhodopsin, the complete loss of the full length 47kDa polypeptide did not occur until between 30 and 60 minutes (figure 23), and up till that time there was only partial loss of the 47kDa band. These results indicate that the microsomal membranes retain their integrity up until 60 minutes, and that the complete digestion of exposed polypeptide will have occurred at this time.

To overcome the problem of maintaining a similar trypsin activity between Nductin-β lac and the control proteins during the digestion, equal volumes of translated Nductin-β lac and β-lactamase were mixed prior to digestion with trypsin. This allowed a direct comparison of the digestion of Nductin-β lac and β-lactamase over the period of the timecourse. At each timepoint of the digest, aliquots were treated in two ways, either the microsomes were isolated directly by centrifugation, or Nductin-b lac was isolated by immunoprecipitation. The centrifugation of the microsomes allowed the direct comparison of Nductin-β lac and β-lactamase digestion. The immunoprecipitation of Nductin-β lac produced better resolved bands, including the presence of a third band between the 22 and 17kDa bands. This third band was probably due to incomplete tryptic digestion of Nductin-β lac at one of the potential tryptic cleavage sites in the β-lac extension closer to the C-terminus of Nductin-β lac (figure 18). The trypsin timecourse results on ice for Nductin-β lac were similar to those at room temperature except that the timeframe over which the various bands appeared and disappeared was much more spread out. As can be seen in figure 24 where β-lactamase was present along with Nductin-β lac, the presence of a stable, uncleaved 22kDa band along

Figure 23. Time course of trypsin digestion of β lactamase and squid rhodopsin in microsomal membranes.

β lactamase and squid rhodopsin were translated *in vitro* in the presence of microsomal membranes before being treated with 0.025% trypsin over a 90 minute period on ice. Prior to the trypsin digestion the microsomal membranes were treated with tetracaine-HCl to a final concentration of 2mM, to stabilise the microsomal membranes. The digest was stopped at the indicated time points by diluting an aliquot of the digestion sample in MP buffer containing aprotinin, after which the microsomal membranes were pelleted by centrifugation and the pellet fraction was visualised by autoradiography, after 12.5% SDS-PAGE.

β lactamase

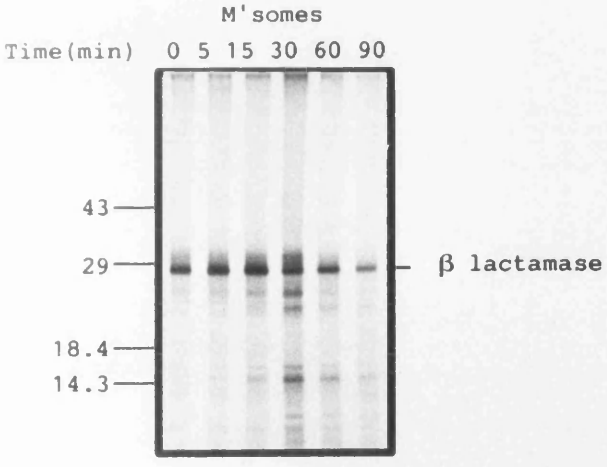

Squid rhodopsin

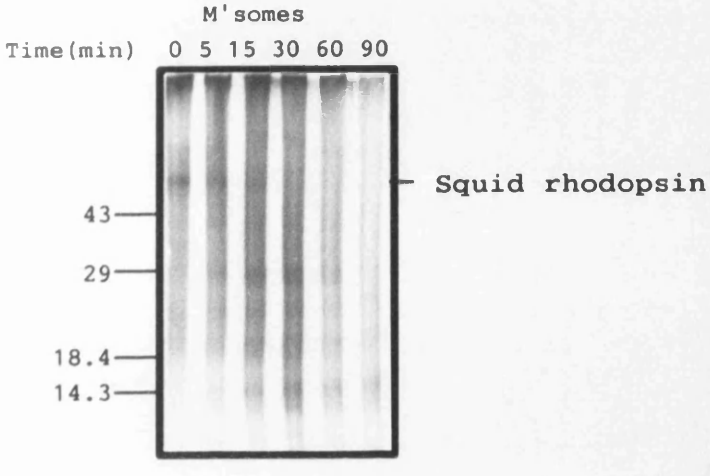

Figure 24. Time course of trypsin digestion of Nductin-β lac and β-lactamase in microsomal membranes.

Nductin-β lac and β-lactamase were separately translated *in vitro* in the presence of microsomal membranes but before being treated with 0.025% trypsin over a 90 minute period on ice, equal volumes of Nductin-β lac and β-lactamase sample were mixed. Prior to the trypsin digestion the microsomal membranes were treated with tetracaine-HCl to a final concentration of 2mM. The digest was stopped at the indicated time points by diluting an aliquot of the sample in MP buffer containing aprotinin, after which the microsomal membranes were pelleted by centrifugation (M'somes). In addition, at each indicated time point a second aliquot was removed and diluted in RIPA buffer containing aprotinin and an immunoprecipitation performed using the N2 antisera (IP). The pellet fraction protein and the immunoprecipitated protein was visualised by 12.5% SDS-PAGE and autoradiography.

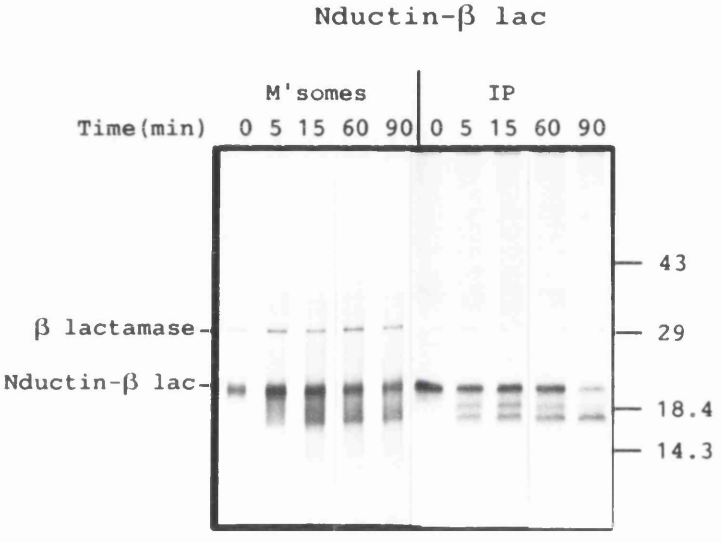
Nductin-β lac
M'somes
IP
Time(min) 0 5 15 60 90 0 5 15 60 90
β lactamase
Nductin-β lac
43
29
18.4
14.3

with the cleaved 17kDa band occurred when trypsin had no access to the lumen of the microsomes and there was no loss of β-lactamase signal. The presence of the two bands was stable between 30 and 60 minutes, suggesting that all the exposed Nductin-β lac had been cleaved and that the presence of an uncleaved population was a real result, not an artefact of incomplete digestion. The 22kDa band was believed to represent a population of Nductin-β lac whose membrane orientation was opposite to that of the cleaved 17kDa form of Nductin-β lac. This digestion pattern was predicted if Nductin-β lac had been inserted in both orientations into the microsomal membranes (figure 18).

3.3.6.4. Chemical modification of ductin by fluorescein-5-maleimide (FM).

The result from the trypsin digest of Nductin-β lac that suggest the presence of dual orientations is contrary to the generally accepted view that membrane proteins have a single membrane orientation. In an effort to provide confirmation of the dual orientation of Nductin-β lac an alternative strategy was used which was based on cysteine replacement (Jones et al, 1994, 1995). A cysteine-free form of Nductin has previously been prepared which retains wild-type activity in the V-ATPase complex when expressed in *vat c* (Nelson and Nelson, 1990; Harrison et al, 1994). Replacement of the residues at position 6 (N-terminus of helix 1) and 44 (loop between helices 1 and 2) (Figure 25) by cysteine had no deleterious effects on V-ATPase activity and was accessible to reaction in the whole V-ATPase with the water soluble reagent fluorescein-5-maleimide (FM). The reaction caused a slight shift in the size of the Nductin polypeptide that could be detected by SDS-PAGE. Cysteine residues exposed to the cytosolic face will be accessible to hydrophilic reagents while those on the lumenal side should be inaccessible. As residues 6 and 44 are on opposite sides of the membrane (Fig 25), it should be possible to use their availability to reaction with FM as a marker for the orientation of the ductin polypeptide in the microsomal membrane. As with the trypsin digestion of

Figure 25. Disposition of Nductin in the bilayer showing the positions of the residues replaced by cysteine, S6 and S44.

The single cysteine replacement mutants of Nductin, S6C and S44C, flank the first transmembrane region of Nductin and are extramembranous (see Finbow et al., 1992; Jones et al., 1995).

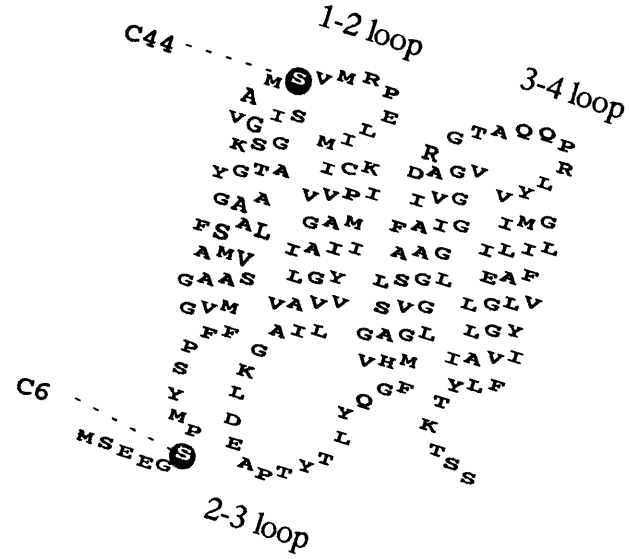
1-2 loop
3-4 loop
C44
C6
2-3 loop

Nductin-β lac three possibilities can be envisioned for the FM labelling of either cys6 or cys44. If the N-terminus of Nductin is cytoplasmically located then cys6 will be labelled with FM but cys44 will not, whereas if the N-terminus is lumenally located then cys6 will not label but cys44 will. If on the other hand the N-terminus is located on both the lumenal face and the cytoplasmic face due to dual orientations then both cys6 and cys44 will partially label with FM.

Firstly, to optimise the conditions for labelling with FM, microsomal membranes containing the mature β-lactamase were incubated at different concentrations of FM. The conditions during an *in vitro* translation are reducing, which inhibits the action of the FM, thus high enough concentrations of FM have to be present during the labelling to overcome the reducing conditions and to allow a complete reaction, but without causing the permeabilisation of the microsomal membranes. The mature form of β-lactamase contains two cysteine residues and reaction with FM in the presence of SDS results in a detectable shift of the polypeptide (figure 26B), which suggests that any permeabilisation of the microsomal membranes will be detected from the labelling of β-lactamase by FM. β-lactamase was translated in the presence of microsomal membranes after which it was diluted five-fold then treated with FM at concentrations of 0, 0.25 , 0.5, 1.0 and 1.5 mM. Excess β-mercaptoethanol was added after 60 minutes to mop up unreacted FM before centrifuging the samples to pellet the microsomal membranes.

At 0.25mM and 0.5mM FM there was no detectable shift in the migration of β-lactamase, but above these concentrations a fraction of the β-lactamase was labelled by FM, as seen by its altered migration (Figure 26A). This indicates that the microsomal membranes are impermeable to the FM at the concentrations 0.25mM and 0.5mM, but above this concentration the FM can gain access to the lumenal contents of the microsomal membranes.

Figure 26. Labelling of β-lactamase by fluorescein-5-maleimide (FM).

A) β-lactamase was translated *in vitro* in the presence of microsomal membranes, after which it was labelled for 60 minutes at 30°C with different concentrations of FM shown above each lane as mM. The FM labelling was performed once the translation mix had been diluted five-fold into either phosphate buffered saline (P) or MP buffer (M), to test the effect of different buffers on the permeability of the microsomal membranes. The microsomes were isolated from the reaction mixture by centrifugation and the labelled proteins visualised by 8% SDS-PAGE and autoradiography. B) Microsomal membranes containing *in vitro* translated β-lactamase were either pelleted by centrifugation then resuspended in an equal volume of MP buffer, after which they were labelled for 60 minutes at 30°C by 1mM FM in the presence (+) of 1% SDS, or were treated with 1mM FM in the absence (-) of SDS prior to being collected by centrifugation. No dilution of the translation mix prior to FM labelling was performed. After FM labelling the microsomal membrane proteins were directly visualised by 12.5% SDS-PAGE and autoradiography.

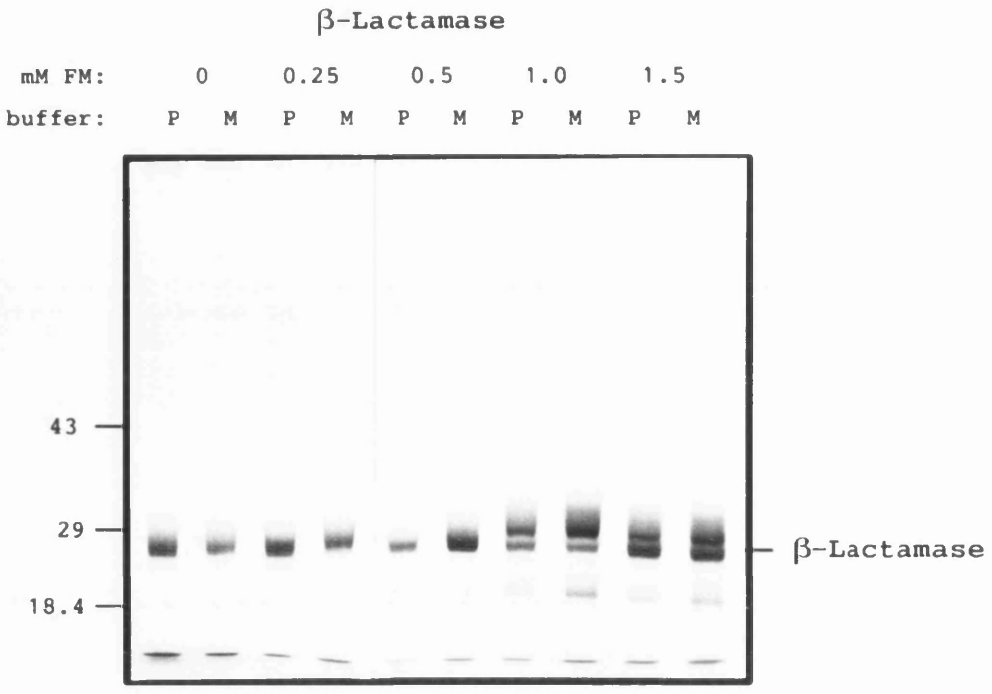
β-Lactamase
mM FM: 0 0.25 0.5 1.0 1.5
buffer: P M P M P M P M P M
43
29
18.4
β-Lactamase

A

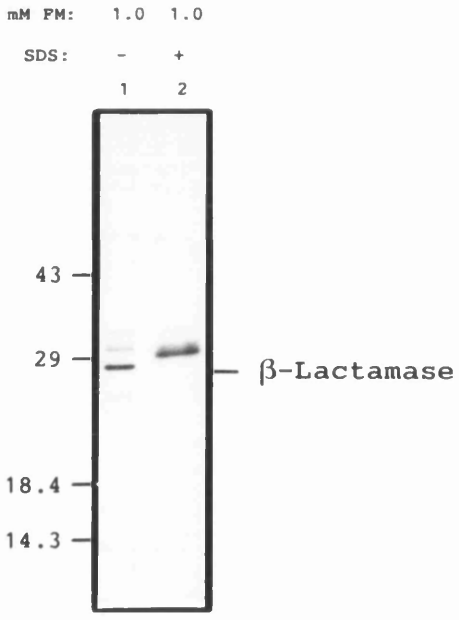
mM FM: 1.0 1.0
SDS: - +
1 2
43
29
18.4
14.3
β-Lactamase

B

The two cysteine replacement mutants, cys6 and cys44, were analysed for their reactivity with FM under a number of conditions and FM concentrations. Two sets of labelling conditions were used, firstly the same as had been used for the labelling of β-lactamase, and secondly where there was no dilution of the samples prior to addition of FM to a final concentration of 1.0mM and 3.0mM. The second set of conditions had been used during the initial labelling studies, with the first set of conditions used later to increase the amount of FM present in relation to the protein of the *in vitro* translation mix. The final concentration of FM could not be increased since it was insoluble at higher concentrations, therefore the protein to be labelled was diluted instead. Using the first set of conditions the cys44 mutation exhibited approximately half labelling at the lowest concentrations (0.25mM and 0.5mM), but at 1.5mM, when the membrane was permeable, there is a more complete reaction of the polypeptide with FM (Figure 27B). The fact that the level of labelling of cys44 was stable between 0.25mM and 0.5mM at approximately half labelling, suggests that all the available cys44 cysteine residues had been modified by FM. When the FM labelling of cys44 was performed using the second set of conditions, the labelling pattern was the same as before (figure 27A) with partial labelling at 1mM FM and more complete labelling at 3mM, once the membranes were FM permeable. Cys44 was also labelled with FM in the presence of SDS (figure 28), which should have had the effect of exposing all cysteine residues to modification. This was indeed found to be the case, since the FM labelling of cys44 was increased compared to labelling in the absence of SDS.

The cys6 mutant was treated with FM using the same set of conditions as for cys44, except that there was no treatment at 1.5mM FM after dilution in MP buffer. The maximum level of labelling (at 0.5mM figure 27B and 1.0mM figure 27A) for cys6 that could be obtained before the microsomes became permeable to FM was only partial. Once the microsomal membranes became permeable to FM,

Figure 27. Labelling of the cys6 and cys44 substitutions of Nductin by FM. Microsomal membranes containing the *in vitro* translated cys6 (C6) (lanes 1 and 2) and cys44 (C44) (lanes 3 and 4) substitutions of Nductin were labelled for 60 minutes at 30°C with the different concentrations of FM shown above each lane as mM. Two sets of conditions were used, A) no dilution of the translation mix prior to FM labelling and B) dilution of the translation mix five-fold prior to FM labelling. After FM labelling the microsomal membranes were collected by centrifugation and the proteins visualised by 12.5% SDS-PAGE and autoradiography.

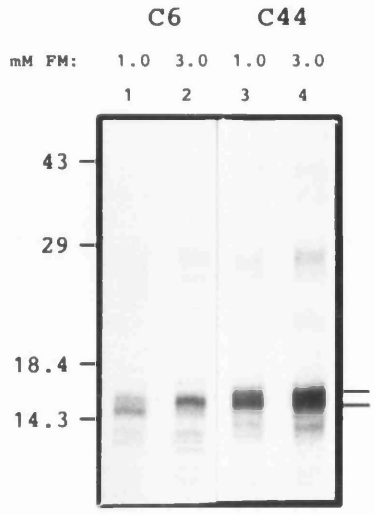
C6
C44
mM FM:
1.0
3.0
1.0
3.0
1
2
3
4
43
29
18.4
14.3

A

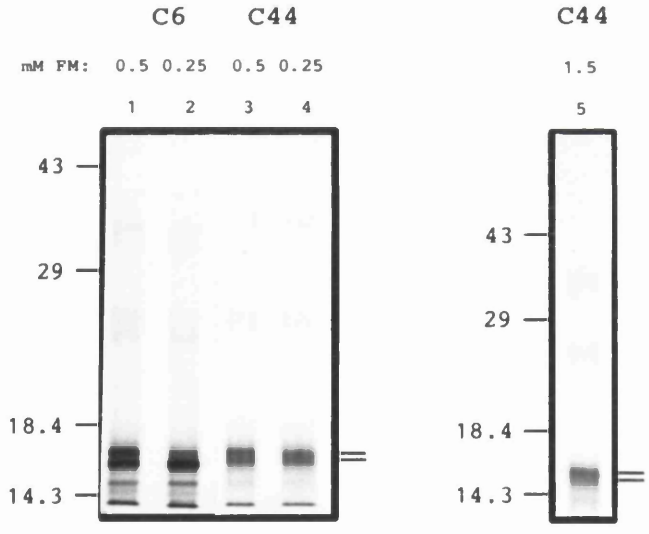
C6
C44
C44
mM FM:
0.5
0.25
0.5
0.25
1.5
1
2
3
4
5
43
29
18.4
14.3
43
29
18.4
14.3

B

Figure 28. Labelling of the cys6 and cys44 substitutions of Nductin by FM in the presence of SDS.

Microsomal membranes containing the *in vitro* translated cys6 (C6) (lanes 1 and 2) and cys44 (C44) (lanes 3 and 4) substitutions of Nductin were either pelleted by centrifugation then resuspended in an equal volume of MP buffer after which they were labelled for 60 minutes at 30°C by 1mM FM in the presence (+) of 1% SDS, or were treated with 1mM FM in the absence (-) of SDS prior to being collected by centrifugation. No dilution of the translation mix prior to FM labelling was performed. After FM labelling the microsomal membrane proteins were directly visualised by 12.5% SDS-PAGE and autoradiography.

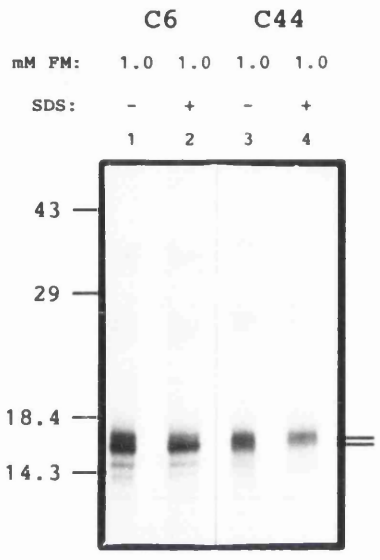
C6
C44
mM FM:
1.0
1.0
1.0
1.0
SDS:
-
+
-
+
1
2
3
4
43
29
18.4
14.3

cys6 was labelled to a much greater extent than before (figure 27B, lane 2 and figure 27A, lane 2). The labelling of cys6 in the presence of SDS was actually lower than in the absence of SDS (figure 28) which was unexpected and the reason unknown. The maximum labelling of cys6 and cys44 when the microsomal membranes retained their impermeability to FM was only partial in both cases. These two residues are on opposites sides of the lipid bilayer, so the labelling pattern for cys6 and cys44 can be best explained if ductin has two orientations in the membrane.

3.3.7. The role of charge in determining the orientation of Nductin-β lac.

The charge of the N-terminus has been implicated as a possible determinant of orientation (Parks and Lamb, 1991, 1993). All forms of ductin so far sequenced have been found to have acidic residues present at their N-termini and it was postulated that these acidic residues may play a role in determining the orientation of ductin. In Nductin, there are two glutamic acid residues at positions 3 and 4 of the N-terminal region (Figure 6). To test the importance of these two residues they were exchanged for either alanine or lysine, and the effect that changes in charge at the N-terminus had on the orientation profile of Nductin-β lac was assayed. The alanine substitution changed the N-terminal charge from -2 to 0, while the lysine substitution created an N-terminus of charge +2. The previous studies on the influence of N-terminal charge indicated that changes of the magnitude to be carried out are likely to lead to a change in the orientation of Nductin-β lac (Parks and Lamb, 1991, 1993).

The N-terminus of Nductin was mutated by using the same PCR strategy as had been used previously to construct the original Nductin-β lac fusion protein (figure 19), the only difference being in the forward primer containing the T7 RNA polymerase site. For each N-terminal mutant the 3' end of that primer was

extended to cover the residues at positions 3 and 4 and the appropriate changes in the nucleotide sequence were included such that the glutamic acid residues were replaced with either alanine using *T7 Nductin AA* (table 8) to produce NductinAA-β lac, or lysine using T7 *Nductin KK* to produce NductinKK-β lac (table 8). As before, capped mRNA was transcribed directly from the final PCR DNA construct and used for the *in vitro* translation of NductinAA-β lac and NductinKK-β lac.

The two N-terminal mutants of Nductin-β lac were treated in the same manner as for the wild type Nductin-β lac, and as before full length β-lactamase was included as a control for the access of trypsin to the lumen of the microsomal membranes. No immunoprecipitation was performed because the major epitope of the N2 antisera appears to be located at the N-terminus and was adversely affected by the mutations introduced at the N-terminus. The trypsin digestion profile of NductinAA-β lac and NductinKK-β lac did not significantly alter from that seen for Nductin-β lac (Figure 29 and figure 30); two bands were observed, one of which was the uncleaved polypeptide while the lower band corresponded in size to the core transmembrane region after removal of the β-lactamase extension. The lack of any change in the orientation profile of Nductin-β lac after substitution of the N-terminal glutamic acids was surprising in light of the previously published data highlighting the importance of charge.

3.3.8. Orientation of VMA11.

It is likely that the ductin-related protein VMA11 shares some of the same biochemical properties as ductin such as the mechanism of membrane insertion. Therefore, the orientation of VMA11 was investigated using the same technique as for Nductin, the addition of a trypsin sensitive C-terminal extension based on β-lactamase. This extension was added to the C-terminus of VMA11 using the internal oligonucleotides *VMA11 T4A sense* and *VMA11 T4A antisense* (table 7),

Figure 29. Time course of trypsin digestion of NductinKK-β lac and β-lactamase in microsomal membranes.

NductinKK-β lac and β-lactamase were separately translated *in vitro* in the presence of microsomal membranes, but before being treated with 0.025% trypsin over a 90 minute period on ice, equal volumes of NductinKK-β lac and β-lactamase sample were mixed. Prior to the trypsin digestion the microsomal membranes were treated with tetracaine-HCl to a final concentration of 2mM. The digest was stopped at the indicated time points by diluting an aliquot of the sample into MP buffer containing aprotinin, after which the microsomal membranes were pelleted by centrifugation (M'somes). The pellet fraction protein was visualised by 12.5% SDS-PAGE and autoradiography.

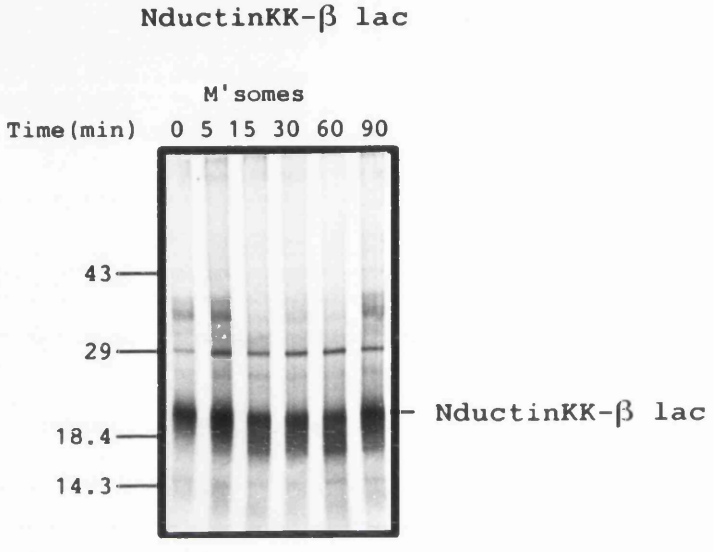
NductinKK-β lac
M'somes
Time(min) 0 5 15 30 60 90
43
29
18.4
14.3
NductinKK-β lac

Figure 30. Time course of trypsin digestion of NductinAA-β lac and β-lactamase in microsomal membranes.

NductinAA-β lac and β-lactamase were separately translated *in vitro* in the presence of microsomal membranes, but before being treated with 0.025% trypsin over a 90 minute period on ice, equal volumes of NductinAA-β lac and β-lactamase sample were mixed. Prior to the trypsin digestion the microsomal membranes were treated with tetracaine-HCl to a final concentration of 2mM. The digest was stopped at the indicated time points by diluting an aliquot of the sample into MP buffer containing aprotinin, after which the microsomal membranes were pelleted by centrifugation (M'somes). The pellet fraction protein was visualised by 12.5% SDS-PAGE and autoradiography.

NductinAA-β lac

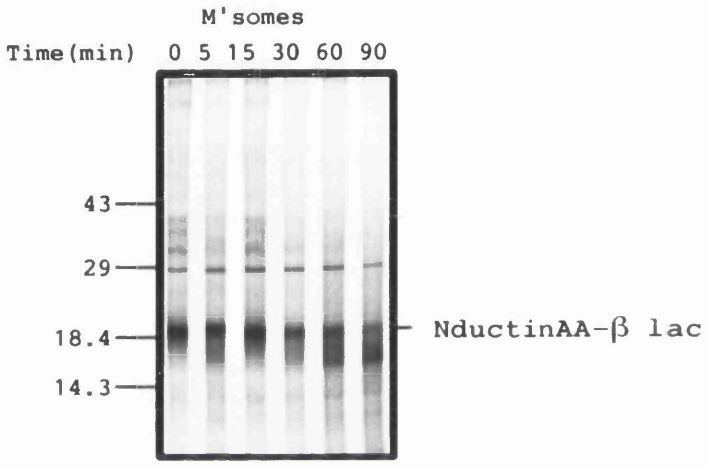

and the flanking primers *T7 VMA11* (table 8) and β-*lac 3'anti* (table 2), employing the same PCR strategy as had been used to make Nductin-β lac, to produce VMA11-β lac. Capped RNA was transcribed (Ambion) directly from the full length purified PCR product for use in the *in vitro* translation reaction.

When VMA11-β lac was expressed *in vitro* in the presence of microsomal membranes then treated with 0.025% trypsin over the same timecourse as used previously, it exhibited a similar double band profile as had been seen for Nductin-β lac (figure 31). There was an uncleaved population of VMA11-β lac, as well as a cleaved population that corresponded in size to the core transmembrane region after removal of the β-lactamase extension. As for Nductin-β lac, this was interpreted as indicating that VMA11-β lac had been inserted into the microsomal membranes with dual orientations.

3.3.9. The assembly of ductin complexes.

3.3.9.1. Introduction.

The membrane complexes of either the V-ATPase or the gap junction contain six ductin polypeptides, and in the gap junction the six ductin polypeptides are arranged symmetrically around a central aqueous channel (Holzenburg et al., 1993). EM analysis of the mediatophore complex also suggests an oligomeric complex of ductin similar to the connexon (see section 1.6.3.). Therefore, it was examined whether Nductin expressed in the microsomal membrane could self-associate and in some way approximate the assembled ductin found in either of these final forms.

Figure 31. Time course of trypsin digestion of VMA11-β lac and β-lactamase in microsomal membranes.

VMA11-β lac and β-lactamase were separately translated *in vitro* in the presence of microsomal membranes, but before being treated with 0.025% trypsin over a 90 minute period on ice, equal volumes of VMA11-β lac and β-lactamase sample were mixed. Prior to the trypsin digestion the microsomal membranes were treated with tetracaine-HCl to a final concentration of 2mM. The digest was stopped at the indicated time points by diluting an aliquot of the sample into MP buffer containing aprotinin, after which the microsomal membranes were pelleted by centrifugation (M'somes). The pellet fraction protein was visualised by 12.5% SDS-PAGE and autoradiography.

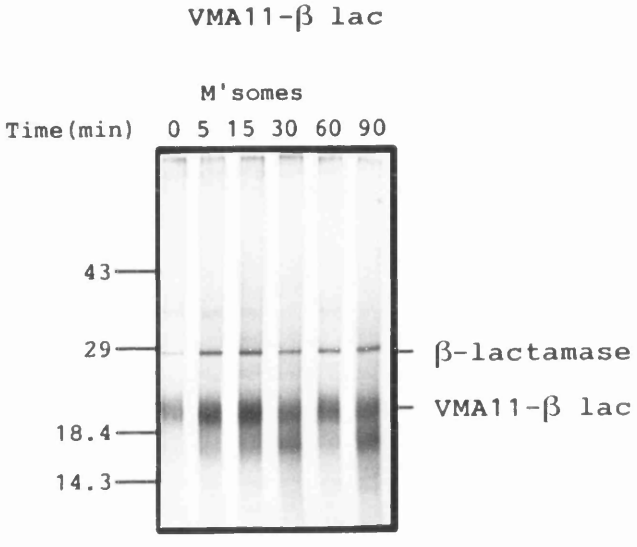
VMA11-β lac
M'somes
Time(min) 0 5 15 30 60 90
43
29
18.4
14.3
β-lactamase
VMA11-β lac

3.3.9.2. Immunoprecipitation of ductin complexes.

The self-assembly of ductin was investigated by the co-immunoprecipitation, after *in vitro* expression, of Nductin-β lac and the bovine form of ductin (Bductin), using the N2 antisera. The Nductin-β lac fusion polypeptide was used instead of Nductin to allow a clear distinction on SDS-PAGE of the *Nephrops* and bovine forms since both would otherwise migrate at 16kDa.

Bductin and Nductin-β lac capped mRNA was mixed before being added to the *in vitro* translation reaction. A number of different ratios (1:3, 1:1, and 3:1) of Bductin to Nductin-β lac mRNA were used in the translation to produce different ratios of Bductin and Nductin-β lac polypeptide for the immunoprecipitation. There was little or no observable cross-reactivity between Bductin and the N2 antisera (figure 32, lane 8). The Bductin was found co-immunoprecipitated with Nductin-β lac for each of the three mRNA ratios tried (Figure 32, lanes 9, 10 and 11). When the Nductin-β lac polypeptide was limiting compared to Bductin, at the mRNA ratio of 3:1, Bductin and Nductin-β lac were co-immunoprecipitated in equal amounts, as was the case when the two polypeptides were translated in equal quantities, at the 1:1 mRNA ratio. These results suggested that the association between Nductin-β lac and Bductin was specific and not a result of the aggregation of hydrophobic polypeptides. In addition, the association between Bductin and Nductin-β lac was not a result of binding after the microsomes had been solubilised in the RIPA buffer since mixing of Bductin and Nductin-β lac after solubilisation in RIPA buffer did not lead to any association between the two forms of ductin (figure 32, lane 6).

The specificity of the ductin self-association was tested by co-expressing either Nductin or Nductin-β lac with a number of other polypeptides of varying

Figure 32. Self-assembly of ductin complexes.

Capped mRNA encoding Nephrops ductin or the fusion protein Nductin-β lac was co-translated in the presence of microsomes with mRNA encoding bovine ductin (Bductin). On the left is shown the microsomal fraction and on the right the corresponding immunoprecipitation performed using the N2 antisera. Lanes 1 and 2 show the translation products of mRNA encoding for Nductin-β lac and bovine ductin translated separately. Lanes 3 to 5 show a co-translation of the above mRNA's in approximate ratios of 1:3, 1:1 and 3:1 respectively. Lanes 7 and 8 shows the immunoprecipitation (IP) from the microsomes from lanes 1 and 2 respectively and lane 6 shows the IP from an equal mix of lanes 1 and 2 after first solubilising the microsomal membranes in RIPA buffer. Lanes 9 to 11 show the IP of the microsomes shown in lanes 3 to 5. The protein samples were visualised by 12.5% SDS-PAGE and autoradiography.

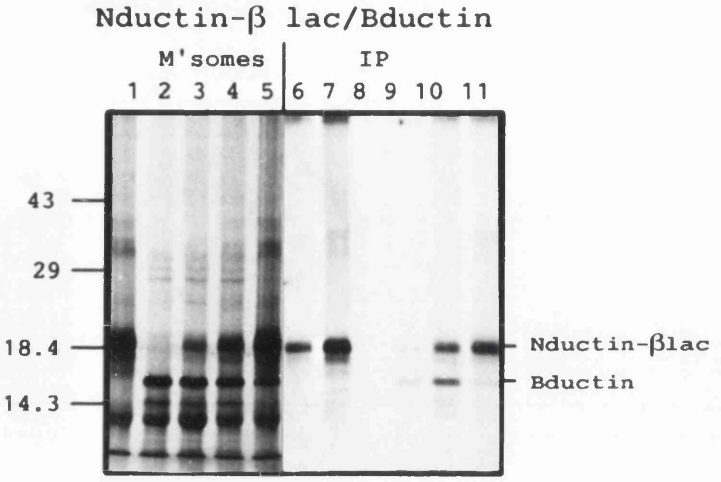
Nductin-β lac/Bductin
M'somes
IP
1 2 3 4 5 6 7 8 9 10 11
43
29
18.4
14.3
Nductin-βlac
Bductin

homology with Nductin. Three polypeptides were used; VMA11 (70% homology), PPA1 (40% homology) and squid rhodopsin (no homology). For each of these polypeptides the same protocol was used as had been used for Nductin-β lac and Bductin, that is repeating the immunoprecipitation with different ratios of co-expressed polypeptides. To allow a clear distinction between polypetides, Nductin-β lac was co-expressed with VMA11 then the immunoprecipitation performed with the N2 antisera. There was no cross-reactivity between VMA11 and the N2 antisera (figure 33, lane 5). As for Bductin, VMA11 was co-immunoprecipitated in a specific manner with Nductin-β lac, and as before the two polypeptides were brought down in equal amounts when Nductin-β lac was limiting (figure 33). This was not the case when PPA1 was co-expressed with Nductin, since little PPA1 was co-immunoprecipitated with Nductin, when using the N2 antisera (figure 34). When the PPA1 polypeptide was present in excess of the Nductin polypeptide (figure 34, lane 3) only a small amount of PPA1 polypeptide was co-immunoprecipitated, less than the equal amounts observed for VMA11 and Bductin (figure 34, lane 8). A similar observation was made for Nductin and rhodopsin when the two polypeptides were co-expressed and Nductin immunoprecipitated with the N2 antisera (figure 35). A small amount of squid rhodopsin was immunoprecipitated along with Nductin (figure 35, lane 8) when the two polypeptides were present in the translation mix in near equal amounts (figure 35, lane 3). This was likely to be the result of a non-specific association since a small amount of squid rhodopsin was also present in lane 7 even though the amount of Nductin polypeptide present in the original translation mix (figure 35, lane 2) was very low.

Figure 33. Association of Nductin-β lac with VMA11.

Capped mRNA encoding Nductin-β lac was co-translated *in vitro* with mRNA encoding the VMA11 polypeptide, in the presence of microsomes . On the left is shown the microsomal fraction (M'somes) and on the right the corresponding immunoprecipitation (IP) using the N2 antisera. Lane 1 shows the translation products of a single mRNA species encoding for the VMA11 polypeptide. Lanes 2 to 4 show a co-translation of Nductin-β lac and VMA11 in approximate mRNA ratios of 1:3, 1:1 and 3:1, respectively. Lanes 5 shows the immunoprecipitation from the microsomes from lane 1. Lanes 6 to 8 show the IP of the microsomes shown in lanes 2 to 4. The protein samples were visualised by 12.5% SDS-PAGE and autoradiography.

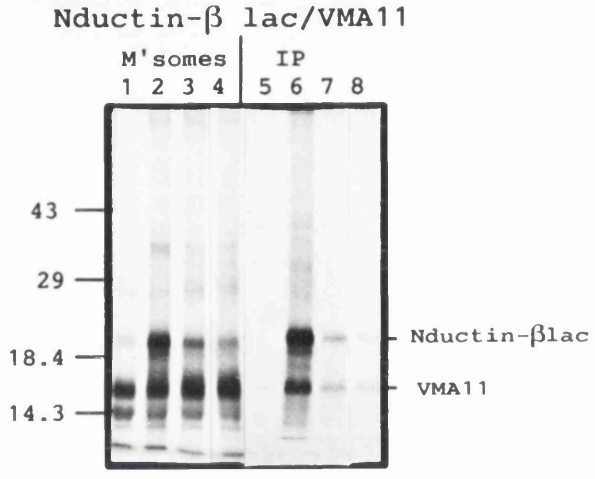
Nductin-β lac/VMA11
M'somes
IP
1 2 3 4 5 6 7 8
43
29
18.4
14.3
Nductin-βlac
VMA11

Figure 34. Non-association of Nductin with PPA1.

Capped mRNA encoding Nductin-β lac was co-translated in the presence of microsomes with mRNA encoding PPA1. On the left is shown the microsomal fraction (M'somes) and on the right the corresponding immunoprecipitation (IP) performed using the N2 antisera. Lanes 1 and 5 show the translation products of mRNA encoding for Nductin and PPA1 translated separately. Lanes 2 to 4 show a co-translation of the above mRNA's in approximate ratios of 1:3, 1:1 and 3:1 respectively. Lanes 6 and 10 shows the IP from the microsomes from lanes 1 and 5 respectively and lane 11 shows the IP from an equal mix of lanes 1 and 5 after first solubilising the microsomal membranes in RIPA buffer. Lanes 7 to 9 show the IP of the microsomes shown in lanes 2 to 4. The protein samples were visualised by 12.5% SDS-PAGE and autoradiography.

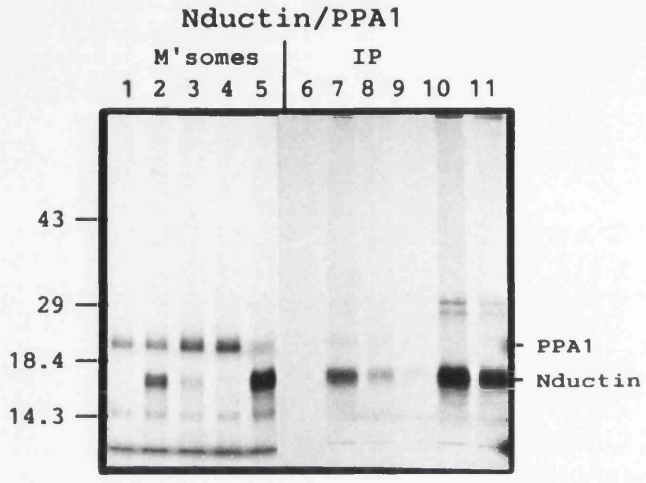
Nductin/PPA1
M'somes
IP
1 2 3 4 5 6 7 8 9 10 11
43
29
18.4
14.3
PPA1
Nductin

Figure 35. Non-association of Nductin with squid rhodopsin.

Capped mRNA encoding Nductin was co-translated *in vitro* in the presence of microsomes with mRNA encoding the squid rhodopsin polypeptide. On the left is shown the microsomal fraction (M'somes) and on the right the corresponding immunoprecipitation (IP) using the N2 antisera. Lane 4 shows the translation products of a single mRNA species encoding the squid rhodopsin polypeptide. Lanes 1 to 3 show a co-translation of Nductin and squid rhodopsin in approximate mRNA ratios of 1:3, 1:1 and 3:1, respectively. Lanes 5 shows the IP from the microsomes from lane 4, while lane 9 shows the IP of squid rhodopsin and Nductin mixed after translation and dilution in RIPA buffer. Lanes 6 to 8 show the IP of the microsomes shown in lanes 1 to 3. The protein samples were visualised by 12.5% SDS-PAGE and autoradiography.

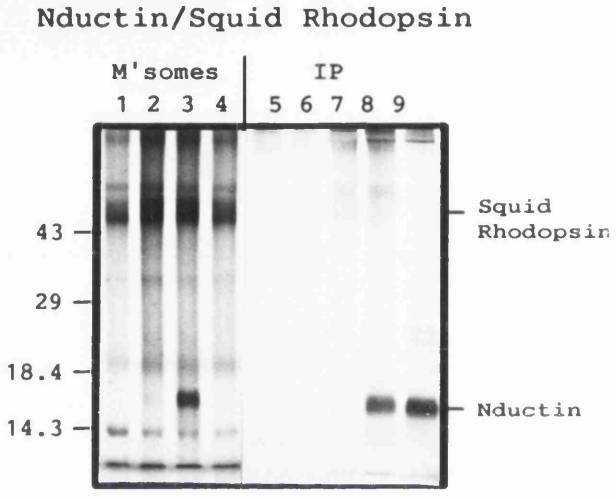
Nductin/Squid Rhodopsin
M'somes
IP
1 2 3 4 5 6 7 8 9
43
29
18.4
14.3
Squid
Rhodopsin
Nductin

3.3.9.3. The assembly of Bductin E139R

A mutant form of Bductin, E139R, has been shown to have a decreased binding affinity for the BPV1 E5 oncoprotein and to have transforming activity when stably expressed in NIH3T3 cells (Andresson et al., 1993). One possible explanation for the properties of E139R is that it is defective for assembly and that this can act in a dominant negative manner to knockout the endogenous ductin activity, thus causing transformation. To test whether the assembly of E139R was in fact altered, it was coexpressed with Nductin-β lac during an *in vitro* translation reaction and an immunoprecipitation performed using N2 antisera. The same conditions were used as had been used for wild type Bductin, and E139R was found co-immunoprecipitated with Nductin-β lac with no discernible alteration in the binding efficiency (Figure 36). The replacement of the essential glutamic acid in the fourth transmembrane region with lysine does not cause a disruption in the self-assembly of ductin, so the phenotype of E139R must be caused by the disruption of some other ductin property.

3.3.9.4. Chemical modification of ductin complexes by FM.

The investigation of the self-association of ductin was extended by the same cysteine replacement mutants of ductin that had been used previously to map the location of a proposed aqueous channel in the V_0 sector of the V-ATPase (Jones et al, 1994, 1995). Three single cysteine replacement mutants were available, cys25, cys27, and cys29 (Figure 37), each of which is located in the middle of the first transmembrane domain of ductin, but on different faces of the helix. This means

Figure 36. Self-assembly of ductin complexes is not disrupted by the E139R mutation.

Capped mRNA encoding the fusion protein Nductin-β lac was co-translated in the presence of microsomes with mRNA encoding the mutant Bductin, E139R. On the left is shown the microsomal fraction (M'somes) and on the right the corresponding immunoprecipitation (IP) performed using the N2 antisera. Lanes 1 and 5 show the translation products of mRNA encoding for E139R and Nductin-β lac translated separately. Lanes 2 to 4 show a co-translation of the above mRNA's in approximate ratios of 1:3, 1:1 and 3:1 respectively. Lanes 6 and 10 shows the IP from the microsomes from lanes 1 and 5 respectively and lane 11 shows the IP from an equal mix of lanes 1 and 5 after first solubilising the microsomal membranes in RIPA buffer. Lanes 7 to 9 show the IP of the microsomes shown in lanes 2 to 4. The protein samples were visualised by 12.5% SDS-PAGE and autoradiography.

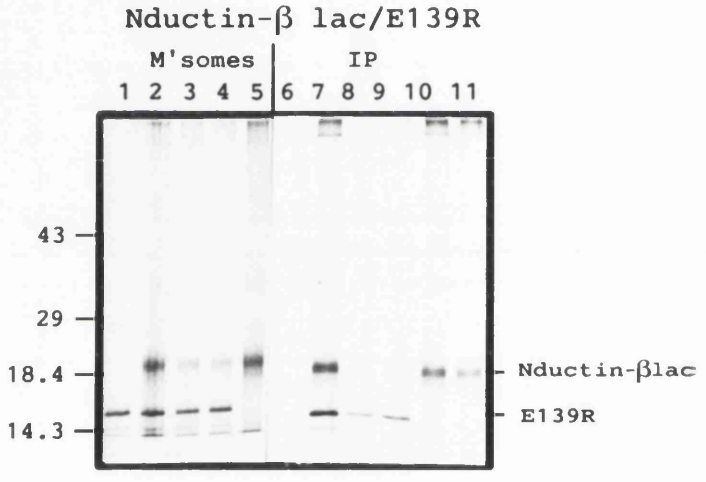
Nductin-β lac/E139R
M'somes
IP
1 2 3 4 5 6 7 8 9 10 11
43
29
18.4
14.3
Nductin-βlac
E139R

Figure 37. Disposition of Nductin in the bilayer showing the positions of the residues replaced by cysteine, S25, L27 and A29.

The single cysteine replacement mutants of Nductin, S25C, L27C and A29C, are present in the middle of the first transmembrane region of Nductin (see Finbow et al., 1992; Jones et al., 1995).

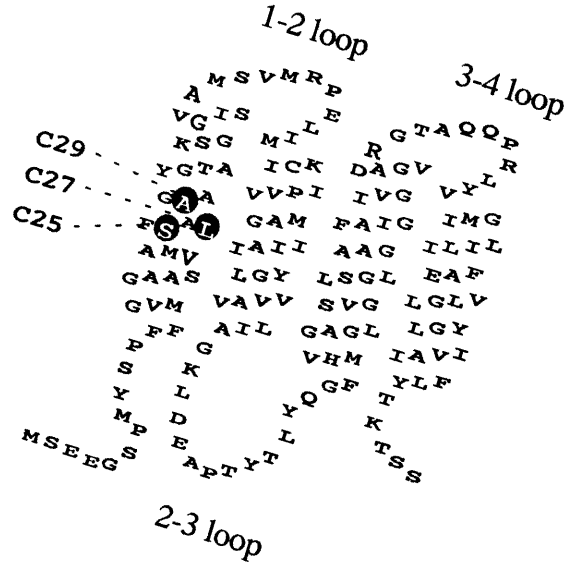
1-2 loop
3-4 loop
C29
C27
C25
2-3 loop

that the FM will have different accessibility to, and labelling of, the three residues, which can be visualised by changes in the migration of the polypeptides after FM modification. When Cys25, as part of the whole V-ATPase complex, was treated with FM it was not chemically modified (Jones et al., 1995). In contrast, when cys29 was treated under the same conditions it was modified, as seen by the increase in electrophoretic mobility of cys29. The results of the FM labelling of cys25 and cys29 isolated from the V-ATPase complex were in agreement with the predictions made from the model of ductin structure (Jones et al., 1995). Using the same model it was predicted that cys27 would be labelled by FM after being isolated from the V-ATPase, but this was found not to be the case. As well as these three residues other cysteine replacement mutants in the first transmembrane region were available and labelled by FM, and found to be modified in a manner consistent with predictions made from the model of ductin structure (Jones et al., 1995).

The same two sets of FM labelling conditions were used to label cys25, cys27 and cys29 as had been used for the labelling of cys6 and cys44. These conditions allowed the cysteine replacement polypeptides to be studied when the microsomal membranes were either FM impermeable or FM permeable. Cys25 was at best only poorly labelled by FM (figure 39, lane 1) and generally was not labelled at all (figure 38A, lanes 1 and 2). Full labelling of the cys25 polypeptide was only obtained in the presence of SDS (figure 39, lane 2). When cys27 and cys29 were treated with FM they were both labelled and, as with the cys6 and cys44 mutants, only partial labelling could be obtained before the microsomal membranes became permeable to the FM (figure 38A, lanes 3 and 5, and figure 38B, lanes 1 and 2). Once the FM gained access to the lumen of the microsomes the labelling of cys27 and cys29 increased to near complete labelling (Figure 38A, lanes 4 and 5). Cys27 and cys29 were also treated with FM in the presence of SDS, where cys27 was found to be almost fully labelled (figure 39, lane 4). In contrast, the level of cys29

Figure 38. Labelling of the cys25, cys27 and cys29 substitutions of Nductin by FM.

Microsomal membranes containing the *in vitro* translated cys25 (C25) (lanes 1 and 2), cys27 (C27) (lanes 3 and 4) and cys29 (C29) (lanes 5 and 6)substitutions of Nductin were labelled for 60 minutes at 30°C with the different concentrations of FM shown above each lane as mM. Two sets of conditions were used, A) no dilution of the translation mix prior to FM labelling and B) dilution of the translation mix five-fold prior to FM labelling (only cys27 was labelled under these conditions; lanes 1, 2 and 3). After FM labelling the microsomal membranes were collected by centrifugation and the proteins visualised by 12.5% SDS-PAGE and autoradiography.

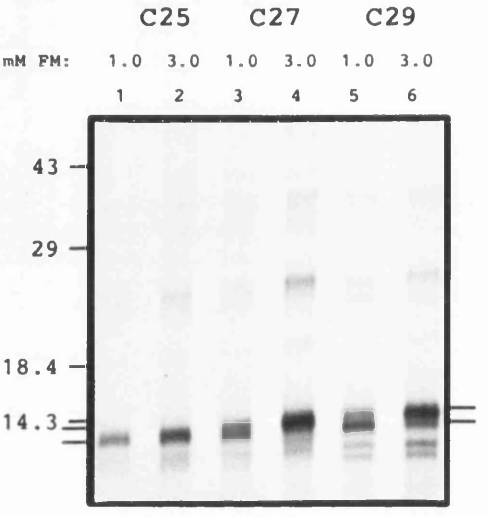
C25
C27
C29
mM FM:
1.0
3.0
1.0
3.0
1.0
3.0
1
2
3
4
5
6
43
29
18.4
14.3

A

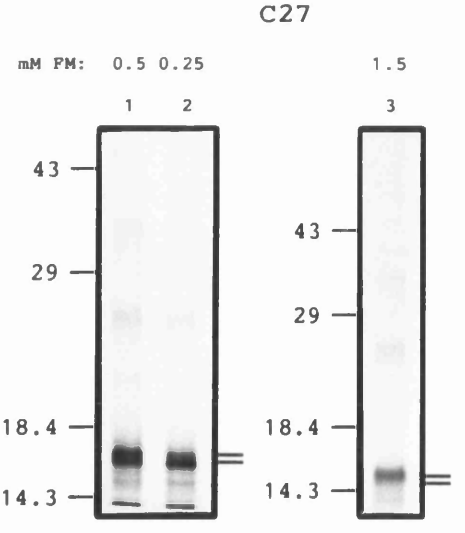
C27
mM FM:
0.5
0.25
1.5
1
2
3
43
29
18.4
14.3
43
29
18.4
14.3

B

Figure 39. Labelling of the cys25, cys27 and cys29 substitutions of Nductin by FM in the presence of SDS.

Microsomal membranes containing the *in vitro* translated cys25 (C25) (lanes 1 and 2), cys27 (C27) (lanes 3 and 4) and cys29 (C29) (lanes 5 and 6) substitutions of Nductin were either pelleted by centrifugation then resuspended in an equal volume of MP buffer, after which they were labelled for 60 minutes at 30°C by 1mM FM in the presence (+) of 1% SDS, or were treated with 1mM FM in the absence (-) of SDS prior to being collected by centrifugation. No dilution of the translation mix prior to FM labelling was performed. After FM labelling the microsomal membrane proteins were directly visualised by 12.5% SDS-PAGE and autoradiography.

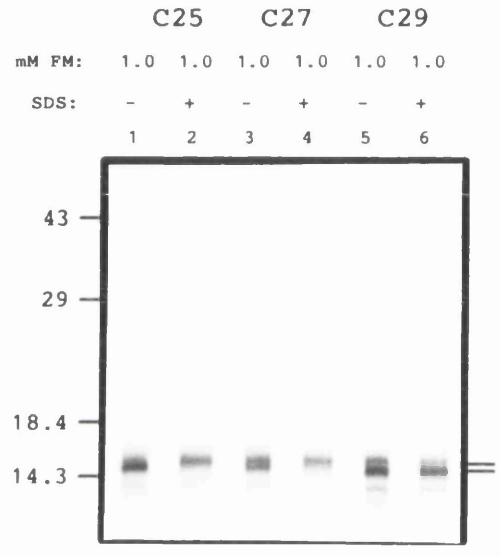
C25
C27
C29
mM FM: 1.0 1.0 1.0 1.0 1.0 1.0
SDS: - + - + - +
1 2 3 4 5 6
43
29
18.4
14.3

FM labelling decreased in the presence of SDS as compared to labelling in the absence of SDS (figure 39, lanes 5 and 6). This lack of FM labelling for cys 29 in the presence of SDS was also observed for cys6 and again the reason for it was unknown. Of the three residues tested only the accessibility to FM of cys27 was different from that obtained when the FM labelling was performed on the mutants when isolated from the whole V-ATPase complex (Jones et al., 1995). The ability of the hydrophilic FM to modify a cysteine residue present at either position 27 or 29 of helix 1 indicates that these two residues are exposed to an aqueous environment that is accessible to FM.

3.4. Discussion

3.4.1. The *in vitro* translation system.

The use of the *in vitro* translation system has allowed an outstanding question concerning ductin, that of how it becomes incorporated into the gap junction and the V-ATPase with two opposite orientations, to be studied and resolved. Two techniques were used to study the orientation of ductin, the trypsin cleavage of a trypsin sensitive extension on the C-terminus of Nductin (section 3.3.6.3.), and the FM labelling of single cysteine residues on opposite faces of the Nductin polypeptide (section 3.3.6.4.). Confidence in the result that ductin has dual orientations comes from the demonstration that ductin is capable of self-assembling into an oligomeric complex that contains an aqueous channel (section 3.3.9.). The ability to assemble demonstrates that the *in vitro* translation system is capable of supporting the proper folding and association of ductin, at least for the early stages of the generation of oligomeric ductin assemblies. Thus, there is no reason to believe that the results obtained using the *in vitro* translation system do not also apply *in vivo*, though it would be desirable to confirm the results in an *in vivo* system.

Similar types of experiments have been performed on a number of other proteins and in a number of different systems. One such example is the hepatitis B virus envelope protein which has been studied using both *in vitro* translation (Ostapchuk et al., 1994) and transiently transfected cells (Bruss et al., 1994), with essentially the same results obtained in both systems. The newly synthesised Large (L) envelope protein was found to have a different membrane topology from that of the mature L protein. The N-terminal region of the L protein is thought to undergo a post-translational translocation event to produce the mature topology (Bruss et al., 1994; Ostapchuk et al., 1994). The canine microsomal membranes have been successfully used to study the mechanism of translocation and a number of important advances have been made (Walter and Lingappa, 1986). It would seem reasonable to accept the results obtained concerning the dual orientation of ductin as being representative of the process that occurs *in vivo* considering the reproducibility of previously published work obtained from the *in vitro* system.

The *in vitro* system can only be used to study the earliest events in the biogenesis of membrane proteins, such as membrane insertion and early processing events. Later events such as glycosylation processing and the assembly of mature complexes cannot be studied and instead requires the use of more complete systems, like transfected COS cells. Attempts to recreate protein-protein interactions *in vitro* may only be partially successful since unknown factors that impinge on interacting proteins will prove very hard to substitute. At least in complete cellular systems such unknown factors are likely to be present and allow the interaction of interest to be studied. Thus, to continue and extend the study of ductin's assembly into either the gap junction or the V-ATPase it may prove necessary to use a different system that can support a more complete assembly process.

Chapter 4. General Discussion

4.1. Role of the conserved loop regions

Due to the multisubunit nature of the V-ATPase complex the number of inter-subunit interactions that are important for assembly will be expected to be large. Even the number of potential interactions between the four subunits that constitute the V_0 sector (Kane et al., 1992; Bauerle et al., 1993) would be extensive, which makes the task of identifying sites of interactions difficult especially considering the lack of structural information concerning V_0. One possible approach to understanding the structure of V_0 is to make use of the structural information that has been obtained on ductin after it was isolated as the gap junction connexon, that is, a hexamer of ductin polypeptides arranged around a central aqueous channel (Holzenburg et al., 1993).

In support of a common structure is the fact that ductin is also present in the V-ATPase complex as a hexamer (Sun et al., 1987; Arai et al., 1988). In addition, there is the presence of an aqueous channel in the V_0 sector, comprising helix 1 of ductin, which was inferred from the labelling pattern by FM of ductin cysteine replacement mutants isolated from the V-ATPase complex (Jones et al., 1995). The consistency between the results obtained from the FM labelling of ductin and the gap junction derived model of ductin would suggest that the structure of ductin in both complexes is very similar and as such the model can be used to predict potential sites of interaction for ductin when it is in the V-ATPase complex.

At the start of this thesis work the candidate regions of ductin for a role in both the gap junction and the V-ATPase were the conserved loops between helices 1-2 and 3-4. In the V-ATPase these regions are thought to be sites of contact with other subunits, while in the gap junction they are thought to be the sites of contact between apposing connexons. This suggests ductin has one orientation in the V-

ATPase and another in the gap junction. The results presented in section 3.2.8. can be best explained on the proposed orientation of ductin in the V-ATPase.

The 1-2 loop chimera was able to form a functional V-ATPase, though with a much reduced activity compared to the wild-type complex. This indicates that the 1-2 loop region is important for the activity of ductin but that the chimera is still able to assemble with the other V-ATPase subunits into an active complex. Therefore, the chimeric polypeptide may fold in a similar manner as the wild-type ductin. The reduction in V-ATPase activity is thus likely to be due to an alteration in the direct interaction between the 1-2 loop region and other V-ATPase subunits and not an indirect effect such as misfolding of the polypeptide. From this it would seem that the predicted position of the 1-2 loop is correct and it is exposed to the cytoplasmic face of the membrane where it can interact with other V-ATPase subunits. The inactivity of the 3-4 loop chimera could be a result of the same fault as the 1-2 loop chimera, a faulty connection within the assembled V-ATPase, alternatively the inactivity could be due to another problem such as faulty assembly of the V-ATPase complex due to misfolding of the 3-4 loop chimera. However, the ability of VMA11 to bind to Nductin, as demonstrated in the *in vitro* translation system, suggests that it is the transmembrane regions and not the loop regions that determine the folding and self-assembly of ductin (see section 4.5.). It would seem reasonable though to expect that the 3-4 loop chimera phenotype is a more extreme version of the 1-2 loop chimera phenotype since if the 1-2 loop region is cytoplasmic then so will the 3-4 loop region. A cytoplasmic location for the 3-4 loop region and a crucial interaction with other V-ATPase subunits would explain the inactivation of the V-ATPase when the 3-4 loop region is exchanged with the equivalent region of VMA11.

The location of the N- and C- termini of ductin in the lumen of the vacuoles when part of the V-ATPase complex has only been indirectly observed. One such

observation was the difference between cys6 and cys44 in their formation of intermolecular disulphide bonds that was a consequence of the orientation of ductin in the V-ATPase, with cys6 lumenally located and cys44 exposed to the cytoplasm (Jones et al., 1995). As such, these mutants encountered different oxidising conditions which lead to disulphide bond induced dimerisation of cys6 under natural conditions, but not of cys44, dimerisation of which only occurred during isolation and was prevented by addition of NEM. A second study, using anti-peptide antibodies directed against the N-terminal region of ductin to label chromaffin granule membranes showed that these antibodies only bound to the lumenal surface of these V-ATPase containing membranes (Finbow et al., 1993), and this again suggests that the N-terminus of ductin was lumenally located. While in a third study, the C-terminus of ductin was modified by a six histidine extension, which did not cause the inactivation of ductin in the V-ATPase complex (Harrison et al., 1994) and is therefore not important for activity. This suggests that the C-terminus is sufficiently distant from other subunits of the V-ATPase complex not to cause inactivation. In a fourth study, an inactive form of ductin with the R34N mutation was rescued by extragenic second site suppresser mutations (Supek et al., 1992). The suppresser mutations were assumed to be present on V-ATPase subunits that were in contact with the conserved loop region that contained R34N, and that this region was located on the cytoplasmic face of the membrane.

The results obtained in this thesis concerning the activity of the ductin loop chimeras provides additional evidence to that already described above which supports the orientation of ductin being N-and C- termini lumenally exposed when it is in the V-ATPase complex. The activity of the loop chimeras of Nductin was significantly reduced or inactive compared to wild type levels, indicating that the conserved loop regions of ductin are important for the activity of ductin. This was predicted from the model of ductin which placed these loop regions at the interface

between ductin and the other V-ATPase subunits where they would play an important role in intersubunit association.

The results from the expression of the ductin loop chimeras does not provide data on which subunits of the V-ATPase it is that this region interacts with, but the importance of these regions in the activity of ductin was demonstrated. By analogy with the F-ATPase subunit *c* loop region, the ductin 3-4 loop region may be important in coupling proton translocation through V_0 with the ATP hydrolysis in V_1. In the F-ATPase subunit *c*, mutation of the conserved polar loop region consistently leads to the same phenotype, that of decoupling (Mosher et al., 1985; Fraga et al., 1994). It would be interesting to test the 3-4 loop chimera for an equivalent decoupling effect in the V-ATPase. Previous attempts at isolating the V-ATPase complex from cells expressing the defective chimeric polypeptides had failed due to low yields of vacuolar membranes. However, a new constitutive expression vector is available that provides a substantial increase in expression, and this may overcome the problem. Also, it may prove possible to test the effect that the ductin loop chimeras have on GJIC by expressing the chimeras in a model system for communication between cells, though at the moment such a system is unavailable.

Recent mutational analysis of ductin aimed at identifying residues involved in the translocation of protons indicates that the essential glutamic acid in helix 4 may lie in a crevice that is formed between helix 3 and helix 4 (Y.-I. Kim, University of Leeds; personnel communication) instead of facing into the centre of the four helical bundle, as had been originally modelled. This new location for the essential glutamic acid is similar to what has been suggested for the location of the equivalent residue in subunit c, which has been ascribed to a crevice between the two helical segments (Fillingame et al., 1992). In ductin, the potential crevice containing the essential glutamic acid is in close proximity to the 3-4 loop region

identified in this study as being essential for ductin activity. This close proximity may be to allow a linkage in some manner between the passage of protons along the helix 3 and helix 4 crevice and the other subunits of the V-ATPase that are in contact with the 3-4 loop region.

One way to identify potential sites of interaction with the 3-4 loop and 1-2 loop regions would be to isolate second site suppressor mutations that resulted in the restoration of the V-ATPase activity, as has been done previously for yeast ductin by N. Nelson (Supek et. al., 1992; 1994). In these studies suppressor mutations were selected for by either mutating inactive forms of the ductin polypeptide and screening for active forms of the polypeptide, or by mutagenising cells at low ethyl methanesulphonate levels then selecting for revertants. These techniques were successful in identifying a number of residues that could lead to a suppression of the inactive ductin phenotype. In one case, K34N, all the suppressor mutations were extragenic (Supek et al., 1992), suggesting an interaction with the other subunits of the V-ATPase for this residue. The sites at which second site suppressor mutations occur may correspond to the pathway that links proton translocation with ATP hydrolysis, as has already been suggested for the F-ATPase where suppressor mutants of subunit *c* polar loop mutants occur in the F_1 subunit ε (Zhang et al., 1994; Capaldi et al., 1994). If the 3-4 loop region of ductin does perform a similar role to that of the subunit *c* polar loop region then it may be possible to replace the 3-4 loop region with the polar loop region of subunit *c*, with the aim of showing a conservation of function between the two regions, if they are interchangeable.

4.2. Role of VMA11

VMA11 and ductin are very similar at the amino acid sequence level (70%; Umemoto, 1991), thus it was not surprising to find that in terms of the biochemical

properties studied in this thesis ductin and VMA11 have a number of features in common . Like ductin, VMA11 was inserted into microsomal membranes with dual orientations, and it was able to bind to ductin when the two proteins were co-expressed. These observations tend to suggest that the function of VMA11 will be similar to that of ductin, that is, a membrane channel protein, but with some crucial differences that provide the basis of their different activities. It has been suggested that VMA11 could be involved in the assembly of the V-ATPase enzyme, but not a part of the final complex since no VMA11 polypeptide was isolated from the V-ATPase complex (Umemoto, 1991). The ability of VMA11 to bind to ductin may not be relevant to the *in vivo* situation since *in vivo* VMA11 may not encounter ductin at all, or at least until after it is no longer capable of binding to ductin. If VMA11 does bind to ductin *in vivo* to enable assembly, VMA11 would need to be extracted from the resulting complex, which would seem to be an inefficient process especially considering ductin is capable of self-assembly in the absence of VMA11. If this is the case then there would appear to be no need for VMA11 to assist in the self-assembly of ductin, but that does not rule out a role for VMA11 in the assembly of the other V_0 subunits.

An alternative function for VMA11 could be that it provides a different ion specificity from that of ductin or that it forms the channel forming component of a non-vacuolar located V-ATPase-type enzyme. A non-vacuolar V-ATPase has been suggested as the location of the STV1 polypeptide since it localises to a different compartment from the homologous vacuolar-located protein, VPH1 (Manolson et al., 1994) (see section 1.6.4.2.). One of the problems in trying to identify the role of VMA11 has been the inability to isolate the polypeptide (Umemoto, 1991). This may be due to a low expression level and/or a non-vacoular localisation. One way round this problem would be to tag VMA11 with an epitope, such as c-myc, and use the available antibodies against c-myc to either localise the tagged polypeptide or to try and isolate the polypeptide by

immunoprecipitation. Alternatively, further studies on Nductin to VMA11 changes may provide a "*Nephrops*" protein with VMA11 activity.

The inability of any of the chimeric ductins, even with the additional changes, F24L and Y31I, to functionally replace the VMA11 activity indicates that the difference in activity between ductin and VMA11 is caused by more widespread changes throughout the polypetides than at first thought. A candidate region for further modification is in the third transmembrane helix of ductin on the same helical face as S103, since this residue is thought to be part of the crevice that contains the essential glutamic acid on helix 4, and as such may be involved in the translocation of protons (figure 40) (Y-I Kim, Leeds University; personal communication). If it proves possible to change the activity of ductin to that of VMA11 then this may help to identify residues involved in proton translocation in the V-ATPase complex.

4.3. Orientation of ductin in microsomal membranes.

To begin an investigation into the orientation of ductin it was necessary to define the mechanism by which ductin became inserted into the lipid bilayer. As would be expected from its location and disposition, in the vacuolar membrane as part of the V-ATPase, and the plasma membrane as part of the gap junction, the efficient synthesis of Nductin during *in vitro* translation is dependant upon the presence of microsomal membranes. This suggests the involvement of the SRP, in the same manner as had been observed for the acetylcholine receptor δ subunit (Walter and Blobel, 1981), and it therefore seems likely that in eukaryotic cells ductin is synthesised on ER bound ribosomes and inserted directly into the endoplasmic reticulum.

Figure 40. A model depicting the relative position of residues on the surfaces of the four α-helix bundle of Nductin.

The two residues, F24 and Y31, are thought to lie in the interface between helices 1 and 4. The three residues, S25, L27 and A29, have been positioned to reflect their relative labelling by FM when replaced by cysteine. L27 and A29 were labelled by FM, so are thought to face into the central aqueous channel, while S25 was not labelled by FM, so it has been positioned away from the central channel. The residue S103 is thought to line the crevice between helices 3 and 4 in the region of the essential E140 (modified from Finbow et al., 1995).

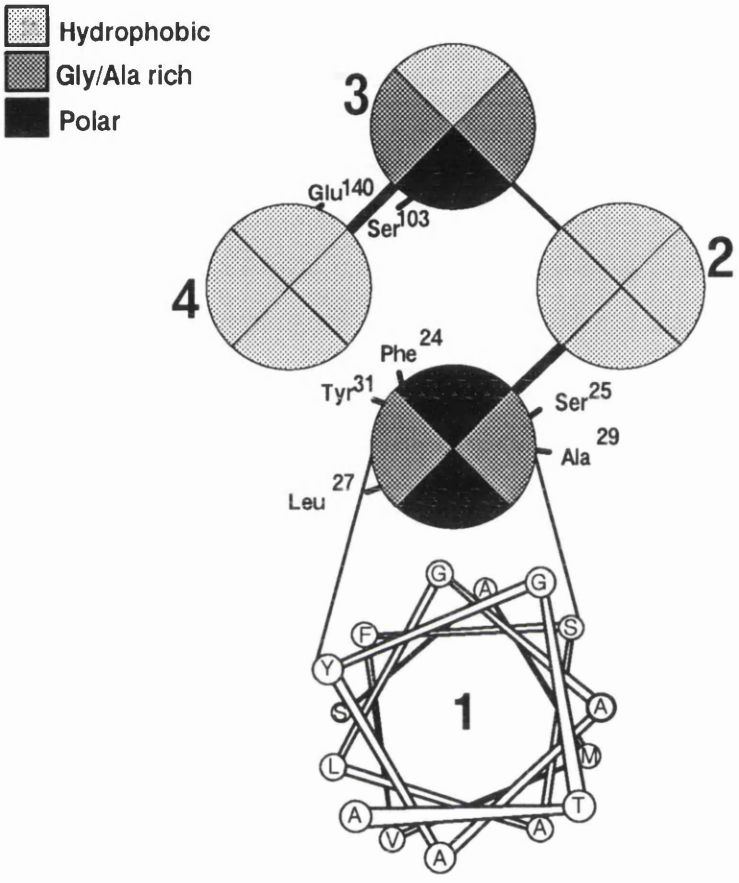
Hydrophobic
Gly/Ala rich
Polar
3
2
4
1
Glu140
Ser103
Phe24
Tyr31
Ser25
Ala29
Leu27
G
A
G
F
S
Y
S
A
L
M
A
T
V
A
A

The consensus view on the orientation of membrane proteins is that they are inserted with a single orientation and that the translocation machinery is responsible for the accurate insertion of the membrane proteins (von Heijne, 1995). Ductin is one of the first native proteins to be shown to have dual orientations after insertion into the membrane. As such, ductin challenges the consensus view on membrane protein insertion and sets a precedent for the insertion of membrane proteins with dual orientations. The insertion of ductin with dual orientations provides an explanation for previous studies on ductin which showed that the N-terminus of ductin was cytoplasmic in the gap junction (Finbow et al, 1992, 1993). In contrast, in the V-ATPase, mutagenesis studies and the maintenance of V-ATPase activity after addition of a poly histidine tail at the C-terminus of ductin, suggested that the N-terminus had a lumenal location (Supek et al., 1992, 1994; Harrison et al, 1994; Jones et al, 1994).

In a similar fashion to that of ductin, VMA11 was shown after trypsin cleavage of the fusion polypeptide, VMA11-β lac to be inserted into the microsomal membrane with dual orientations. What this result indicates is that the phenomena of dual orientations is not restricted to ductin, and from this is the question of where are the signals in ductin and VMA11 that give rise to this dual orientation. As mentioned above, the highest level of homology between the two proteins occurs in the transmembrane regions, so it would seem likely that the signals that cause the dual orientation are contained within the transmembrane regions. This agrees with the results on the effect of N-terminal charge on the orientation of ductin, as described below.

Although ductin appears to contradict current opinion, it is important to recognise that little is known about what governs orientation of polytopic membrane proteins. One reason for believing ductin has dual orientations is the confidence in

the predicted membrane disposition of ductin, that is, as a four α-helical bundle embedded in the lipid bilayer. The original predictions on ductin's disposition made on the basis of hydropathy plots have since been confirmed and extended by a variety of techniques. One such technique was FTIR which showed that ductin was composed mainly of α-helical regions (Holzenburg et al., 1993). Such a statement can not be made for other well studied membrane proteins whose structure are not well understood, like the acetyl choline receptor (ACh R). The transmembrane portion of the ACh R subunits were originally modelled as four α-helices but once the structure of the ACh R was resolved to 9Å only a single α-helix, that of M2, could be identified in the transmembrane region, thus creating uncertainty over the validity of the earlier predictions (Unwin, 1993; Hucho et al., 1994). This example illustrates the danger in relying solely on predictions from hydropathy profiles as the basis for interpreting topological results from membrane proteins.

The insertion of ductin in dual orientations at the time of its synthesis provides a means for ductin to become incorporated into both the gap junction and the V-ATPase while keeping the two complexes segregated (figure 41). In this manner the cell is able to utilise the channel properties of ductin in two different complexes and eliminates the need to re-invent a channel protein. Because of the vectorial nature of the other subunits of the V_0 sector they would be able to distinguish between the two orientations of ductin and bind only to the vacuolar orientation of ductin. As yet it is not clear as to how the ductin present in the mediatophore relates to the ductin present in the other two complexes, though it is likely to act as the channel component of the mediatophore.

The signals which might direct the dual orientation of ductin have not yet been identified. The relative disposition of charged residues, especially positive charges, in extramembranous domains are thought to be major determinants of orientation

Figure 41. Proposed scheme of the insertion of ductin leading to dual orientations and the segregation of the assembly of the V_0 of the V-ATPase from the connexon of gap junction.

Ductin is inserted into the ER membrane in dual orientations where it self-assembles into an oligomeric complex, in this model assumed to be a hexamer. The two orientations are then differentially transported so that ductin with the N- and C- termini exposed to the cytoplasm becomes incorporated into the gap junction, while ductin with the N- and C- termini exposed to the ER lumen becomes incorporated into the V-ATPase complex.

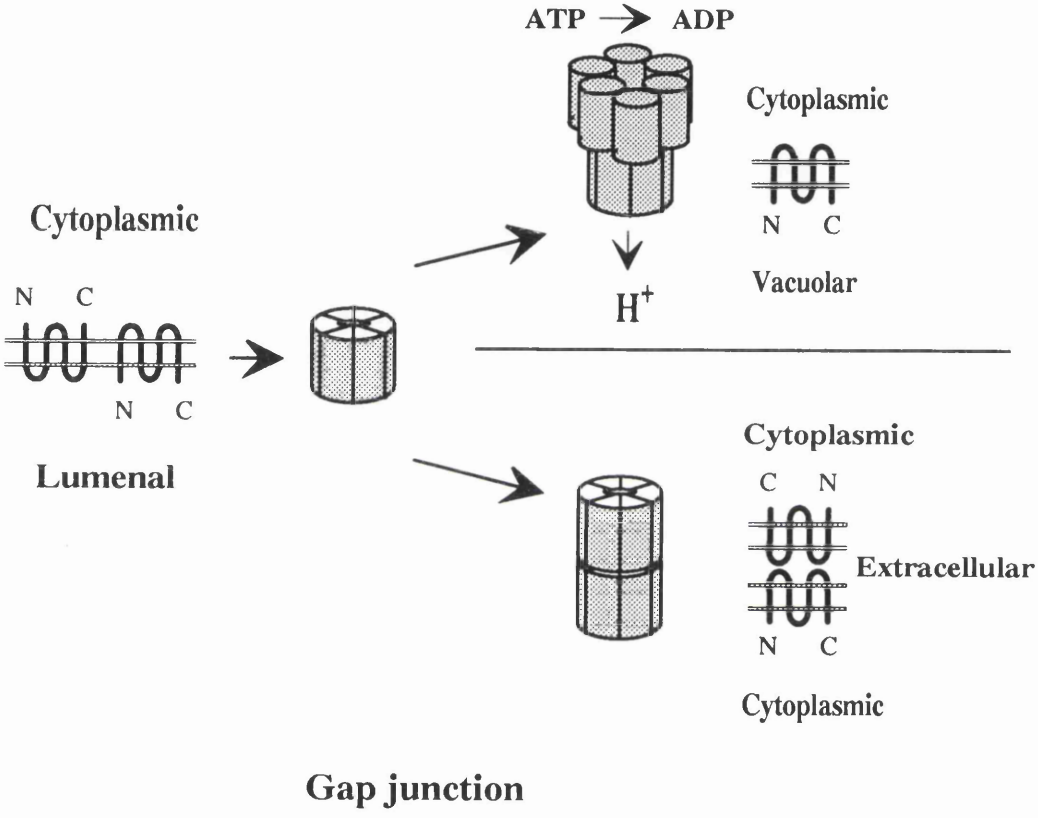
V-ATPase
ATP → ADP
Cytoplasmic
N C
Vacuolar
H+
Cytoplasmic
N C
Lumenal
Cytoplasmic
C N
Extracellular
N C
Cytoplasmic
Gap junction

(Gafvelin and von Hjeine, 1994). Changing conserved acidic residues at the N-terminus for basic or neutral residues appears to have had no effect on the ratio of the two orientations, indicating that the charge of the N-terminal region is not a factor in determining the dual orientation of ductin. A possible alternative signal containing region might be the transmembrane domains of the first and second helices. There is some basis for believing that this may be the case since work on type III transmembrane proteins showed that this orientation was determined in part by the length of the transmembrane segment as well as the N-terminal charge (Sakaguchi et al., 1992; Parks and Lamb, 1993).

One way to test the importance of the transmembrane regions would be to create chimeric forms of ductin that had this region replaced with the equivalent portion of a multimembrane pass protein known to have a single orientation, and then test the orientation of the resulting chimeric polypeptide. By systematically replacing portions of the transmembrane segments it should be possible to identify the regions responsible for the dual orientation. A possible candidate protein for such a study is squid rhodopsin, which is known to have a single membrane orientation, the N-terminus being located in the lumen and the C-terminus being exposed to the cytoplasm (Ryba et al., 1993). An alternative approach, aimed at conferring dual orientation onto a protein of known single orientation may also identify the signals that result in a dual orientation. Again squid rhodopsin would seem a suitable candidate protein since its orientation can be readily determined from cleavage of the C-terminal region by endoproteinase glu-c (V8 proteinase) (Ryba et al., 1993). Once the signals that determine the dual orientation of ductin are known it may prove possible to manipulate ductin such that it is inserted in a single orientation. This would then allow the specific targeting of either the gap junction or the V-ATPase complex with altered forms of ductin and to test the effect this has.

The generation of the orientation of type I and type II membrane proteins has been explained within the context of the hairpin model of protein insertion. This model proposes that the signal sequence is presented to the translocation site as an α-helical hairpin, with cleavage of the signal sequence generating the type I topology and non-cleavage generating the type II topology (Shaw et al., 1988). This model is less useful in explaining how the type III membrane orientation is generated, in which the signal sequence also acts as a membrane anchor and is not cleaved, resulting in the N-terminus being located in the lumen of the ER membrane, the opposite location as predicted by the hairpin loop model. There is no reason to believe that the standard translocation machinery is not capable of generating this orientation since there is evidence that this machinery is responsible for the type III orientation (Hull et al., 1988), so there is no need to invoke an alternative mechanism of insertion for ductin.

To test this, it may be worth investigating the ER machinery that gives rise to the dual orientation; is it the same as the basic translocation machinery based on the Sec61 complex (Gorlich and Rapoport, 1993) or are there additional factors responsible? The ability of the minimal translocaton machinery to insert both type I and type II proteins in their correct orientation (Gorlich and Rapoport, 1993) suggests that the orientation of ductin will also be determined by the Sec61 complex, without the aid of additional factors. A reconstituted system containing the SRP receptor and the Sec61 complex could be used to test the insertion and orientation of ductin and to identify the minimal translocation machinery required for a polytopic membrane protein. In addition, it should be possible to repeat, using ductin loaded with photoactivatable lysine analogues, the cross-linking experiments that confirmed the location of the Sec61 complex at the heart of the translocation machinery (Mothes et al., 1994). Such studies showed that the number of preprolactin residues in contact with the Sec61 complex was 40 after cleavage of the signal sequence, but before cleavage there were 80 residues in

contact with the Sec61 complex. These results are consistent with the hairpin model of insertion, and that before cleavage of the signal sequence the 80 residues in contact with the Sec61 complex are arranged so as to span the membrane twice within the translocation channel. Using ductin in place of the preprolactin in this system might confirm or refute the hairpin model as the basis for explaining the insertion of ductin and more generally other polytopic membrane proteins that do not have a cleaved signal sequence.

4.4. Assembly of ductin complexes

Once inserted into the membrane, ductin can self-associate, as shown by the ability of Bductin to bind to Nductin-β lac. This association suggests assembly of membrane complexes containing ductin takes place in the endoplasmic reticulum, as is the case for other oligomeric complexes (Hurtley and Helenius, 1989). This association is specific since no binding of ductin to polytopic membrane proteins of limited (PPA1) or no homology (squid rhodopsin) was observed. Ductin can also bind to the VMA11 polypeptide, which has 70% identity to ductin, with the conserved residues being concentrated in the transmembrane regions. This suggests that binding between ductin and VMA11 polypeptides occurs primarily within the transmembrane domains, as might be expected for these hydrophobic polypeptides.

The ability of ductin to bind to itself and VMA11 suggests that ductin folds with the correct secondary and tertiary structure once inserted into the microsomal membranes. In addition, it has recently been found that ductin binds to the transforming E5 polypeptide of bovine papillomavirus type 1 in microsomal membranes (Faccini et al., 1995), which further supports the idea that the folding and assembly of ductin *in vitro* is functionally equivalent to that of ductin *in vivo*. Whether folding is spontaneous or somehow directed by chaperones, e.g. BiP, is

not known. However, the small amount of ductin polypeptide exposed as extramembranous regions would suggest that there is minimal opportunity for the involvement of BiP or other ER chaperones. The apparent normal folding and self-association of ductin leads to the possibility that other polytopic membrane proteins which have short extramembranous domains, such as the ductin progenitor subunit *c* proteolipid of the F_0, might likewise spontaneously fold and assemble into oligomeric complexes (see below).

The labelling of residues deep in the first transmembrane domain by fluorescein-5-maleimide (FM) suggested the presence of an aqueous pore in the oligomeric complex detected by the co-immunoprecipitation of Nductin-β lac and Bductin. Such a pore has been detected in EM images of the connexons of gap junctions after negative staining (Holzenburg et al., 1993) and by the FM labelling of ductin isolated from the V-ATPase complex (Jones et al., 1995). Of interest is that FM only labels approximately half of the cys27 and cys29 polypeptides until the FM was able to cross the microsomal membrane, when near full labelling was achieved. This suggested that there is some kind of occlusion in the nascent oligomeric complex that prevents access to the FM from one side of the oligomeric complex and that the dual orientation of ductin results in FM having only partial access to the assembled oligomeric complex. The presence of an occlusion is consistent with the assumption that the V_0 sector is impermeable to protons and larger molecules after removal of the V_1 sector or after re-constitution in liposomes (Harrison et al., 1994). Closed connexons have also been predicted from studies examining gap junction structure (Unwin and Ennis, 1984). However, there is one difference compared with FM labelling in the V-ATPase complex, which is that cys27, predicted to face into the centre of the pore (figure 41) (Finbow et al, 1992), is not labelled efficiently in the whole V-ATPase but is labelled in the microsomal membrane. The reason for this difference may be that the ductin oligomeric

complex is modified during the assembly of the V-ATPase complex by the presence of the other subunits.

The Bductin mutant E139R was available with which to test the effect on assembly of the substitution of the conserved essential glutamic acid for lysine. E139R was co-immunoprecipitated with Nductin-β lac in the same ratio as had the wild type Bductin, indicating that the substitution had no effect on the ability of Bductin to assemble with Nductin-β lac. The transforming effect that has been reported for this mutation (Andresson et al., 1993) is probably not due to faulty assembly of this polypeptide, but instead due to alteration of some other activity of ductin, such as the channel properties or the association of other polypeptides with ductin.

An understanding of the process that leads to the assembly of ductin complexes should also be applicable to a number of other membrane channel families e.g. the aquaporins, that consist of multi-subunit assemblies (Walz et al., 1994). The assembly of another multi-subunit complex, the ACh R, is via a multistep process involving the rapid formation of a trimer of subunits followed by the slower addition of the last two subunits to produce the full pentameric assembly (Green and Claudio, 1993). During this process an important factor is thought to be the folding of the large extramembranous domains by factors in the lumen of the ER. Similarly the folding of the VSV G protein ectodomain has been shown to involve the lumenal chaperone proteins BiP (GRP78) (Machamer et al., 1990)and calnexin (Hammond, 1994). The ectodomain folding of both the ACh R subunits and the VSV G protein may be able to influence the way in which the transmembrane regions of these polypeptides interact with themselves. This is not the case for ductin which has only the most minimal regions exposed to the ER lumen, so it is unlikely that there is any involvement of lumenal factors in the folding and assembly of ductin. If this is the case then what are the forces that determine the self-assembly of the ductin polypeptides?

The folding and assembly of integral membrane proteins is thought to occur in a two step process, with the formation of a stable helix followed by the association of the helices into the tertiary/quaternary structure (von Heijne, 1995). The association of transmembrane regions has been studied in a number of proteins, including bacteriorhodopsin and glycophorin A. The dimerisation of glycophorin A is mediated by its transmembrane domain and was shown to be the result of a specific helix-helix association (Lemmon et al., 1992). In this study what were considered relatively conservative changes were capable of disrupting the association mediated by the transmembrane region, indicating that a high degree of specificity was involved at the dimer interface. The transmembrane segments of bacteriorhodopsin can be considered as independently folding units since a functional polypeptide can be generated from the association of the first two transmembrane segments with the other five transmembrane segments after reconstitution of the chymotrypsin cleaved polypeptide (Popot et al., 1987). The ability of these two fragments to fold into a native structure during reconstitution suggests that the folding of these polypeptides is primarily determined by local properties of the sequence and not by the presence of either the rest of the protein or the biosynthetic machinery. The general outline of the principles involved in the assembly of membrane proteins, those of independently folding units that are capable of very specific associations, seems likely to apply to ductin at both the tertiary and quaternary level.

It should be possible to identify the regions within ductin that contribute to the process of self-assembly by systematically replacing the transmembrane regions of ductin with the equivalent region of PPA1. PPA1 is homologous to ductin but is unable to associate with ductin in the *in vitro* system (figure 34), so exchanging transmembrane domains between the two proteins should minimise disruption of the tertiary structure while allowing the effects on quaternary structure to be

studied, since an association competent domain from ductin will have been replaced with an association incompetent domain from PPA1. By testing the ability of these ductin/PPA1 chimeras to self-assemble and to assemble with ductin the regions involved in assembly may be mapped. A panel of ductin/PPA1 chimeric polypeptides could also be used to investigate the role of individual transmembrane domains in the binding of other proteins to ductin. One such protein is the BPV1 E5 oncogene which has been shown to bind to ductin in the *in vitro* translation system (Faccini et al., 1995) and in a number of other expression systems, such as transient transfection of COS cells (Goldstein and Schlegel, 1990). In contrast, the PPA1 polypeptide was unable to bind to E5 in the *in vitro* translation system, thus making it possible to use the ductin/PPA1 chimeric polypeptides to map the E5 binding site on ductin.

If the assembled form of ductin found *in vitro* contains the same aqueous channel found in the final gap junction and V-ATPase complexes then this initial assembly process probably provides the basis for the further assembly of ductin containing complexes. The assembly of the V-ATPase is already known to occur in the ER (Myers and Forgac, 1993) so the self-assembly of a ductin complex in this region is not surprising, but the site of assembly for the gap junction has not been established so the identification of the ER as the site of the initial assembly process is a beginning in the understanding of how the whole process of gap junction assembly occurs. One of the intriguing results obtained from the FM labelling is the presence of an occlusion in the ductin complex that only allows the FM access to the single cysteine residues from one side of the membrane. The detection of this occlusion now allows it to be mapped, by altering the sites of the single cysteine residue to different locations in the aqueous channel. If this occlusion is the result of a "closed" ductin hexamer channel then it may prove possible to "open" the channel by mutation, and so determine the residues or regions of ductin involved in opening the channel.

References.

Abrahams, J.B., Lutter, R., Todd, R.J., Van Raaij, M.J., Leslie, A.G.W. and Walker, J.E. (1993). Inherent assymetry of the structure of F_1-ATPase from bovine heart at 6.5 Å resolution. *EMBO J.*, **12**, 1775-1780.

Abrahams, J.B., Leslie, A.G.W., Lutter, R., and Walker, J.E. (1994). Structure at 2.8 Å of F_1-ATPase from bovine heart mitochondria. *Nature*, **370**, 621-628.

Anderson, D.J., Walter, P. and Blobel, G. (1982). Signal recognition protein is required for the integration of acetylcholine receptor δ subunit, a transmembrane glycoprotein, into the endoplasmic reticulum membrane. *J. Cell Biol.*, **93**, 501-506.

Andresson, T., Sparkowski, J. and Schlegel, R. (1993). Mutants of the 16 K pore-forming protein of the vacuolar ATPase: loss of BPV-1 E5 oncoprotein binding is accompanied by aquisition of transforming activity. Abstract for the 12th International Pappilomavirus Conference, Baltimore, 12th Sept.-1st Oct. 1993.

Anraku, Y., Umemoto, N., Hirata, R. and Wada, Y. (1989). Structure and function of the yeast vacuolar membrane proton ATPase. *J. Bioenerg. Biomembr.*, **21**, 589-603.

Apperson, M., Jensen, R.E., Suda, C., Witte, C. and Yaffe, M.P. (1990). A yeast protein, homologous to the proteolipid of the chromaffin granule proton-ATPase, is important for cell growth. *Biochem. Biophys. Res. Commun.*, **168**, 574-579.

Arai, H., Terres, G., Pink, S. and Forgac, M. (1988). Topography and subunit stoichiometry of the coated vesicle proton pump. *J. Biol. Chem.* **263**, 8796-8802.

Arai, H., Berne, M. and Forgac, M. (1987). Inhibition of the coated vesicle proton pump and labeling of a 17,000-dalton polypeptide by *N,N'* dicyclohexylcarbodiimde. *J. Biol. Chem.* **251**, 11006-11011.

Arkin, I.T., Adams, P.D., MacKenzie, K.R., Lemmon, M.A., Brunger, A.T. and Engelman, D.M. (1994). Structural organisation of the pentameric transmembrane α-helices of phospholamban, a cardiac ion channel. *EMBO J.*, **13**, 4757-4764.

Azarnia, S., Reddy, S., Kmiecik, T.E., Shalloway, D. and Loewenstein, W.R. (1988). The cellular *src* gene product regulates junctional cell-to-cell communication. *Science*, **239**, 398-401.

Bauerle, C., Ho, M.N., Lindorfer, M.A. and Stevens, T.H. (1993). The *Saccharomyces cerevisiae VMA6* gene encodes the 36-kDa subunit of the vacuolar H^+-ATPase membrane sector. *J. Biol. Chem.*, **268**, 12749-12757.

Beltran, C. and Nelson, N. (1992) The membrane sector of the vacuolar H^+-ATPase by itself is impermeable to protons. *Acta Physiol. Scand.*, **145**, 40-46.

Beltran, C., Kopecky, J., Pan, Y.C., Nelson, H. and Nelson, N. (1992). Cloning and mutational analysis of the gene encoding subunit c of yeast vacuolar H^+-ATPase. *J. Biol. Chem.*, **267**, 774-779.

Beltzer, J.P., Fiedler, K., Fuhrer, C., Geffen, I., Handschin, C., Wessels, H.P. and Spiess, M. (1991). Charged residues are major determinants of the transmembrane orientation of a signal-anchor sequence. *J. Biol. Chem.*, **266**, 973-978.

Bianchet, M., Ysern, S., Hullihen, J., Pederson, P.L and Amzel, L.M. (1991). Mitochodrial ATP synthase: quaternary structure of the F_1 moiety at 3.6 Å determined by X-ray diffraction. *J. Biol. Chem.*, **266**, 21197-21201.

Birman, S., Israel, M., Lesbats, B. and Morel, N. (1986). Solubilisation and partial purification of a presynaptic membrane protein ensuring calcium-dependant acetylcholine release from proteoliposomes. *J. Neurochem.*, **47**, 433-444.

Birman, S., Meunier, F.-M, Lesbats, B., Le Caer, J.-P and Israel, M. (1990) A 15 kDa proteolipid found in mediatophore preparations from *Torpedo* electric organ present high sequence homology with the bovine chromaffin granule protonophore. *FEBS Letts.*, **250**, 293-296.

Blobel, G. (1980). Intracellular protein topogenesis. *Proc. Natl. Acad. Sci. USA*, **77**, 1496-1500.

Boekema, E.J., van Heel, M. and Graber, P. (1988) Structure of the ATP synthase from chloroplasts studied by electron microscopy and image processing. *Biochim. Biophys Acta*, **932**, 354-361.

Bohrmann, J. (1993). Antisera against a channel -forming 16 kDa protein inhibit dye-coupling and bind to cell membranes in Drosophila ovarian follicles. *J. Cell. Sci.*, **105**, 513-518.

Bowman, B.J., Dschida, W.J., Harris, T. and Bowman, E.J. (1989) The vacuolar ATPases of *Neurospora crassa* contains an F_1-like structure. *J. Biol. Chem.*, **264**, 15506-15512.

Breckenridge, L.J. and Almers, W. (1987) Currents through the fusion pore during exocytosis of a secretory vesicle. *Nature*, **317**, 814-817.

Brochier, G., Gulik-Krzywicki, T., Lesbats, B., Dedieu, J.C. and Israel, M. (1992). Calcium-induced acetylcholine release and intramembrane particle occurrence in proteoliposomes equipped with mediatophore. *Biol. Cell*, **74**, 225-230.

Brodsky, J.L. and Schekman, R. (1993). A sec63p-BiP complex from yeast is required for protein translocation in a reconstituted proteoliposome. *J. Cell Biol.*, **123**, 1355-1363.

Bruss, V., Lu, X., Thomssen, R. and Gerlich, W.H. (1994). Post-translational alterations in transmembrane topology of the hepatitus B virus large envelope protein. *EMBO J.*, **13**, 2273-2279.

Burnett, S., Jareborg, N. and DiMaio, D. (1992). Localisation of bovine papillomavirus type 1 E5 protein to transformed basal keratinocytes and permissive differentiated cells in fibropapilloma tissue. *Proc. Natl. Acad. Sci. USA*, **89**, 5665-5669.

Capaldi, R.A., Aggeler, R., Turina, P. and Wilkens, S. (1994). Coupling between catalytic sites and the proton channel in F_1F_0-type ATPases. *T.I.B.S.*, **19**, 284-289.

Caspar, D.L.D., Goodenough, D.A., Makowski, L. and Phillips, W.C. (1977). Gap junction structures: I correlated electron micrsocopy and X-ray diffraction. *J. Cell Biol.*, **74**, 605-627.

Cavalli, A., Eder-Colli, L., Dunant, Y., Loctin, F. and Morel, N. (1991). Release of acetylcholine by *Xenopus* oocytes injected with mRNAs from cholinergic neurons. *EMBO J.*, **10**, 1671-1675.

Cavalli, A., Dunant, Y., Leroy, C., Meunier, F.M., Morel, N. and Israel, M. (1993). Antisense probes against mediatophore block transmitter release in oocytes primed with neuronal mRNAs. *Euro. J. Neuroscience*, **5**, 1539-1544.

Claudio, T., Paulson, H.L., Green, W.N., Ross, A., Hartman, D.S. and Hayden, D. (1989). Fibroblasts transfected with *Torpedo* actetylcholine receptor β-, γ-, and δ-subunit cDNAs express functional receptors when infected with a retroviral a recombinant. *J. Cell Biol.*, **108**, 2277-2290.

Cohen, B.D., Goldstein, D.J., Rutledge, L., Vass, W.C., Lowy, D.R., Schlegel, R. and Schiller, J.T. (1993). Transformation-specific interaction of the bovine papillomavirus E5 oncoprotein with the platelet-derived growth factor receptor transmembrane domain and the epidermal growth factor receptor cytoplasmic domain. *J. Virol.*, **67**, 5303-5311.

Conrad, M., Bubb, V.J. and Schlegel, R. (1993). The human papillomavirus type 6 and 16 E5 proteins are membrane-associated proteins which associate with the 16-kilodalton pore-forming protein. *J. Virol.*, **67**, 6170-6178.

Conrad, M., Goldstein, D., Andresson, T. and Schlegel, R. (1994). The E5 protein of HPV-6, but not HPV-16, associates efficiently with cellular growth factor receptors. *Virol.*, **200**, 796-800.

Crider, B.P., Xie, X.-S. and Stone, D.K. (1994). Bafilomycin inhibits proton flow through the H^+ channel of the vacuolar proton pumps. *J. Biol. Chem.*, **269**, 17379-17381.

Crowley, K.S., Reinhart, G.D. and Johnson, A.E. (1993). The signal sequence moves through a ribosomal tunnel into a noncytoplasmic aqueous environment at the ER membrane early in translocation. *Cell*, **73**, 1101-1115.

Crowley, K.S., Liao, S., Worrel, V.E., Reinhart, G.D. and Johnson, A.E. (1994). Secretory proteins move through the endoplasmic reticulum membrane via an aqueous, gated pore. *Cell*, **78**, 461-471.

Dahl, G., Miller, T., Paul. D, Voellmy, R. and Werner, R. (1987) Expression of functional cell-cell channels from cloned rat liver gap junction complementary DNA. *Science*, **235**, 1280-1283.

Dehaan, R.L. (1988). Dynamic behaviour of cardiac gap junctions. In *Gap Junctions*, ed. Hertzberg, E.L. and Johnson, R.G., pp305-320, Alan Liss Inc., New York.

Deisenhofer, J., Epp, O., Miki, K., Huber, R. and Michel, H. (1985). Structure of the protein subunits in the photosynthetic reaction centre of *Rhodopseudomonas viridis* at 3Å resolution. *Nature*, **318**, 618-624.

Denda, K., Konishi, J., Oshima, T., Date, T. and Yoshida, M. (1989). A gene encoding the proteolipid subunit of *Sulfolobus acidocaldarius* ATPase complex. *J.Biol. Chem.*, **264**, 7119-7121.

Dermietzel, R., Volker, M., Hwang, T.-K., Berzborn, R.J. and Meyer, H.E. (1989). A 16 kDa protein co-isolating with gap junctions from brain tissue belonging to a class of proteolipids of the vacuolar H^+-ATPases. *FEBS letts.*, **253**, 1-5.

Dermietzel, R., Hwang, T.K. and Spray, D.S. (1990). The gap junction family: structure, function, and chemistry. *Anat. Embryol.*, **182**, 517-528.

Deshaies, R.J. and Schekman, R. (1987). A yeast mutant defective at an early stage in import of secretory protein precursors into the endoplasmic reticulum. *J. Cell Biol.*, **105**, 633-645.

Deshaies, R.J., Sanders, S.L., Feldheim, D.A. and Schekman, R. (1991). Assembly of yeast Sec proteins involved in translocation into endoplasmic reticulum into a membrane-bound multisubunit complex. *Nature*, **349**, 806-807.

DiMaio, D., Guralski, D. and Schiller, J.T. (1986). Translation of open reading frame E5 of bovine papillomavirus is required for its transforming activity. *Proc. Natl. Acad. Sci. USA*, 83, 1797-1801.

Doherty, R.D. and Kane, P.M. (1993). Partial assembly of the yeast vacuolar H^+-ATPase in mutants lacking one subunit of the enzyme. *J. Biol. Chem.*, **268**, 16845-16851.

Dschida, W.J. and Bowman, B.J. (1992). Structure of the vacuolar ATPase from *Neurospora crassa* as determined by electron microscopy. *J. Biol. Chem.*, **267**, 18783-18789.

Duff, K.C., Gilchrist, P.J., Saxena, A.M. and Bradshaw, J.P. (1994) Neutron diffraction reveals the site of amantadine blockade in the influenza A M2 ion channel. *Virology*, **202**, 277-283.

Elble, R. (1992). A simple and efficient procedure for transformation of yeasts. *BioTechniques*, **13**, 18-20.

Faccini, A.M., Cairney, M., Anderson, R., Finbow, M.E., Campo, M.S. and Pitts, J.D. (1995). The bovine papillomavirus type 4 E8 protein binds to ductin in a cell-free system; down-regulation of gap junctional intercellular communication in cells transformed by BPV-4. (in prep.).

Falk, M. M., Kumar, N. M., and Gilula, N. B. (1994). Membrane insertion of gap junction connexins: polytopic channel forming membrane proteins. *J. Cell Biol.*, **127**, 343-355.

Feldheim, D. and Schekman, R. (1994). Sec72p contributes to the selective recognition of signal peptides by the secretory polypeptide translocation complex. *J.Cell Biol.*, **126**, 935-943.

Filligame R.H., Oldenburg, M. and Fraga, D. (1991). Mutation of alanine 24 to serine in subunit *c* of the Escherichia coli F_1F_0-ATP synthase reduces reactivity of aspartyl 61 with dicyclohexylcarbodiimide. *J. Biol. Chem.*, **266**, 20934-20939.

Fillingame, R.H. (1992). Subunit *c* of F_1F_0ATP synthase: structure and role in transmembrane energy transduction. *Biochim. Biophys. Acta*, **1101**, 240-243.

Fillingame, R.H., Girvin, M.E., Fraga, D. and Zhang, Y. (1992). Correlations of structure and function in H^+ translocating subunit *c* of F_1F_0ATP synthase. *Ann. N. Y. Acad. Sci.*, **671**, 323-334.

Finbow, M.E. and Pitts, J.D. (1981). Pereability of junctions between animal cells: Intercellular exchange of various metabolites and a vitamin derived cofactor. *Exp. Cell Res.*, **131**, 1-13.

Finbow, M.E., Shuttleworth, J., Hamilton, A.E. and Pitts, J.D. (1983). Analysis of vertebrate gap junction protein. *EMBO J.*, **2**, 1479-1486.

Finbow, M.E., Buultjens, T.E.J., Lane, N.J., Shuttleworth, J. and Pitts, J.D. (1984). Isolation and characterisation of arthropod gap junctions. *EMBO J.*, **3**, 2271-2278.

Finbow, M.E., Buultjens, T.E.J., John, S., Kam, E., Meagher, L. and Pitts, J.D. (1986). Molecular structure of the gap junctional channel. *Ciba symp.*, **125**, 92-107.

Finbow, M.E., Pitts, J.D., Goldstein, D.J., Schlegel, R. and Findlay, J.B.C. (1991). The E5 oncoprotein target: a 16-kDa channel-forming protein with diverse functions. *Molec. Carcinogen.*, **4**, 430-434.

Finbow, M.E., Eliopoulos, E.E., Jackson, P.J., Keen, J.N., Meagher, L., Thompson, P., Jones, P. and Findlay. J.B.C. (1992). Structure of a 16 kDa integral membrane protein that has identity to the putative proton channel of the vacuolar H^+-ATPase. *Protein Eng.*, **5**, 7-15.

Finbow, M.E. and Meagher, L. (1992). Connexins and the vacuolar proteolipid-like 16-kDa protein are not directly associated with each other but may be components of similar or the same gap junctional complexes. *Exp. Cell Res.*, **203**, 280-284.

Finbow, M.E., and Pitts, J.D. (1993). Is the gap junction channel- *the connexon*- made of connexin or ductin? *J. Cell Sci.*, **106**, 463-472.

Finbow, M.E., John, S., Kam, E., Apps, D.K. and Pitts,J.D. (1993). Disposition and orientation of ductin (DCCD-reactive vacuolar H^+-ATPase subunit) in mammalian membrane complexes. *Exp. Cell Res.*, **207**, 261-270.

Finbow, M.E., Goodwin, S., Meagher, L., Lane, N.J., Keen, J., Findlay, J.B.C. and Kaiser, K. (1994). Evidence that the 16 kDa proteolipid (subunit c) of the vacuolar H^+-ATPase and ductin from gap junctions are the same polypeptide in *Drosophila* and *Manduca*: molecular cloning of the *Vha16k* gene from *Drosophila*. *J. Cell Sci.*, **107**, 1817-1824.

Finbow, M. E., Harrison, M., and Jones, P. (1995). Ductin- a proton pump component, a gap junction channel and a neurotransmitter release channel. *Bioessays*, **17**, 247-255.

Flagg-Newton, J., Simpson, I. and Loewenstein, W.R. (1979). Permeability of cell-cell membrane channels in mammalian cell junctions. *Science*, **205**, 404-409.

Forgac, M. (1992). V-type ATPases, *J. Bioenerg. Biomem- minireview series*, **24**, 339-350.

Forgac, M. (1989). Structure and function of the vacuolar class of ATP-driven proton pumps. *Physiol. Rev.*, **69**, 765-796.

Foster, D.L. and Fillingame, R.H. (1982). Stoichiometry of subunits in the H^+-ATPase complex of *Escherichia coli*. *J. Biol. Chem.*, **257**, 2009-2015.

Foury, F. (1990). The 31-kDa polypeptide is an essential subunit of the vacuolar ATPase in *Saccharomyces cerevisiae*. *J. Biol. Chem.*, **265**, 18554-18560.

Fraga, D., and Fillingame , R.H. (1989). Conserved polar loop region of Escherichia coli subunit *c* of the F_1F_0 H^+-ATPase. *J. Biol. Chem.*, **264**, 6797-6803.

Fraga, D., Hermolin, J. and Fillingame, R.H. (1994). Transmembrane helix-helix interactions in F0 suggested by suppressor mutations to ala^{24} > asp/asp^{61} > gly mutant of ATP synthase subunit *c*. *J. Biol. Chem.*, **269**, 2562-2567.

Fraga, D., Hermolin, J., Oldenburg, M., Miller, M.J. and Fillingame, R.H. (1994). Arginine 41 of subunit *c* of *Escherichia coli* H^+-ATP synthase is essential in binding and coupling of F_1 to F_0. *J. Biol. Chem.*, **269**, 7532-7537.

Franchini, G., Mulloy, J.C., Koralnik, I.J. Lo Monico, A., Sparkowski, J.J, Andresson, T., Goldstein, D.J and Schlegel, R. (1993) The human T-cell leukemia/lymphotrophic virus type I p12' protein cooperates with the E5 oncoprotein of bovine papillomavirus in cell transformation and binds the 16-kilodalton subunit of the vacuolar H^+-ATPase. *J. Virol.*, **67**, 7701-7704.

Frydman, J., Nimmesgern, E., Ohtsuka, K. and Hartl, F.U. (1994). Folding of nascent polypeptide chains in high molecular mass assembly with molecular chaperones. *Nature*, *370*, 111-117.

Gafvelin, G., and von Hjeine, G. (1994). Topological "fustration" in multispanning E. coli inner membrane proteins. *Cell*, **77**, 401-412.

Gilmore, R. (1993). Protein translocation across the endoplasmic reticulum: a tunnel with toll booths at entry and exit. *Cell*, **75**, 589-592.

Girvin, M.E. and Fillinghame, R.H. (1993) Hairpin folding of subunit *c* of the F_1F_0 ATP synthase: ^1H NMR resonance assignments and NOE analysis. *Biochem.*, **32**, 12167-12177.

Girvin, M.E. and Fillinghame, R.H. (1994) Helical structure and folding of subunit *c* of the F_1F_0 ATP synthase: ^1H distance measurements to nitroxide-derivatized aspartyl-61. *Biochem.*, **33**, 665-674.

Gogarten, J.P., Kibak, H., Dittrich, P., Taiz, L., Bowman, E.J., Bowman, B.J., Manolson, M.F., Poole, R.J., Date, T., Oshima, T., Konishi, J., Denda, K. and Yoshida, M. (1990). The evolution of the vacuolar H^+-ATPase: implications for the origin of the eukaryotes. *Proc. Natl. Acad. Sci. USA*, **86**, 6661-6665.

Goldstein, D.J. and Schlegel, R. (1990). The E5 oncoprotein of bovine papillomavirus binds to a 16 kd cellular protein. *EMBO J.*, **9**, 137-146.

Goldstein, D.J., Finbow, M.E., Andresson, T., McLean, P., Smith, K., Bubb, V. and Schlegel, R. (1991). Bovine papillomavirus E5 oncoproteins binds to the 16K component of the vacuolar H^+-ATPases. *Nature*, **352**, 347-349.

Goldstein, D.J., Andresson, T., Sparkowski, J.J. and Schlegel, R. (1992a). The BPV-1 E5 protein, the 16 kDa membrane pore-forming protein and the PDGF receptor exist in a complex that is dependant on hydrophobic transmembrane interactions. *EMBO J.*, **11**, 4851-4859.

Goldstein, D.J., Kulke, R., DiMaio, D. and Schlegel, R. (1992b). A glutamine residue in the membrane-associating domain of the bovine papillomavirus type 1 E5 oncoprotein mediates its binding to a transmembrane component of the vacuolar H^+-ATPase. *J. Virol.*, **66**, 405-413.

Goldstein, D.J., Li, W., Wang, L.-M., Heidaran, M.A., Aaronson, S., Shinn, R., Schlegel, R. and Pierce, J.H. (1994). The bovine papillomavirus type 1 E5 transforming protein specifically binds and activates the β-type receptor for the platelet-derived growth factor but not other related tyrosine kinase-containing receptors to induce cellular transformation. *J. Virol.*, **68**, 4432-4441.

Gorlich, D., Prehn, S., Hartmann, E., Kalies, K.-U. and Rapoport, T.A. (1992a). A mammalian homologue of SEC61p and SECYp is associated with ribosomes and nascent polypeptides during translocation. *Cell*, **71**, 489-503.

Gorlich, D., Hartmann, E., Prehn, S. and Rapoport, T.A. (1992b). A protein of the endoplasmic reticulum involved early in polypeptide translocation. *Nature*, **357**, 47-52.

Gorlich, D. and Rapoport, T.A. (1993). Protein translocation into proteoliposomes reconstituted from purified components of the endoplasmic reticulum membranes. *Cell*, **75**, 615-630.

Green, W.N. and Claudio, T. (1993). Acetylcholine receptor assembly: subunit folding and oligomerisation occur sequentially. *Cell*, **74**, 57-69.

Guthrie, C. and Fink, G.R. (1991). Guide to yeast genetics and molecular biology. *Meth. Enzymol.*, **194**, Academic Press Inc.

Hall, M.D., Hoon, M.A., Ryba, N.J., Pottinger, J.D., Keen J.N., Saibil, H.R., and Findlay, J.B. (1991). Molecular cloning and primary structure of squid (*Loligo forbesi*) rhodopsin, a phospholipase C-directed G-protein-linked receptor. *Biochem J.*, **274**, 35-40.

Hammond, C., Braakman, I. and Helenius, A. (1994). Role of N-linked oligosaccharide recognition, glucose trimming, and calnexin in glycoprotein folding and quality control. *Proc. Natl. Acad. Sci. USA*, **91**, 913-917.

Hammond, C. and Helenius, A. (1994). Folding of VSV G protein: sequential interaction with BiP and calnexin. *Science*, **266**, 456-458.

Harrison, M.A., Jones, P.C., Kim, Y.-I., Finbow, M.E. and Findlay, J.B.C. (1994). Functional properties of a hybrid vacuolar H^+-ATPase in *Saccharomyces*

cells expressing the *Nephrops* 16-kDa proteolipid. *Eur. J. Biochem.*, **221**, 111-120.

Hartmann, E., Rapoport, T.A. and Lodish, H.F. (1989). Predicting the orientation of eukaryotic membrane-spanning proteins. *Proc. Natl. Acad. Sci.*, **86**, 5786-5790.

Harvey, W.R and Nelson N. (1992). V-ATPases. *J. Exp. Biol.*, **172**, 1-485.

Hasebe, M., Hamada, H., Moriyama, Y., Maeda, M. and Futai, M. (1992). Vacuolar H^+-ATPase genes, the presence of four genes including pseudogene for the 16 kDa proteolipid in the human genome. *Biochim. Biophys. Res. Comm.*, **183**, 856-863.

Hax, W.M.A., van Venrooji, G.E.P.M. and Vossenberg, J.B.J. (1974). Cell communication: a cyclic-AMP mediated phenomenon. *J. Mem. Biol.*,**19**, 253-266.

Henderson, R., Baldwin, J.M., Ceska, T.A., Zemlin, F., Beckmann, E. and Downing, K.H. (1990). Model for the structure of bacteriorhodopsin based on high-resolution electron cryo-microscopy. *J. Mol. Biol.*, **213**, 899-929.

Hermolin, J., and Fillinghame, R. H. (1989). H^+-ATPase activity of the *Escherichia coli* F_1F_0 is blocked after reaction of dicyclohexylcarbodiimide with a single proteolipid (subunit c) of the F_0 complex. *J. Biol. Chem.*, **253**, 3796-3803.

Hiebert, S.W., Paterson, R.G. and Lamb, R.A. (1985). Hemagglutinin-neuraminidase protein of the paramyxovirus simian virus 5: nucleotide sequence of the mRNA predicts an N-terminal membrane anchor. *J. Virol.*, **54**, 1-6.

High, S., and Dobberstein, D. (1992). Mechanisms that determine the transmembrane disposition of proteins. *Curr. Opin. Cell Biol.*, **4**, 581-586.

High, S., Andersen, S.S.L., Gorlich, D., Hartmann, E., Prehn, S., Rapoport, T.A. and Dobberstein, B. (1993). Sec61p is adjacent to nascent type I and type II signal-anchor proteins during their membrane insertion. *J. Cell Biol.*, **121**, 743-750.

High, S., Martoglio, B., Gorlich, D., Andersen, S.S.L., Ashford, A.J., Giner, A., Hartmann, E., Prehn, S., Rapoport, T.A., Dobberstein, B. and Brunner, J. (1993). Site-specific photocross-linking reveals that sec61p and TRAM contact different regions of a membrane-inserted signal sequence. *J. Biol. Chem.*, **268**, 26745-26751.

High, S. and Stirling, C.J. (1993). Protein translocation across membranes: common themes in divergent organisms. *T.I.C.B.*, **3**, 335-339.

Hirata, R., Ohsumi, Y., Nakano, A., Kawasaki, H., Suzuki, K. and Anraku, Y. (1990). Molecular structure of a gene, *VMA1*, encoding the catalytic subunit of H^+-translocating adenosine triphosphate from vacuolar membranes of *Saccharomyces cerevisiae*. *J. Biol. Chem.*, **265**, 6726-6733.

Hirata, R., Umemoto, N., Ho, M.N., Ohya, Y., Stevens, T.H. and Anraku, Y. (1993). *VMA12* is essential for assembly of the vacuolar H^+-ATPase subunits onto the vacuolar membrane in *Saccharomyces cerevisiae*. *J. Biol. Chem.*, **268**, 961-967.

Ho, M.N., Hill, K.J., Lindorfer, M.A. and Stevens, T.H. (1993). Isolation of vacuolar membrane H^+-ATPase-deficient yeast mutants; the *VMA5* and *VMA4* genes are essential for assembly and activity of the vacuolar H^+-ATPase. *J. Biol. Chem.*, **268**, 221-227.

Ho, M.N., Hirata, R., Umenoto, N., Ohya, Y., Takatsuki, A., Stevens, T.H. and Anraku, Y. (1993). *VMA13* encodes a 54-kDa vacuolar H^+-ATPase subunit required for activity but not assembly of the enzyme complex in *Saccharomyces cerevisiae*. *J. Biol. Chem.*, **268**, 18286-18292.

Hoh, J.H., Lal, R., John, S.A., Revel, J.-P. and Arnsdorf, M.F. (1991). Atomic force microscopy and dissection of gap junctions. *Science*, **253**, 1405-1408.

Holzenburg, A., Jones, P.C., Franklin, T., Pali, T., Heimburg, T., Marsh D., Findlay, J.B.C. and Finbow, M.E. (1993). Evidence for a common structure for a class of membrane channels. *Eur. J. Biochem.*, **213**, 21-30.

Hoppe, J., Schairer, H.U. and Sebald, W. (1980). The proteolipid of a mutant ATPase from *Eschirichia coli* defective in H^+-conduction contains a glycine instead of the carbodiimide-reactive aspartyl residue. *FEBS lett.*, **109**, 107-111.

Hoppe, J., Schairer, H.U., Friedl, P. and Sebald, W. (1982). An asp-asn substitution in the proteolipid subunit of the ATP synthase from *Eschirichia coli* leads to a non-functional proton channel. *FEBS lett.*, **145**, 21-24.

Horwitz, B.H., Burkhardt, A., Schlegel, R. and DiMaio, D. (1988). 44-amino-acid E5 transforming protein of bovine papillomavirus requires a hydrophobic core and specific carboxyl-terminal amino-acids. *Mol. Cell. Biol.*, **8**, 4071-4078.

Hubbard, S.C. and Ivatt, R.J. (1981). Synthesis and processing of asparagine-linked oligosaccharides. *Annu. Rev. Biochem.*, **50**, 555-583.

Hucho, F., Gorne-Tschelnokow, U. and Strecker, A. (1994). b-structure in the membrane-spanning part of the nicotinic acetylcholine receptor (or how helical are transmembrane helices?). *T.I.B.S.*, **19**, 383-387.

Hurtley, S.M., and Helenius, A. (1989). Protein oligomerisation in the endoplasmic reticulum. *Ann. Rev. Cell Biol.*, **5**, 277-307.

Israel, M., Morel, N., Lesbats, B., Birman, S. and Manranche, R. (1986). Purification of a presynaptic membrane protein that mediates a calcium-dependant translocation of aceetylcholine. *Proc. Natl. Acad. Sci. USA*, **83**, 9226-9230.

Israel, M. and Dunant, Y. (1993). Acetylcholine release, from molecules to function. *Prog. Brain Res.*, **98**, 219-233.

Israel, M., Morel, N. and Lesbats, B. (1992). Evidence for an association of the 15-kDa proteolipid of the mediatophore with a 14-kDa polypeptide. *J. Neurochem.*, **56**, 2046-2052.

Israel, M., Lesbats, B. and Bruner, J. (1993). Glutamate and acetyl choline release from cholinergic nerve terminals, a calcium control specificity of the release mechanism. *Neurochem. Int.*, **22**, 52-57.

Israel M., Lesbats, B., Morel, N., Manaranche, R., Gulik-Krzywicki, T. and Dedieu, J.C. (1984). Reconstitution of a functional synaptosomal membrane possesing the protein constituents involved in acetylcholine translocation. *Proc. Natl. Acad Sci. USA*, **81**, 277-281.

Jackson, R.C. and Blobel, G. (1977). Post-translational cleavage of presecretory proteins with an extract of rough microsomes from dog pancreas containing signal peptidase activity. *Proc. Natl. Acad. Sci. USA*, **74**, 5598-5602.

Johnson, R.G., Hammer, M., Sheridan, J.D., and Revel, J.-P. (1974). Gap junction formation between reaggregated novikoff hepatoma cells. *Proc. Natl. Acad. Sci. USA*, **71**, 4536-4540.

Jones, P.C., Harrison, M.A., Kim, Y.-I., Finbow, M.E. and Findlay, J.B.C. (1994). Structure and function of the proton conducting sector of the vacuolar H^+-ATPase. *Biochem. Soc. Transact.*, **22**, 805-809.

Jones, P. C., Harrison, M. A., Kim, Y.-I., Finbow, M. E., and Findlay, J. B. (1995). The first putative transmembrane helix of the vacuolar H^+-ATPase proteolipid lines a pore in the V_0 membrane sector. *J. Biol. Chem.*, (submitted).

Kakinuma, Y., Kakinuma, S., Takase, K., Konishi, K., Igarashi, K. and Yamato, I. (1993). A gene encoding the 16-kda proteolipid subunit of *Enterococcus hirae* Na^+-ATPase complex. *Biochem. Biophys. Res. Comm.*, **195**, 1063-1069.

Kalies, K.-U., Gorlich, D. and Rapoport, T.A. (1994). Binding of ribosomes to the rough endoplasmic reticulum mediated by the sec61p-complex. *J. Cell Biol.*, **126**, 925-934.

Kam, E., Melville, L. and Pitts, J.D. (1986). Patterns of junctional communication in skin. *J. Invest. Dermatol.*, **87**, 748-753.

Kane, P.M., Yamashiro, C.T. and Stevens, T.H. (1989). Biochemical characterisation of the yeast vacuolar H^+-ATPase. *J. Biol. Chem.*, **264**, 19236-19244.

Kane, P.M., Kuehn, M.C., Howald-Stevenson, I. and Stevens, T.H. (1992). Assembly and targeting of peripheral and integral membrane subunits of the yeast vacuolar H^+-ATPase. *J. Biol. Chem.*, **267**, 447-454.

Kluge, C. and Dimroth, P. (1993). Specific protection by Na^+ or Li^+ of the F_1F_0-ATPase of *Propiogenium modestum* from the reaction with dicyclohexylcarbodiimide. *J. Biol. Chem.*, **268**, 14557-14560.

Krogstad, D.J. and Schlesinger, P. (1987). Acid -vesicle function, intracellular pathogens, and the action of chloroquine against Plasmodium falciparum. *N. Eng. J. Med.*, **317**, 542-549.

Kuhlbrandt, W., Wang, D.N. and Fujiyoshi, Y. (1994). Atomic model of plant light-harvesting complex by electron crystallography. *Nature*, **367**, 614-621.

Kuki, M., Noumi, T., Maeda, M., Amemura, A. Futai, M. (1988). Functional domains of ε subunit of *Escherichia coli* H^+-ATPase (F_0F_1). *J. Biol. Chem.*, **263**, 17437-17442.

Kulke, R., Horwitz, B.H., Zibello, T. and DiMaio, D. (1992). The central hydrophobic domain of the bovine papillomavirus E5 transforming protein can be replaced by many hydrophobic amino acid sequences containing a glutamine. *J. Virol.*, **66**, 505-511.

Kumar, N. M., and Gilula, N. B. (1992). Molecular biology and genetics of gap junction channels. *Semin. Cell Biol.*, **3**, 3-16.

Kutay, U., Ahnert-Hilger, G., Hartmann, E., Wiedenmann, B. and Rapoport, T.A. (1995). Transport route for synaptobrevin via a novel pathway of insertion into the endoplasmic reticulum membrane. *EMBO J.*, **14**, 217-223.

Lamb, R.A., Zebedee, S.L. and Richardson, C.D. (1985). Inluenza virus M_2 protein is an integral membrane protein expressed on the infected-cell surface. *Cell*, **40**, 627-633.

Laubinger, W., Deckers-Hebestreit, G., Altendorf, K. and Dimroth, P. (1990) A hybrid sdenosinetriphosphatase composed of F_1 of *Escherichia coli* and F_0 *of Propionigenium modestum* is a functional sodium ion pump. *Biochem.*, **28**, 5347-5352.

Lawrence, T.S., Beers, W.H. and Gilula, N.B. (1978). Transmission of hormonal stimulation by cell-to-cell communication. *Nature*, **272**, 501-506.

Leitch, B., and Finbow, M.E. (1990). The gap junction-like form of a vacuolar proton channel component appears not to be an artefact of isolation: an immunocytochemical localisation study. *Exp. Cell Res.*, **190**, 218-226.

Lemmon, M.A., Flanagan, J.M., Hunt, J.F., Adair, B.D., Bormann, B.-J., Dempsey, C.E. and Engelman, D.M. (1992). Glycophorin A dimerisation is driven

by specific interactions between transmembrane α-helices. *J. Biol. Chem.*, **267**, 7683-7689.

Lipp, J., Flint, N., Haeuptle, M.-T. and Dobberstein, B. (1989). Structural requirements for membrane assembly of proteins spanning the membrane several times. *J. Cell Biol.*, **109**, 2013-2022.

Lo, C.W. and Gilula, N.B. (1979). Gap junctional communication in the preimplantation mouse embryo. *Cell*, **18**, 399-409.

MacDonald, C. (1985). Gap junctions and cell-cell communication. *Essays Biochem.*, **21**, 86-118.

Machamer, C.E., Doms, R.W., Bole, D.G., Helenius, A. and Rose, J.K. (1990). Heavy chain binding protein recognices incompletely disulphide-bonded forms of vesicular stomatis virus G protein. *J. Biol. Chem.*, **265**, 6879-6883.

Makowski, L., Caspar, D.L.D., Phillips, W.C. and Goodenough, D.A. (1977). Gap junction structures: II analysis of X-ray diffraction data. *J. Cell Biol.*, **74**, 628-644.

Makowski, L., Caspar, D.L.D., Phillips, W.C., Baker, T.S. and Goodenough, D.A. (1984). gap junction structures VI. Variation and conservation in connexon conformation and packing. *Biophys. J.*, **45**, 208-218.

Mandel, M., Moriyama, Y., Hulmes, J.D., Pan, Y.-C., Nelson, H. and Nelson, N. (1988). cDNA sequence encoding the 16-kDa proteolipid of chromaffin granules implies gene duplication in the evolution of H^+- ATPases. *Proc Natl. Acad. Sci. USA*, **85**, 5521-5524.

Manolson., M.F., Proteau, D., Preston, R.A., Stenbit, A., Roberts, B.T., Hoyt, M.A., Preuss, D., Mulholland, J., Botstein, D. and Jones, E.W. (1992). The *VPH1* gene encodes a 95-kDa integral membrane polypeptide required for *in vivo* assembly and activity of the yeast vacuolar H^+-ATPase. *J. Biol. Chem.*, **267**, 14294-14303.

Manolson, M.F., Wu, B., Proteau, D., Taillon, B.E., Roberts, B.T., Hoyt, M.A. and Jones, E.W. (1994). *STV1* gene encodes functional homologue of 95-kDa yeast vacuolar H^+-ATPase subunit Vph1p. *J. Biol. Chem.*, **269**, 14064-14074.

Marquardt, D. and Center, M.S. (1991). Involvement of vacuolar H^+-adenosine triphosphatase activity in multidrug resistance in HL60 cells. *J.Natl. Cancer Inst.*, 83,1098-1102.

Mege, R.-M., Matsuzaki, F., Gallin, W.J., Goldberg, J.I., Cunningham, B.A. and Edelman, G.M. (1988). Construction of epitheliod sheets by transfection of mouse sarcoma cells with cDNAs for chicken cell adhesion molecules. *Proc. Natl. Acad. Sci. USA*, **85**, 7274-7278.

Mesnil, M. and Yamasaki, H. (1993). Cell-cell communication and growth control of normal and cancer cells: evidence and hypothesis. *Molec. Carcinogen.*, **7**, 14-17.

Meyer, A.N., Xu, Y.-F., Webster, M.K., Smith, A.E. and Donoghue, D.J. (1994). Cellular transformation by a transmembrane peptide: structural requirements for the bovine papillomavirus E5 oncoprotein. *Proc. Natl. Acad. Sci. USA*, **91**, 4634-4638.

Miao, G-H., Hong, Z., and Verma, D. P. S. (1992). Topology and phosphorylation of soybean nodulin-26, an intrinsic protein of the peribacteroid membrane. *J. Cell Biol.*, **118**, 481-490.

Miller, M.J., Oldenburg, M. and Fillinghame, R.H. (1990). The essential carboxyl group in subunit c of the F_1F_0 ATP synthase can be moved and H^+-translocating functions retained. *Proc. Natl. Acad. Sci USA*, **87**, 4900-4904.

Mosher, M.E., Peters, L.K. and Fillingame, R.H. (1983). Use of Lambda *unc* transducing bacteriophages in genetic and biochemical characterisation of H^+-ATPase mutants of *Escherichia coli*. *J. Bacteriol.*, **156**, 1078-1092.

Mosher, M.E., White, L.K., Hermolin, J. and Fillingame, R.H. (1985). H^+-ATPase of Escherichia coli. An *uncE* mutation impairing coupling between F_1 and F_0 but not F_0-mediated H^+ translocation. *J. Biol. Chem.*, **260**, 4807-4814.

Mothes, W., Prehn, S. and Rapoport, T.A. (1994). Systematic probing of the environment of a translocating secretory protein during translocation through the ER membrane. *EMBO J.*, **13**, 3973-3982.

Musch, A., Weidmann, M. and Rapoport, T.A. (1992). Yeast sec proteins interact with polypeptides traversing the endoplasmic reticulum membrane. *Cell*, **69**, 343-352.

Musil, L.S., and Goodenough, D.A. (1993). Multisubunit assembly of an integral plasma membrane channel protein, gap junction connexin43, occurs after exit from the ER. *Cell*, **74**, 1065-1077.

Myers, M. and Forgac, M. (1993). Assembly of the peripheral domain of the bovine vacuolar H^+-adenine triphosphatase. *J. Cell. Physiol.*, **156**, 35-42.

Nelson, N. (1992). Organellar proton-ATPases. *Curr. Op. Cell Biol.*, **4**, 654-660.

Nelson, H., Mandiyan, S. and Nelson, N. (1989). A conserved gene encoding the 57-kDa subunit of the yeast vacuolar H^+-ATPase. *J. Biol. Chem.*, **264**, 1775-1778.

Nelson, H., Mandiyan, S., Noumi, T., Moriyami, Y., Miedel, M.C. and Nelson, N. (1990). Molecular cloning of cDNA encoding the c subunit of H^+-ATPase from bovine chromaffin granules. *J. Biol. Chem.*, **265**, 20390-20393.

Nelson, H. and Nelson, N. (1989). The progenitor of ATP synthases was closely related to the current vacuolar H^+-ATPase. *FEBS Lett.*, **247**, 147-153.

Nelson, H. and Nelson, N. (1990). Disruption of genes encoding subunits of yeast vacuolar H^+-ATPase causes conditional lethality. *Proc. Natl. Acad. Sci. USA*, **87**, 3503-3507.

Nezu, J.-I., Motojima, K., Tamura, H.-I and Ohkuma, S. (1992) Molecular cloning of a rat liver cDNA encoding the the 16 kDa subunit of the vacuolar H^+-ATPase; organellar and tissue distribution of the 16 kDa proteolipids. *J. Biochem.*, **112**, 212-219.

Ng, D.T.W. and Walter, P. (1994). Protein translocation across the endoplasmic reticulum. *Curr. Opin. Cell. Biol.*, **6**, 510-516.

Nicchitta, C.V. and Blobel,G. (1993). Lumenal proteins of the mammalian endoplasmic reticulum are required to complete protein translocation. *Cell*, **73**, 989-998.

Nilson, L.A. and DiMaio, D. (1993). Platelet-derived growth factor receptor can mediate tumorigenic transformation by the bovine papillomavirus E5 protein. *Mol. Cell. Biol.*, **13**, 4137-4145.

Noumi, T., Beltran, C., Nelson, H. and Nelson, N. (1991). Mutational analysis of yeast vacuolar H^+-ATPase. *Proc. Natl. Acad. Sci. USA*, **88**, 1938-1942.

Ooi, C.E. and Weiss, J. (1992). Bidirectional movement of a nascent polypeptide across microsomal membranes reveals requirements for vectorial translocation of proteins. *Cell*, **71**, 87-96.

Ostapchuk, P., Hearing, P. and Ganem, D. (1994). A dramatic shift in the transmembrane topology of a viral envelope glycoprotein accompanies hepatitus B viral morphogenesis. *EMBO J.*, **13**, 1048-1057.

Parks, G.D., Hull, J.D. and Lamb, R.A. (1989). Transposition of domains between the M_2 and HN viral membrane proteins results in polypeptides which can adopt more than one membrane orientation. *J. Cell Biol.*, **109**, 2023-2032.

Parks, G.D. and Lamb, R.A. (1991). Topology of eukaryotic type II membrane proteins: importance of N-terminal positively charged residues flanking the hydrophobic domain. *Cell*, **64**, 777-787.

Parks, G.D, and Lamb, R.A. (1993). Role of NH_2-terminal positively charged residues in establishing membrane protein topology. *J. Biol. Chem.*, **268**, 19101-19109.

Pederson, P.L. and Amzell, L.M. (1993). ATP synthases: structure, reaction center, mechanism, and regulation of one nature's most unique machines. *J. Biol. Chem.*, **268**, 9937-9940.

Peng, S-B., Crider, B.P., Xie, X-S. and Stone, D.K. (1994). Alternative mRNA splicing generates tissue-specific isoforms of 116-kDa polypeptide of vacuolar proton pump. *J. Biol. Chem.*, **269**, 17262-17266.

Petti, L., Nilson, L.A. and DiMaio, D. (1991). Activation of the platelet-derived growth factor receptor by the bovine papillomavirus E5 transforming protein. *EMBO J.*, **10**, 845-855.

Petti, L. and DiMaio, D. (1992). Stable association between the bovine papillomavirus E5 transforming protein and activated platelet-derived growth factor receptor in transformed mouse cells. *Proc. Natl. Acad. Sci. USA*, **89**, 6736-6740.

Petti, L. and DiMaio, D. (1994). Specific interaction between the bovine papillomavirus E5 transforming protein and the β receptor for platelet-derived ggrowth factor in stably transformed and acutly transfected cells. *J. Virol.*, **68**, 3582-3592.

Pitts, J.D. and Simms, J.W. (1977). Permeability of junctions between animal cells. Intercellular transfer of nucleotides but not of macromolecules. *Exp. Cell Res.*, **104**, 153-163.

Pitts, J.D., Hamilton, A.E., Kam, E. and Murphy, J.P. (1986). Retinoic acid inhibits junctional communication between animal cells. *Carcinogenesis*, **7**, 1003-1010.

Pitts, J., Kam, E., Melville, L. and Watt, F.M. (1986). Patterns of junctional communication in animal tissues. Ciba symp., **125**, 140-153.

Pitts, J.D., Kam, E. and Morgan, D. (1988). The role of gap junctional communication in growth control and tumorigenesis. In *Gap Junctions*, ed. Hertzberg, E.L. and Johnson, R.G., pp397-409, Alan Liss Inc., New York.

Popot, J.-L., Gerchman, S.-E. and Engelman, D.M. (1987). Refolding of bacteriorhodopsin in lipid bilayers. *J. Mol. Biol.*, **198**, 655-676.

Popot, J.-L. and Changeux, J.-P. (1984). Nicotinic receptor of acetylcholine: structure of an oligomeric integral membrane protein. *Physiol. Rev.*, **64**, 1162-1239.

Poupolo, K., Kumamoto, C., Adachi, I., Magner, R. and Forgac, M. (1992). Differential expression of the "B" subunit of the vacuolar H^+-ATPase in bovine tissue. *J. Biol. Chem.*, **267**, 3696-3706.

Prange, R. and Streeck, R.E. (1995). Novel transmembrane topology of the hepatitus B virus envelope proteins. *EMBO J.*, **14**, 247-256.

Rapoport, T.A. (1992). Transport of proteins across the endoplasmic reticulum. *Science*, **258**, 931-936.

Rothblat, J.A., Deshaies, R.J., Sanders, S.L., Daum, G. and Schekman, R. (1989). Multiple genes are required for proper insertion of secretory proteins into the endoplasmic reticulum in yeast. *J.Cell Biol.*, **109**, 2641-2652.

Ryba, N. J. P., Hoon, M. A., Findlay, J. B. C., Saibil, H. R., Wilkinson, J. R., Heimburg, T., and Marsh, D. (1993). Rhodopsin mobility, structure, and lipid-protein interaction in squid photoreceptor membranes. *Biochemistry*, **32**, 3298-3305.

Saez, J.C., Conner, J.A., Spray, D.C. and Bennett, M.V. (1989). Hepatocyte gap junctions are permeable to the second messanger, inositol 1,4,5-triphosphate, and to calcium ions. *Proc. Natl. Acad. Sci. USA*, **86**, 2708-2712.

Saiki, R.K., Scharf, S., Faloona, F., Mullis, K.B., Horn, G.T., Erlich, H.A. and Arnheim, N. (1985). Enzymatic amplification of b-globin genomic sequences and restriction site analysis for diagnosis of sickle cell anemia. *Science*, **230**, 1350-1354.

Sakaguchi, M., Tomiyoshi, R., Kuroiwa, T., Mihara, K. and Omura, T. (1992). Functions of signal and signal-anchor sequences are determined by the balance between the hydrophobic segment and the N-terminal charge. *Proc. Natl. Acad. Sci. USA*, **89**, 16-19.

Sanders, S.L., Whitfeild, K.M., Vogel, J.P., Rose, M.D. and Schekman, R. (1992). Sec61p and BiP directly facilitate polypeptide translocation into the ER. *Cell*, **69**, 353-365.

Savitz, A.J. and Meyer, D.I. (1993). 180-kD ribosome receptor is essential for both ribosome binding and protein translocation. *J. Cell Biol.*, **120**, 853-863.

Senior, A.E. (1988). ATP synthesis by oxidative phosphorylation. *Physiol. Rev.*, **68**, 177-231.

Shaw, A.S., Rottier, P.J.M. and Rose, J.K. (1988). Evidence for the loop model of signal-sequence insertion into the endoplasmic reticulum. *Proc. Natl. Acad. Sci. USA.* **85**, 7592-7596.

Shih, C.-K., Wagner R., Feinstein S., Kanik-Ennulat C. and Neff N. (1988). Expression of a proteolipid gene from a high copy-number plasmid confers trifluoperazine resistance in *Saccharomyces cerevisiae*. *Mol. Cell Biol.*, 8, 2994-3003.

Siegel, V. and Walter, P. (1988). Functional dissection of the signal recognition particle. *T.I.B.S.*, **13**, 314-316.

Sikerwar, S.S., Downing, K.H. and Glaesser, R.M. (1991). Three-dimensional sructure of an invertebrate intercellular communicating junction. *J. Struct. Biol.*, **106**, 255-263.

Simon, S. and Blobel, G. (1991). Signal peptides open protein-conducting channels in E. coli. *Cell*, **69**, 677-684.

Simpson, I., Rose, B. and Loewenstein, W.R. (1977). Size limit of molecules permeating the junctional membrane channels. *Science*, **195**, 294-296.

Skach, W. R., Shi, L., Calayag, M. C., Frigeri, A., Lingappa, V.R., and Verkman, A. S. (1994). Biogenesis and transmembrane topology of the CHIP28 water channel at the endoplasmic reticulum. *J. Cell Biol.*, **125**, 803-815.

Solioz, M. and Davies, K. (1994). Operon of the vacuolar-type Na^+-ATPase of *Enterococcus hirae*. *J. Biol. Chem.*, **269**, 9453-9459.

Sosinsky, G.E., Baker, T.S., Casper, D.L.D. and Goodenough, D.A. (1990). Correlation analysis of gap junction lattice images. *Biophys. J.*, **58**, 1213-1226.

Sparkowski, J., Anders, J. and Schlegel, R. (1994). Mutation of the bovine papillomavirus E5 oncoprotein at amino acid 17 generates both high- and low-transforming variants. *J. Virol.*, **68**, 6120-6123.

Stirling, C.J., Rothblatt, J., Hosobuchi, M., Deshaies, R. and Schekman, R. (1992). Protein translocation mutants defectivve in the insertion of integral membrane proteins into the endoplasmic reticulum. *Mol. Biol. Cell*, **3**, 129-142.

Stokes, D.L. and Nakamoto, R.K. (1994). Structures of P-type and F-type ion pumps. *Curr. Op. Struct. Biol.*, **4**, 197-203.

Straight, S.W., Hinkle, P.M., Jewers, R.J. and McCance, D.J. (1993). The E5 oncoprotein of human papillomavirus type 16 transforms fibroblasts and effects the downregulation of the epidermal growth factor receptor in keratinocytes. *J. Virol.*, **67**, 4521-4532.

Stroud, R.M., McCarthy, M.P. and Shuster, M. (1990). Nicotinic acetylcholine receptor superfamily of ligand-gated ion channels. *Biochemistry*, **29**, 11009-11023.

Sugrue, R.J. and Hay, A.J. (1991). Structural characteristics of the M2 protein of influenza A viruses: evidence that it forms a tetrameric channel. *Virology*, **180**, 617-624.

Sun, S.-Z, Xie, X.-S. and Stone, D.K. (1987). Isolation and reconstitution of the dicyclohexylcarbodiimide-sensitive proton pore of the clathrin coated vesicle translocating complex. *J. Biol. Chem.*, **251**, 14690-14694.

Supek, F., Supekova, L., Beltran, C., Nelson, H. and Nelson, N. (1992). Structure, function, and mutational analysis of V-ATPases. *Ann. N. Y. Acad. Sci.*, **671**, 284-292.

Supek, F., Supekova, L. and Nelson, N. (1994). Features of vacuolar H+-ATPase revealed by yeast suppressor mutants. *J. Biol. Chem.*, **269**, 26479-26485.

Takase, K., Kakinuma, S., Yamato, I., Konishi, K., Igarashi, K. and Kakinuma, Y. (1994). Sequencing and characterization of the *ntp* gene cluster for vacuolar-type Na^+-translocating ATPase of *Enterococcus hirae*. *J. Biol. Chem.*, **260**, 11036-11043.

Takase, K., Yamato, I. and Kakinuma, Y. (1993). Cloning and sequencing of the A and B subunits of vacuolar-type Na^+-ATPase from *Enterococcus hirae*. *J. Biol. Chem.*, **268**, 11610-11616.

Tam, L.Y., Loo, T.W., Clarke, D.M., and Reithmeier, R.A.F. (1994). Identification of an internal topogenic signal sequence in human band 3, the erythrocyte anion exchanger. *J. Biol. Chem.*, **269**, 32542-325550.

Tibbits, T.T., Casper, D.L.D., Philips, W.C. and Goodenough, D.A. (1990). Diffraction diagnosis of protein folding in gap junction connexons. *Biophys. J.*, **57**, 1025-1036.

Umemoto, N., Ohya, Y.. and Anraku, Y. (1991). *VMA11*, a novel gene that encodes a putative proteolipid, is indispensable for expression of yeast vacuolar membrane H^+-ATPase activity. *J. Biol. Chem.*, **266**, 24526-24532.

Umemoto, N., Yoshihisa, T., Hirata, R. and Anraku, Y. (1990). Roles of the VMA3 gene product, subunit c of the vacuolar membrane H^+-ATPase on vacuolar acidification and protein transport. A study with VMA3-disrupted mutants of saccharomyces cerevisiae. *J. Biol. Chem.*, **265**, 18447-18453.

Unwin, P.N.T. and Ennis, P.D. (1984). Two configurations of a channel-forming membrane protein. *Nature*, **307**, 609-613.

Unwin, N. (1989). The structure of ion channels in membranes of excitable cells. *Neuron*, **3**, 665-676.

Unwin, N. (1993). Nicotinic acetylcholine receptor at 9Å resolution. *J. Mol. Biol.*, **229**, 1101-1124.

Verbavatz, J.-M., Brown, D., Sabolic, I., Valenti, G., Ausello, D.A., Van Hoek,A.N., Ma, T. and Verkman, A.S. (1993). Tetrameric assembly of CHIP28 water channels in liposomes and cell membranes: a freeze-fracture study. *J. Cell Biol.*, **123**, 605-618.

Verrall, S. and Hall, Z.W. (1992). The N-terminal domains of acetylcholine receptor subunits contain recognition signals for the initial steps of receptor assembly. *Cell*, **68**, 23-31.

Vogel, J.P., Misra, L.M. and Rose, M.D. (1990). Loss of BiP/GRP78 function blocks translocation of secretory proteins in yeast. *J. Cell Biol.*, **110**, 1885-1895.

von Heijne, G. (1995). Membrane protein assembly: rules of the game. *BioEssays*, **17**, 25-30.

von Heijne, G. (1984). Analysis of the distribution of charged residues in the N-terminal region of signal sequences: implications for protein export in prokaryotic and eukaryotic cells. *EMBO J.*, **3**, 2315-2318.

Walter, P. and Blobel, G. (1981). Translocation of proteins across the endoplasmic reticulum III. Signal recognition protein (SRP) causes signal sequence-dependant arrest of chain elongation that is released by microsomal membranes. *J. Cell Biol.*, **91**, 557-561.

Walter, P., Gilmore, R., and Blobel, G. (1984). Protein translocation across the endoplasmic reticulum. *Cell*, **38**, 5-8.

Walter, P. and Lingappa, V.R. (1986). Mechanism of protein translocation across the endoplasmic reticulum membrane. *Ann. Rev. Cell Biol.*, **2**, 499-516.

Walz, T., Smith, B.L., Agre, P. and Engel, A. (1994). The three-dimensional structure of human erythrocyte aquaporin CHIP. *EMBO J.*, **13**, 2985-2993.

Wang, Z.-Q. and Gluck, S. (1990). Isolation and properties of bovine kidney brush border vacuolar H^+-ATPase. *J. Biol. Chem.*, **265**, 21957-21965.

Weiss, M.S., Abele, U., Weckesser, J., Welte, W., Schiltz, E. and Schulz, G.E. (1991). Molecular architecture and electrostatic properties of a bacterial porin. *Science*, **254**, 1627-1630.

Wiedmann, B., Sakai, H., Davies, T.A. and Wiedmann, M. (1994). A protein complex required for signal-sequence-specific sorting and transllocation. *Nature*, **370**, 434-440.

Xie, X.-S. and Stone, D.K. (1986). Isolation and reconstitution of the clathrin-coated vesicle proton translocating complex. **J. Biol. Chem.**, **261**, 2492-2495.

Yamashiro, C.T., Kane, P.M., Wolczyk, D.F., Preston, R.A. and Stevens, T.H. (1990). Role of vacuolar acidification in protein sorting and zymogen activation: a genetic analysis of the yeast vacuolar proton-translocating ATPase. *Mol. Cell. Biol.*, **10**, 3737-3749.

Yeager, M. and Gilula, N.B. (1992). Membrane topology and quaternary structure of cardiac gap junction ion channels. *J. Mol. Biol.*, **223**, 929-948.

Yokoyama, K., Akabane, Y., Ishi, N. and Yoshida, M. (1994). Isolation of prokaryotic V_0V_1-ATPase from a thermophilic eubacterium *Thermus thermophilus*. *J. Biol. Chem.*, **269**, 12248-12253.

Zhang, Y., Oldenburg, M. and Fillingame, R.H. (1994). Suppressor mutations in F_1 subunit ε recouple ATP-driven H^+ translocation in uncoupled Q41E subunt *c* mutant of *Escherichia coli* F_1F_0 ATP synthase. *J. Biol. Chem.*, **269**, 10221-10224.

Zhang, J., Feng, Y. and Forgac, M. (1994). Proton conduction and bafilomycin binding by the V_0 domain of the coated vesicle V-ATPase. *J. Biol. Chem.*, **269**, 23518-23523.

Zhang, J., Myers, M. and Forgac, M. (1992). Characterization of the V_0 domain of the coated vesicle (H^+)-ATPase. *J. Biol. Chem.*, **267**, 9773-9778.

Zhang, Y. and Fillingame, R.H. (1994). Essential aspartate in subunit *c* of F_1F_0 ATP synthase. *J. Biol. Chem.*, **269**, 5473-5479.

Gillespie, G.A.J., Somlo, S., Germino, G.G., Weinstat-Saslow, D. and Reeders, S.T. (1991). CpG island in the region of an autosomal dominant polycystic kidney disease locus defines the 5' end of a gene encoding a putative proton channel. *Proc. Natl. Acad. Sci.*, **88**, 4289-4293.

Maniatis, T., Fritsch, E.F. and Sambrook, J. (1989). Molecular cloning; a laboratory manual. Second edition. Cold Spring Harbour Laboratory Press.